REPUBLIC OF IRAQ
MINISTRY OF HIGHER EDUCATION AND SCIENTIFIC RESEARCH
AL-FURAT AL-AWSAT TECHNICAL UNIVERSITY
ENGINEERING TECHNICAL COLLEGE- NAJAF

EXPERIMENTAL INVESTIGATION OF SOME THERMAL APPLICATIONS USING FRESNEL LENS CONCENTRATOR IN IRAQ

A THESIS
SUBMITTED TO THE DEPARTMENT OF MECHANICAL ENGINEERING TECHNIQUES IN POWER AS PARTIAL FULFILLMENT OF THE REQUIREMENTS FOR TECHNICAL MASTER DEGREE IN MECHANICAL ENGINEERING
(THERMAL)

BY
Ahmed Hussein Obaid Mohammed
(B. Sc. Refrigeration & Air-conditioning Eng.)

Supervised by

Assist. Prof.	**Assist. Prof.**
Dr. Assaad Al Sahlani	**Dr. Adel A Eidan**

June 2020

بِسْمِ اللَّهِ الرَّحْمَٰنِ الرَّحِيمِ

قَالُوا سُبْحَانَكَ لَا عِلْمَ لَنَا إِلَّا مَا عَلَّمْتَنَا ۖ إِنَّكَ أَنتَ الْعَلِيمُ الْحَكِيمُ

صَدَقَ اللهُ العَلِيُّ العَظِيم

سورة البقرة :الاية (32)

Acknowledgment

All Praise to ALLAH for his uncountable blessings, assistance during the preparation of this work.

Special thanks to the Dean of Engineering Technical College- Najaf ***Asst.Prof. Dr. Hassanain Ghani Hameed***

Special thanks to the Head of Department of Mechanical Engineering Techniques of Power ***Asst. Prof. Dr. Dhafer Manea Hachim***

I would like to submit my deep respects and sincere gratitude to my supervisors ***Assist. Prof. Dr. Assaad Al Sahlani*** *and* ***Assist. Prof. Dr. Adel A Eidan*** *for their support during the research period and guidance to accomplish this work.*

Special thanks to the members of the department of Mechanical Engineering Techniques of Power for their assistance to me

I also extend my gratitude to all my friends, especially Eng. Ali Kadhym, for their encouragement who support me directly and indirectly to conduct this work.

My deepest thanks and gratitude are due to each member of my family, especially my dearest parents, brothers and sisters for their patience, support and encouragement throughout my life. Special thanks are due also to my wife for her support and patience during the period of my study.

Ahmed Hussein Obaid
2020

I

Supervisor Certification

We certify that this thesis titled " **Experimental Investigation of Some Thermal Applications Using Fresnel Lens Concentrator in Iraq** " which is being submitted by **Ahmed Hussein Obaid** was prepared under our supervision at the Department of Mechanical Engineering Techniques of Power, Engineering Technical College-Najaf, AL-Furat Al-Awsat Technical University, as partial fulfillment of the requirements for the degree of Master of Technical in Thermal Engineering.

Signature:

Name: Assist. Prof. Dr. Assaad Al Sahlani.

(Supervisor)

Date: /   / 2020

Signature:

Name: Assist. Prof. Dr. Adel A Eidan

(Co-Supervisor)

Date: 5 / 7 / 2020

In view of the available recommendation, we forward this thesis for debate by the examining committee.

Signature:

Name: Asst. Prof. Dr. Dhafer Manea Hachim

(Head of Department of Mechanical Engineering Techniques of Power)

Date: 5 / 7 / 2020

The Examing Committee Certification

We certify that we have read this thesis titled "Experimental **Investigation of Some Thermal Applications Using Fresnel Lens Concentrator in Iraq**" which is being submitted by **Ahmed Hussein Obaid** and as Examining Committee, examined the student in its contents. In our opinion, the thesis is adequate for the award of the degree of Master of Technical in Thermal Engineering.

Signature:

Name: Asst. Prof. Dr. Assaad Al Sahlani
Supervisor
Date: /   / 2020

Signature:

Name: Asst. Prof. Dr.Adel A Eidan
(Co-Supervisor)
Date: /   / 2020

Signature:

Name: Asst. Prof. Dr. Ali N. Kadhim
(Member)
Date: 13 / 10 / 2020

Signature:

Name: Lec. Dr Ali W. Abbas
(Member)
Date: /   / 2020

Signature:

Name: Asst. Prof. Dr. Dhafer Manea Hachim
(Chairman)
Date: 12 / 10 / 2020

Approval of the Engineering Technical College- Najaf

Signature:
Name: Asst. Prof. Dr. Hassanain Ghani Hameed
Dean of Engineering Technical College- Najaf
Date: /   / 2020

III

DECLARATION

I hereby declare that the work in this thesis is my own except for quotations and summaries which have been duly acknowledged.

Ahmed Hussein Obaid

Signature:

Date:

Abstract

This work presents an experimental study to utilize Fresnel lens to increasing the concentrator of solar radiation using a solar tracking system. The experimental rig consists of a freely rotating two-axis frame that is controlled by an electronic circuit that implements Arduino and stepper motors as a control system to adjust the position of the Fresnel lens focal by moving the motors accordingly. The focal of the sunray is to be maintained stationary at a fixed position to ensure continuity of heat flow on the absorption system.

The experimental study presents the thermal characteristics of heat focal provided by Fresnel lens. As an initial test, two plates made of different metals are exposed to the focal of the sunlight to study the temperature distribution on the receiver. The experimental tests are performed with local weather condition in Najaf city/Iraq at latitude 31.59 degrees north, 44.19 degrees east, during winter session from November 2019 to February 2020. The results showed that the focal temperature reached as high as 400 °C when the ambient temperature was 20 °C. Observing the results, gives an idea of promising abilities to use the Fresnel lens in a wide range of renewable energy applications such as water desalination, water heating.

For water desalination, two models of a cylindrical with con solar still (10cm and 20cm in height) and for water heating, two models of the heat exchangers, and cubical steel water container are used.

The experimental tests were performed during arbitrary days of January and February 2020. The results showed that the largest cumulative productivity for six hours for the solar still is (500 ml). The experimental tests were conducted on February 2020. The results showed that the highest useful heat gain recorded for the conical pipe heat exchanger is 92 W when the intensity of solar radiation

is 1206 W/m^2 and the ambient temperature is 14 ° C. The highest obtained useful heat gain of the cubical tank heat exchanger was 91 W when the intensity of solar radiation is 1387 W/m^2 and the ambient temperature is 18 ° C. The experimental tests were performed during arbitrary days of November 2019. The results showed that for steel finned cover the highest recorded temperature is 258.6 ° C at the focus when the ambient temperature is 24.6 ° C and the intensity of the solar radiation is 1251 W/m^2. Whereas, the results of using an aluminum finned cover showed that the highest temperature recorded at the focus is 81.3 ° C when the ambient temperature is 22.4 ° C and the intensity of the solar radiation is 1008 W/m^2.

Contents

List of Figures

X

XI

Nomenclature

Symbol	Definition	Unit
AST	apparent solar time	min.
CFR	Circular Fresnel lens	-
CPV	concentrated photovoltaic	-
Cp	specific heat	J/kg°C
DHI	direct Horizontal irradiance	W/m²
DNI	direct normal irradiance	W/m²
E–W	East - West axis	-
ET	equation of time	min.
F	focal length	
GHI	global horizontal irradiance	W/m²
H	prisms height	
H	hour angle	Deg.
I	solar irradiance	W/m²
I	Incident angle on the lens back surface	Deg.
LL	local longitude	Deg.
LST	local standard time	Min.
L	local latitude	Deg.
LFR	Linear Fresnel reflector	-
LFL	Linear Fresnel lens	-
M	mass flow rate	Kg/s
N	day of the year	-
N–S	North – South axis	-
PDC	Parabolic Dish Collector	-
PMMA	Polymethylmethacrylate	-
PTC	Parabolic trough Collector	-

SL	standard longitude	Deg.
T	Temperature	°C
T_i	fluid inlet receiver temperature	°C
T_o	fluid outlet receiver temperature	°C
Z	Solar azimuth angle	Deg.
Greek Symbols		
A	solar altitude angle	Deg.
ɳ	thermal efficiency	%
Δ	solar declination angle	Deg.
β'	refraction angle of the prisms	Deg.
β	slope angle	Deg.
τ_C	transmittance of the cover	
α_C	thermal diffusivity	
Q_u	useful heat gain	W
U_G	overall loss coefficient of the still basin	

Chapter One

INTRODUCTION

1. INTRODUCTION

1.1 General

Energy generation is a significant factor in economic development. During the past century, fossil fuel was used as main energy source but with limited and decreased availability. In addition, fossil fuel pollutes the environment as a result of the emissions of the combustion.

Nowadays, one of the enormous challenges is how to reduce the demand on fossil fuels, using of renewable energy is the best option and has been the subject of research around the world. recently, considerable efforts have been made to find alternative energy sources and improve their efficiency to reduce problems resulting from the use of fossil fuels and the focus on renewable energy use [1].

Humanity requires sources of energy that solve environmental issues with long-term and sustainable capabilities. Solar energy is one of the alternative solutions with its great potentials in many parts of the world. The greatest benefit of solar energy compared to other energy sources is that it is pure and can be generated without any pollution of the atmosphere [2].

Although Iraq has plenty of sources of fossil fuel, it is limited and is expected to be consumed in the next hundred years [3]. And solar energy is the only uninterrupted option that helps to reduce pollution from fossil fuel burning.

1.2 Solar Radiation Resource

Two main components of solar radiation are direct solar radiation and diffuse radiation. The component summation on a horizontal surface called global solar radiation. Where the instantaneous solar radiation unit described by w/m^2. The average total solar radiation unit for a specific location or region represents in kWh/m^2 [4]

1.2.1 Beam Radiation

Beam radiation, also called direct normal irradiance (DNI), is the amount of solar radiation obtained on a surface perpendicular the radiation that comes from the sun without spreading in the atmosphere. Direct radiation is the one that is effective in solar concentrations because it can be reflected or refracted to a focus.

1.2.2 Diffuse Radiation

The diffuse radiation, also known as Diffuse Horizontal Irradiance (DHI), is the amount of radiation received per unit area of the surface of the collector that does not reach directly from the sun. However, its path changed by molecules of the atmosphere, and it comes equally from all sides

1.2.3 Total Solar Radiation

Total solar radiation, also known as global horizontal irradiance (GHI), is the amount of direct and diffuse solar radiation on a horizontal surface received from the sun.

1.2.4 Distribution of Solar Radiation

The distribution of solar radiation depends on the location of the region in relation to longitude and latitude, as shown in Fig. (1.1). The figure shows the annual amount of global horizontal irradiance worldwide varies from (803-2702) kWh/m^2. The annual of direct normal irradiance varies from (365-3652) kWh/m^2 as shown in Fig. (1.2) [5].

Iraq has a great potential of solar energy that can be employed to developed technologies that used in many renewable energy applications. The reason behind that is its geographical location at latitude 31.59 degrees north, 44.19 degrees east, which gives the advantage of a large amount of solar radiation, as shown in Fig. (1.3). The figure shows that the annual amount of global horizontal irradiation is (1753- 2191) kWh/m^2. Fig. (1.4) shows that the annual amount of direct normal irradiance for Iraq is (1680-2410) kWh/m^2.[6]. In addition, Iraq has a long periods

of daylight. For instance, on an annual basis, it is possible to collects more than 3000 hours of solar irradiance in Baghdad [3].
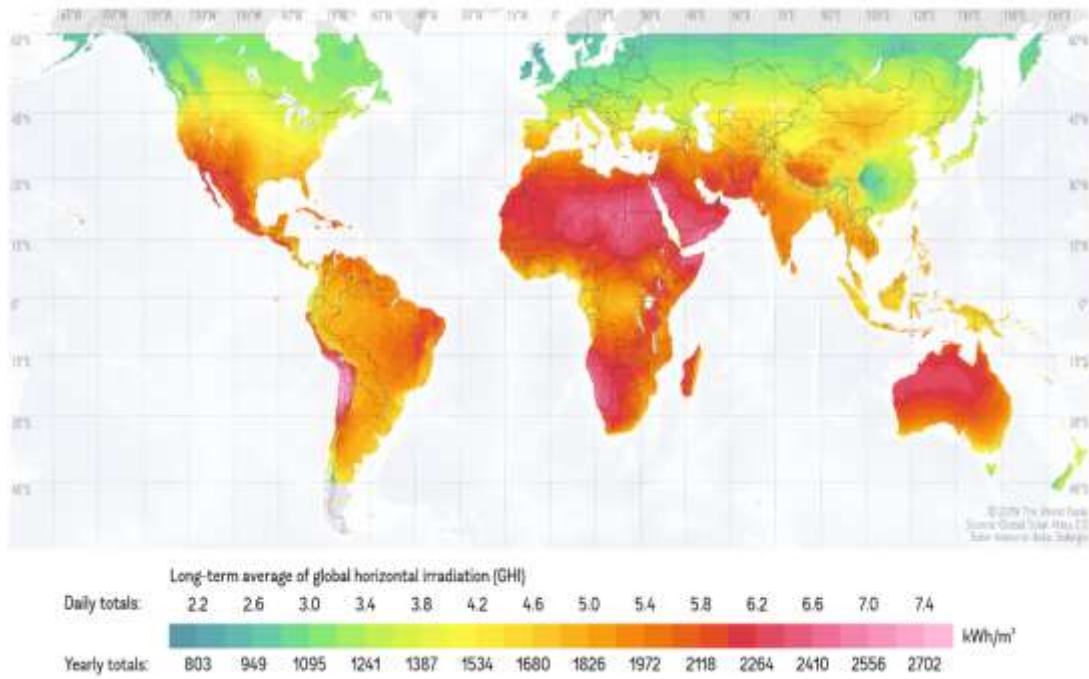
Fig. 1.1: Global horizontal irradiation for world [5].
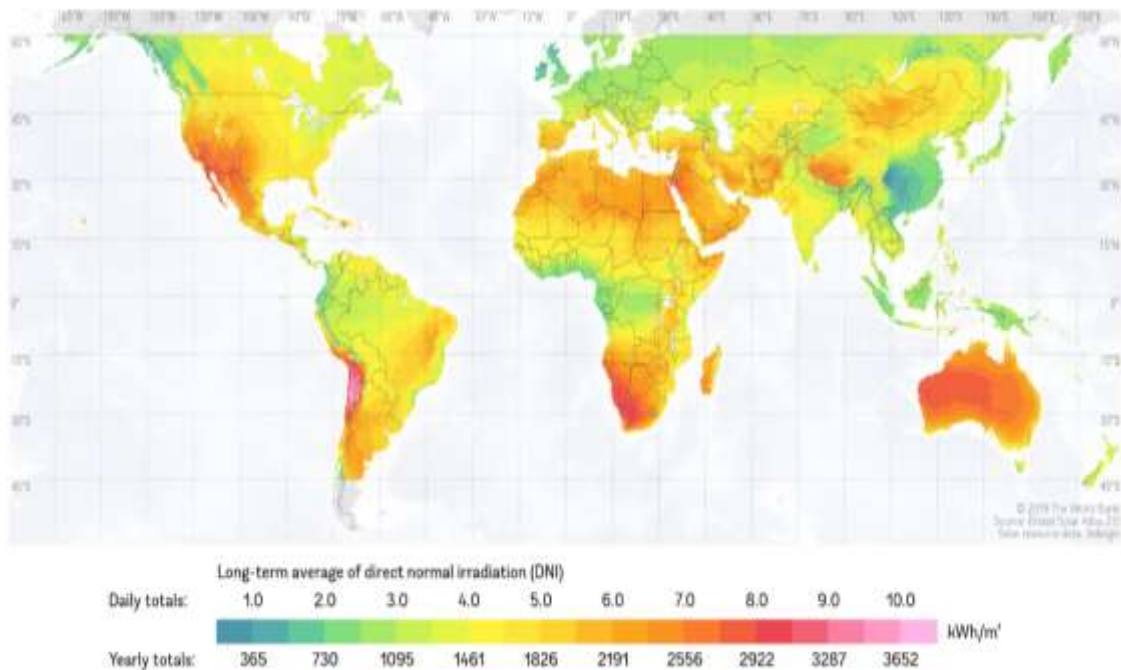
Fig. 1.2: Direct normal irradiance for world [5].
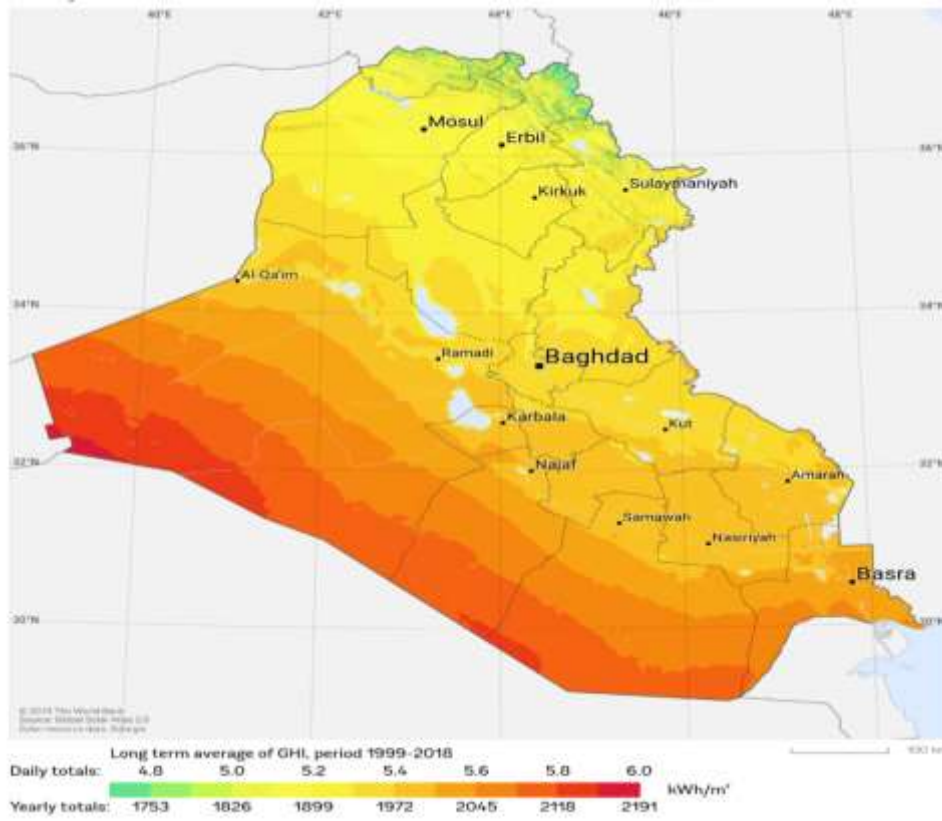
Fig. 1.3: Global horizontal irradiation for Iraq [6].
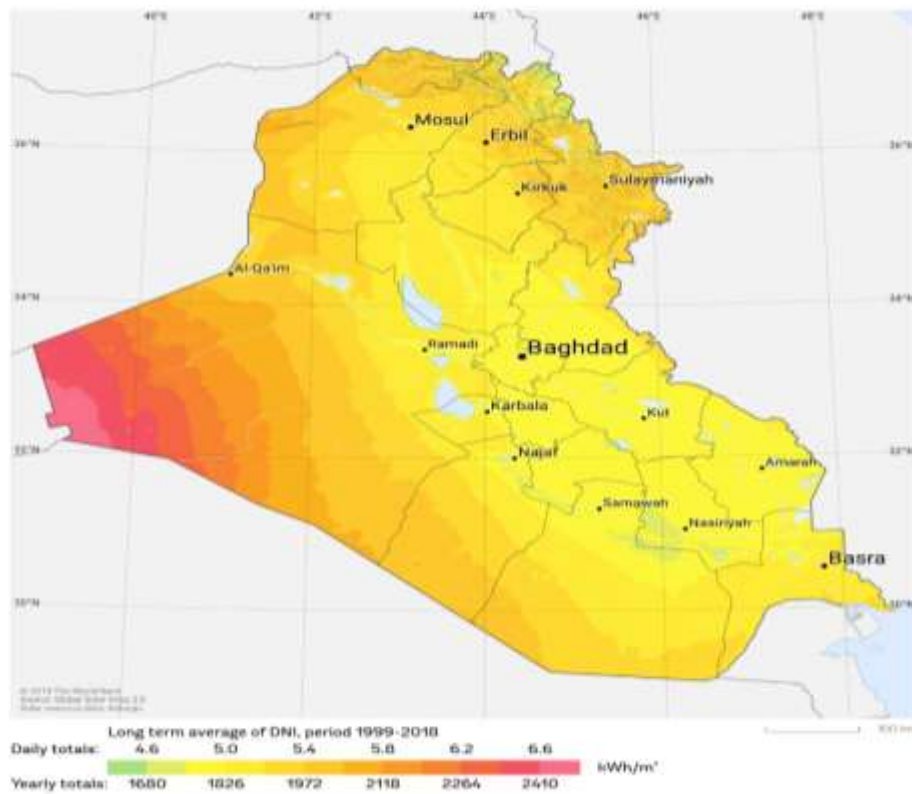
Fig. 1.4: Direct normal irradiance for Iraq [6].

1.3 Solar Concentrators

Solar Energy can be utilized in many different forms, one of which is the solar concentrators. Since long time ago, the solar concentrator systems used sunlight to generate solar thermal energy. Solar concentrators are devices that focus the sunlight from a large area, by reflection or refraction using parabolic or lens, respectively, on a small receiver. Such action increases the amount of solar radiation on surface of the small receiver. There are several types of concentrates as follows [1] [7]:

1.3.1 Parabolic Trough Collector (PTC)

The parabolic trough collector consists of a cylindrical receiver and a parabolic basin. The cylindrical receiver is a pipe along the focal point of the basin. The basin tracks the sun in one axis and heats the fluid that passes through the receiving pipe to about 400 °C, as shown in Fig. (1.5) [8]
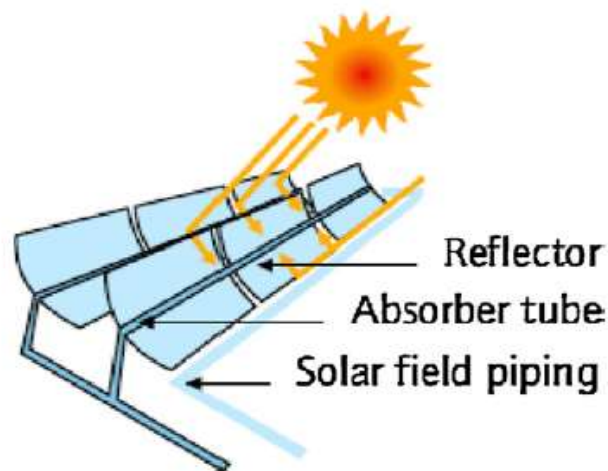
Fig. 1.5: Parabolic trough collector [8]

1.3.2 Linear Fresnel Reflector (LFR)

The linear Fresnel reflector consists of a series of mirrors placed at different angle that reflects the sunlight on a fixed receiver, as shown in Fig. (1.6). Comparing to PT, the LFR shows lower performance[9].
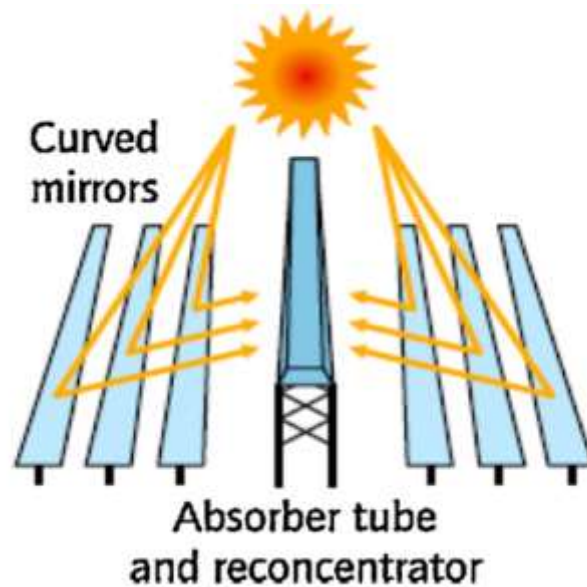
Fig. 1.6: Linear Fresnel reflector [9]

1.3.3 Central Receiver

The central receiver consists of a solar Tower and many of big mirrors, called heliostats, which tracks the sun and act as reflectors of the sunlight. The heliostats focus the sunlight on a receiver located on top of the tower, as shown in Fig. (1.7). the existing liquid heats up to temperatures of about 1500 °C [8].
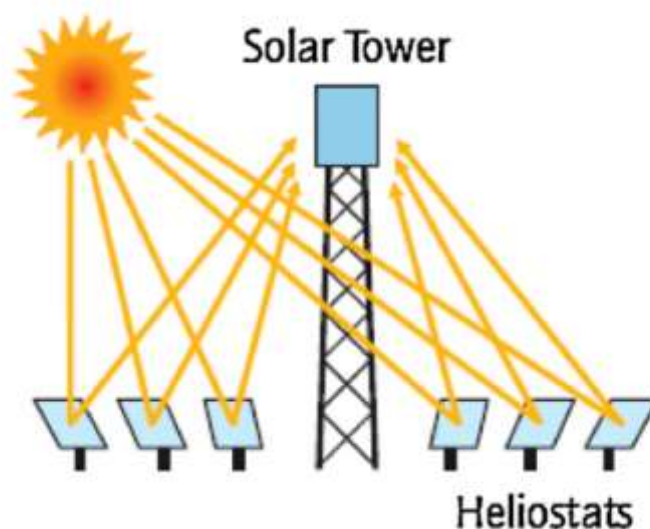
Fig. 1.7: Central receiver [8]

6

1.3.4 Parabolic Dish Collector (PDC)

The parabolic dish collector consists of a parabolic dish-shaped concentrator and a receiver that is placed in the focus to absorb the sunlight reflected on the dish, as shown in Fig. (1.8). The important advantages of PDC systems are their high performance (up to 30%), and modularity (5–50 kW) [9].
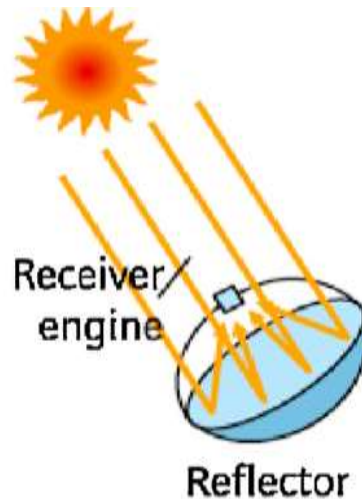
Fig. 1.8: Parabolic dish collector [9]

1.3.5 Fresnel lens Concentrator

Fresnel lens is a solar concentrator with lower volume, lower weight, shorter focal length, and lower manufacturing cost compared to conventional lens [10]. In 1820 Augustin-Jean Fresnel built the first sample, in which the material between the two surfaces was eliminated because the surface consists of a series of concentric grooves, since each groove acts as a single prism.

The angles of the prisms increase as the groove becomes farther from the center. The sunlight passing through each prism is refracted at an angle corresponding to the location of the prism then focuses on a focal point, as shown in Fig. (1.9).

Before the 1950s the lenses were made of glass, then, poly-methyl-meth-acrylate (PMMA) was used to create the lens. The PMMA considered resistant to the side-effects of the sunlight and withstands heat up to 80 °C. the Refractive index of the PMMA lens is 1.49 which considered close to the glass refractive index [11]. In addition, the expected practical life can be up to 30 years [12].
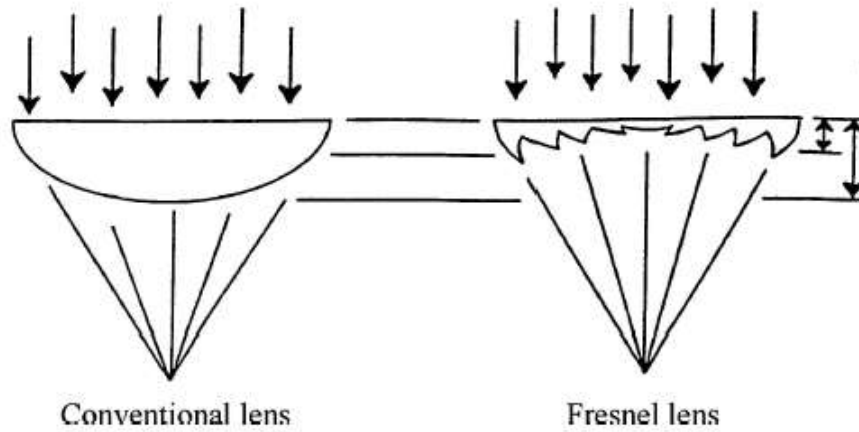
Fig. 1.9: Conventional and a Fresnel lens [7].

There are two Fresnel lens types: Linear and Circular Fresnel lens, described as follows:

Linear Fresnel lens LFL: linear Fresnel lens has a rectangular shape with the grooves formed in parallel lines and a linear focus, as shown in Fig. (1.10-a).

Circular Fresnel lens CFL: In the circular Fresnel lens the grooves are in the form of concentric circles and the focus is in the form of a small circle, as shown in Fig. (1.10-b) [7].

(a)   (b)
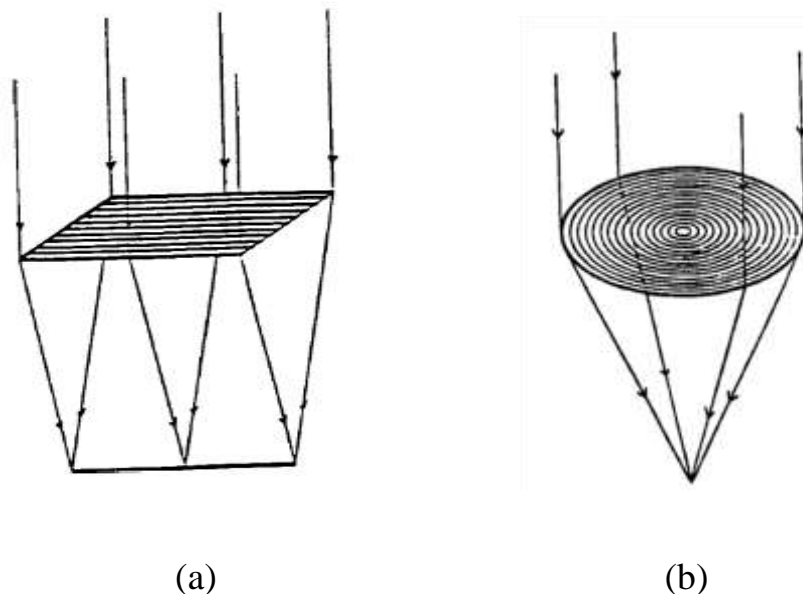
Fig. 1.10: (a) Linear and (b) circular Fresnel

8

1.4 Some Applications of Solar Concentrator

1.4.1 Solar Water Distillation

Water is essential for life for plants, animals and humans. The demand for water for domestic, industrial and agricultural purposes increases significantly due to the large population growth. It is estimated that more than two-thirds of the Earth's surface is known to be filled by water, 97% water on Earth is salt, and 3% fresh water. [13].

Water pollution is due to waste and wastewater, in addition to that the ocean water contains high salinity. In some arid regions the water is scarce and not clean. Therefore, water purification by using solar energy is essential in these areas.

Due to the lack of traditional energy sources in some areas or being expensive, water purification by distillation is one of the most primitive types of water treatment. The treatment process consists of two stages, the evaporation of water by solar energy and condensation of moister air to produce pure water.

The purification of water used in many countries of the world is the solar still device, which has easy steps to manufacture, low maintenance, and economical cost. However, the solar still device has a low productivity [14].

1.4.2 Solar Water Heater

In the last two decades, there has been a significant increase in the use of domestic solar water heater around the world. Solar water heaters are solar thermal applications that convert solar radiation into heat for heating water, cooking, etc. The solar water heater is a reliable process that saves a lot of electricity or fuel. Domestic solar water heating provides close to 60% of the energy needed to heat water annually at household [15].

On the other hand, solar water heaters are used in concentrating solar power plants (CSPPs). Several studies worldwide have shown that the (CSPPs) are economical in generating solar electricity. Where these plants use concentrated solar radiation to achieve the high temperatures needed for processing thermal

power plant dynamics. Which ends with the generation of electrical energy output. The first commercial station was built in California in the late 1980's. In addition, when thermal energy storage (TES) is incorporated into (CSPPs), a great method for converting solar to electricity , which can operate 24 hours a day and seven days a week [3].

1.5 Objectives

The aim of the study is presented in the following:

- Using Fresnel lens to increasing the concentration of solar radiation.
- Using a solar tracking system to be the focal of the sunlight is maintained stationary at a fixed position to ensure continuity of heat flow on the absorption system.
- The experimental rig consists of a freely rotating dual-axis tracking system using two discs to provide an appropriate space in the focus allowing for using various types of thermal applications to benefit from the heat that generated in the focal of the lens.
- Four different applications models are proposed using Fresnel lens concentrator in Iraqi extreme weather.

1.6 Outline of the Thesis

The present thesis is divided into five chapters, as flowing:

- **Chapter one** is a general introduction to the renewable energy, solar radiation resource, solar concentration technology, and finally the Fresnel lens concentrator.
- **Chapter two** presents a review of the literature that is relevant with the topic of the present thesis. These studies include the Fresnel lens concentrator, solar tracking system, solar still, solar water heating.
- **Chapter three** describes the experimental work. A description of the prototype and current apparatus and the solar thermal systems applications.

- **Chapter four** presents the discussion of the experimental results that obtained from various solar thermal systems applications.

- **Chapter five** about the conclusions obtained from the experimental study and provides some recommendations for future

Chapter Two

LITERATURE REVIEW

2. LITERATURE REVIEW

2.1 Introduction

The continuous increase in fossil fuel combustion emissions and the limited resources of conventional fuels are the main driving forces behind efforts to use different energy sources more effectively.

The use of Fresnel lenses for generating electricity and heating water is very powerful equipment for meeting this requirement. Thus, the use of renewable energy is the best option for this reason and has been the subject of research around the world. [16].

In this chapter, works from the literature that study (Fresnel lens, solar tracker, and some applications of solar concentrators) are summaries.

2.2 Fresnel lens

W.T. Xie et. al. (2011) [17] developed and investigated a circular Fresnel lens solar concentrator with different cavity receiver configurations (conical, cylindrical, and spherical receiver), as shown in Fig. (2.1). the prototype collector consisting of high concentration Fresnel lens solar concentrator and a two-axis tracking mechanism.

The different cavity receivers were used to compare the thermal output of the collector. The aperture diameter of all cavities is 50 mm, the vertex angle of the cross-section is set around the conical cavity receiver's symmetrical axis, and a spherical cavity is 60 mm, and the cylindrical cavity depth is set at 50 mm. The result showed that, among the three types of receivers, the best shape was the cone, which has the highest thermal efficiency and the lowest heat loss.

(a)   (b)   (c)
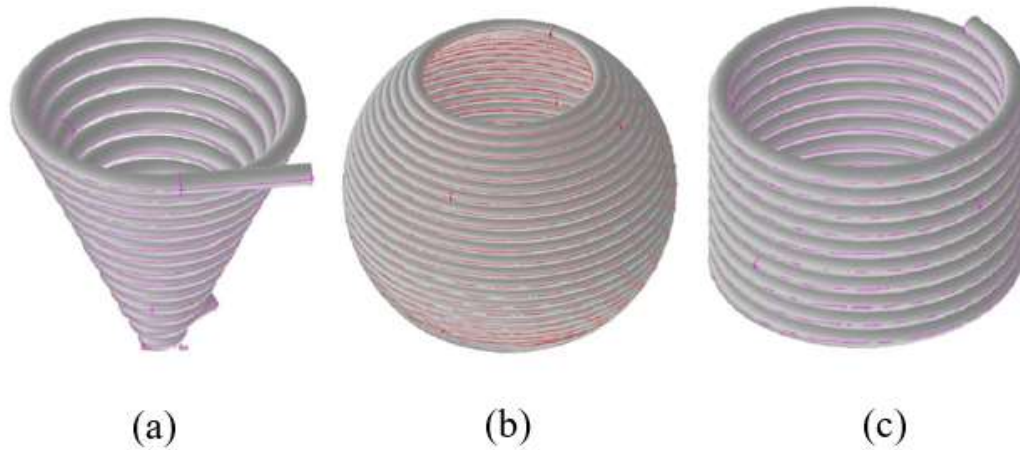
Fig. 2.1: (a) Conical, (b) spherical, and (c)cylindrical cavity receiver [17]

M.M. Valmiki et. al. (2011) [18] presented a circular Fresnel lens as a prototype of a solar cooking stove useful for solar cooking and heating. The stove has a fixed heat area at the focal point of the lens, where the solar tracking device rotates the lens around its focal point, as shown in Fig. (2.2). The tracking is carried out by a rotating motion of two rotating arms holding the lens, and a horizontal rotation of the platform on which the lens system is positioned. The results showed the possibility of obtaining temperatures up to 300 ° C on the stovetop surface. The heat can be used for cooking and internal heating.
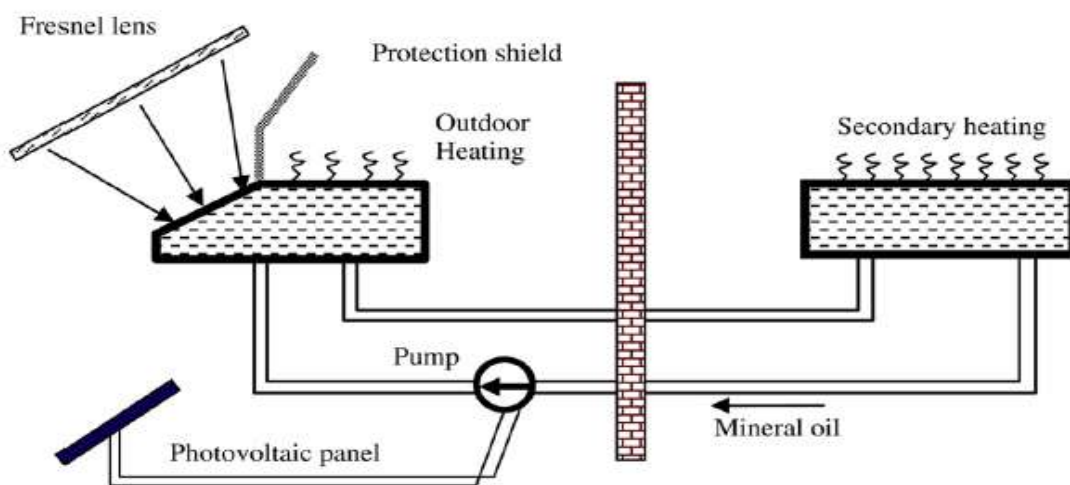
Fig. 2.2: Schematic view of the system [18].

P.J. Sonneveld et. al. (2011) [19] presented a linear Fresnel lens with a concentrated photovoltaic (CPV) system. The goal of the work is to reduce global warming in the summer to reduce the need for cooling. The CPV system absorbs direct solar radiation and allows for the entry of indirect radiation into the greenhouse system. The direct radiation is focused on a photovoltaic/thermal (PV/T) module and converts it into electricity and thermal (hot water) energy, uses a portion of the electricity generated in a tracking system to keep the PV/T module in position. The generated thermal energy can be stored and used for winter heating with a pad and ventilator system or a desalination system as shown in Fig. (2.3).

The result show that the direct radiation resulted in a thermal yield of 56% and an electric yield of 11%. The findings show a promising method for greenhouse system lighting and temperature control, and roof building, simultaneously given that electricity and heat.

Fig. 2.3: Fresnel lenses and modules with PV/T.[19]

Iuliana Soriga, Constantin Neaga (2012) [20] used a linear Fresnel lens solar collector with a cylindrical cavity receiver. The aim of the research is to

calculate the efficiency of the collector using mathematical analysis in Matlab. In the collector being examined, sunlight is centered on the receiver by a linear Fresnel lens to heat up the working substance. The receiver is formed by a copper "U" tube inside a glass vacuum tube, as shown in Fig. (2.4).

The results showed that the design parameters in addition to the effect of the environmental and operational factors on the performance of the collector. In this case, as opposed to the evacuated CPC with the same type of receiver, a higher value for the Fresnel collector output was observed. Though the graphs show clearly the Fresnel collector's supremacy.
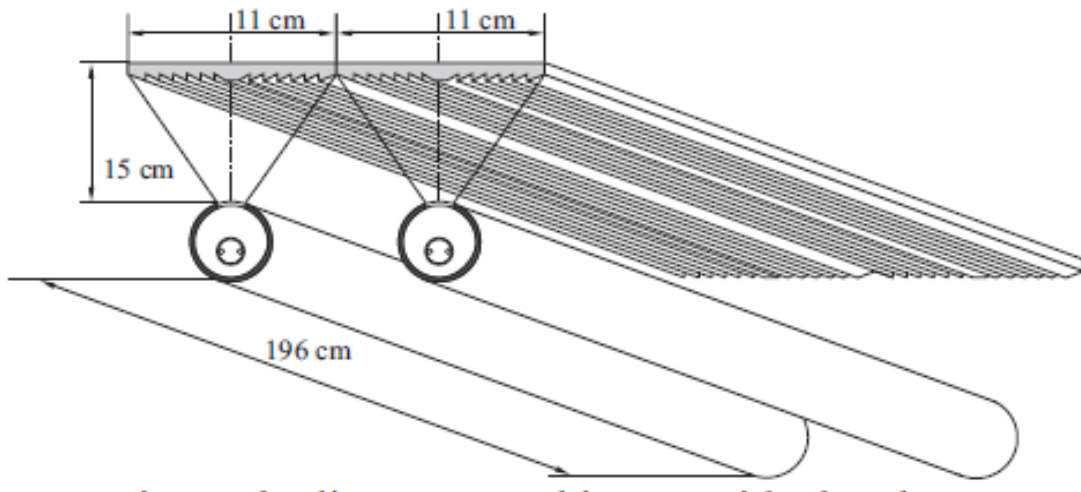
Fig. 2.4: Flat linear Fresnel lenses with absorbers [20].

M. Lin et. al. (2014) [21] presented a linear Fresnel lens solar concentrator with different forms of cavity receiver (triangular, arc cavity, rectangular and semi-circular). The experimental and numerical methods are used to obtain the optimum optical and thermal performance of collector. "five" Small rectangular lenses with inward facing grooves were placed on an stainless-steel frame, each piece of Fresnel lens was 0.4 m long and 0.32 m wide, 0.6 m focal length and 0.001 m prism size, using closed loop, single axis tracking system, as shown in Fig. (2.5). The results showed a better optical and thermal efficiency of the collector with triangular cavity receiver (81.2% and 30% at 120 ℃ respectively) another form of a receiver.

15
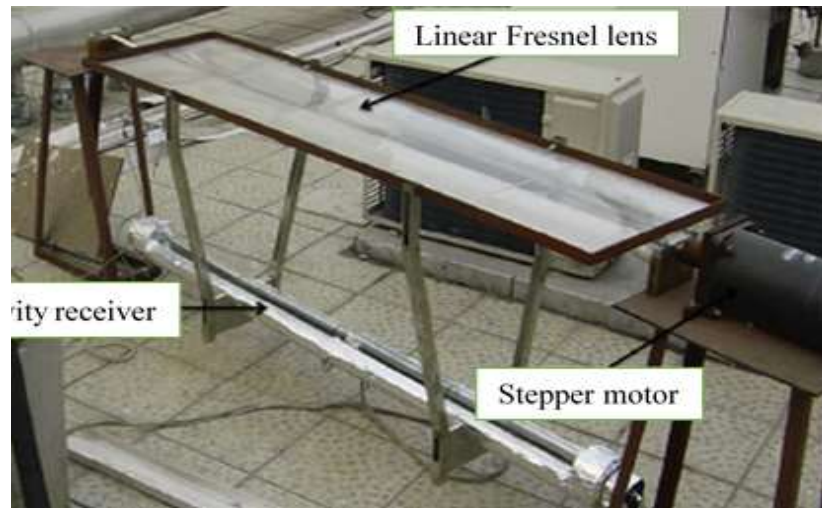
Fig. 2.5: linear Fresnel lens concentrator [21].

T. Prakash Kumar et. al. (2014) [22] developed a Fresnel lens to generate electricity. This model resembles a power plant in a miniature with a Fresnel lens for a heat source and heat exchanger with a heat energy storage tank. The heat that the Fresnel lens produces is used to heat molten salt. The molten salt will be stored in a hot store. Then, this molten salt is transferred to a heat exchanger where it transmits heat to water and turns it into steam. The temperature of the salt in a cold storage tank is then reduced. The salt is pumped from the cold storage tank to the heater, where the salt temperature rises. Steam is used to power a turbine and turbine paired generator that generates electricity, as shown in Fig. (2.6).
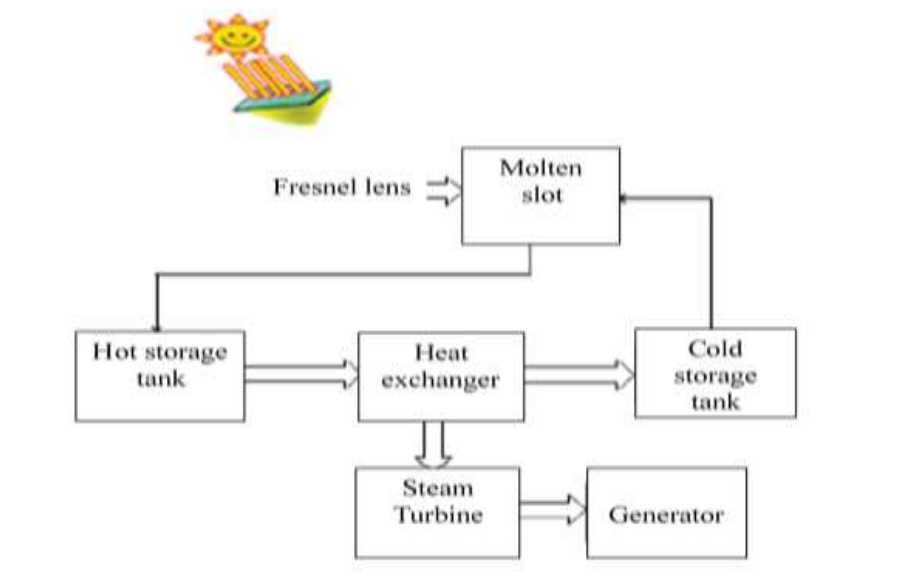
Fig. 2.6: Block diagram representing our prototype [22].

16

M. Hasan Nia et. al. (2014) [11] investigated a circular Fresnel lens with a thermoelectric unit receiver (TE module) for sunlight focuses and electric power generation, respectively. The aim of the work is to generate electricity and heated water, electricity is generated as a result of the heat transfer through the TE module. The solar radiation is concentrated by the Fresnel lens on the oil-filled tanks in the lens focus, as shown in Fig. (2.7). the heat absorbed by the oil is transferred to the water tank connected to the TE module. The results showed that power output is 1.08W with an efficiency of 51.33 % when the intensity of the solar radiation 705.9 W/m^2.

Fig. 2.7: Experimental solar system [11]

M. Imtiaz Hussain et. al. (2015) [12] examined a two types of Fresnel lens collectors, linear Fresnel lens (LFL) and circular Fresnel lens (CFL), to compares the thermal performance characteristics. Both types had the same surface area. The collector's assembly schemes along with a thermally attached storage tanks, 150 L maximum storage capacity, and greenhouses.

The module for greenhouse, thermal storage tank and solar collector was connected through thermally insulated rubber pipes, using programmable, dual axis tracking system, as shown in Fig. (2.8). Two centrifugal pumps were used for each type. The result shows that (CFL) performance is 7-12% higher than (LFL) collector.

(a)   (b)
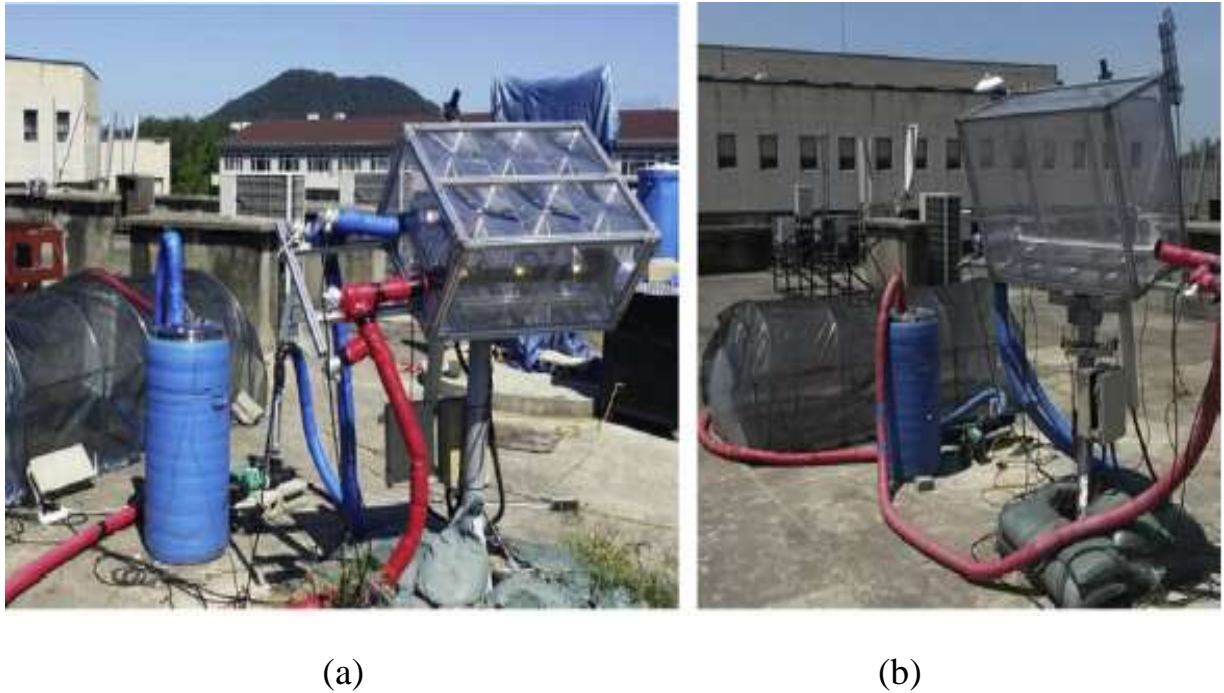
Fig. 2.8: Experimental setup (a) SFL (b) LFL collector system [12].

M. Imtiaz Hussain et. al. (2015) [23] described a circular Fresnel lenses concentrator and U-shaped solar energy receiver with concentrated photovoltaic thermal (CPV/T) to find the maximum possible power generation. The system consisted of eight parts of silicon of glass (SOG) Fresnel lens, a thermal fluid-carrying copper receiver tube and eight triple-junction solar cells against each lens, using dual axis tracking system, as shown in Fig (2.9). The results showed that the energy released depends on the ambient temperature and the intensity of the solar radiation.
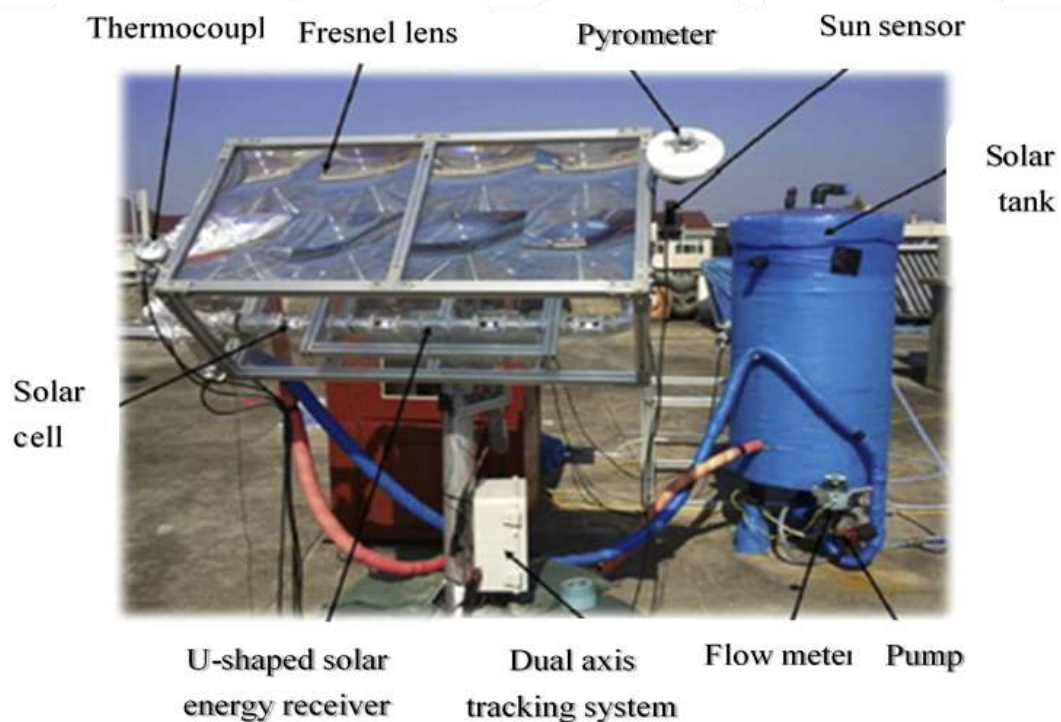
Fig. 2.9: Photograph of experiment setup [23].

Tsung Chieh Cheng et. al. (2016) [24] use a circular Fresnel lens with the sun tracking device and two optical cells are installed to supply the tracking device with electrical power. The device is used in solar thermal applications (such as the Stirling engine). The concentrated solar tracking system of altitude-azimuth type biaxial as shown in Fig. (2.10) the following subsystems are included in this study: solar cells and batteries, control system, structural mechanism, and Fresnel lens.

The results showed that when focusing the sunlight on the Stirling engine's heating head, temperatures of more than 1000 °C were obtained, and it was found that when the intensity of the solar irradiance decreases, it causes a slight decrease in the temperature of the heating head due to the latent heat of copper, as well as a slight loss of heat in the heating head.
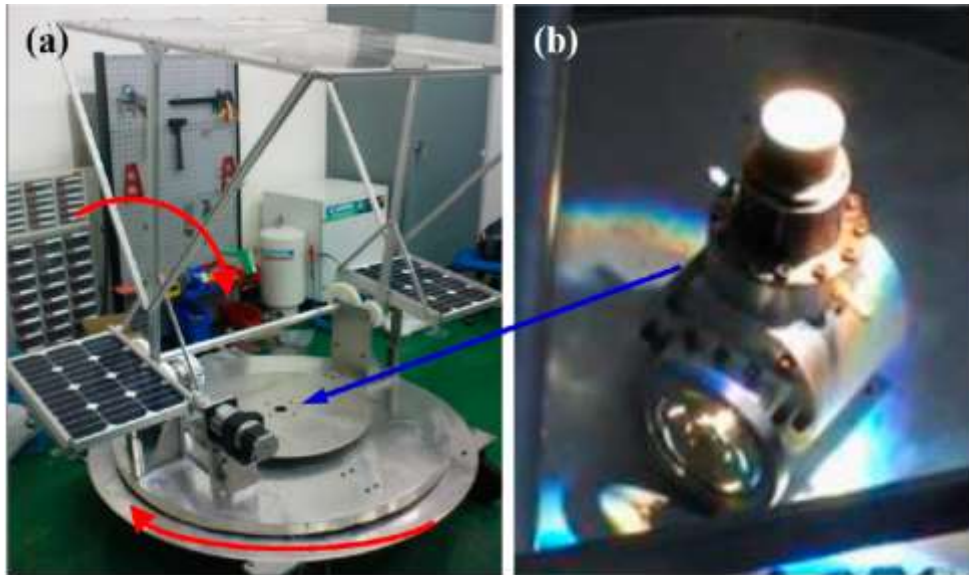
Fig. 2.10: dual-axis tracking system: (a) system photograph; (b) Sunlight focussed on the Stirling engine's heating head in the solar center tracker (arrow pointing) [24].

Simoni Perini et. al. (2017) [25] presented a number of a PMMA Fresnel lens solar concentrator with a receiver pipe heat transfer configuration . It determine the performance of the collector using experiment and theoretical analysis. The concentrator consists of three modules, each module consists of 36 Fresnel lens having a whole aperture area of 75 m^2, the length of each lens is 1 m and width is 0.7 m. The receiver is a 13 meters carbon steel pipe, with closed loop, dual axis tracking system, as shown in Fig. (2.11).

The results showed that the collector's efficiency was limited to less than 20%. The reason for the lower efficiency due to the losses of energy due to the optical loss in the lens and the low solar absorption of the receiver pipe [25].

Figure 2.11 Experimental test scheme at Bourne, UK .[25]

Nawar Saif Al-Dohani1 et. al. (2018) [26] developed a Fresnel lens to generate steam and electricity. The device consists of a Fresnel lens with a heat exchanger. The heat produced from a focal point of the Fresnel lens is concentrated into the heat exchanger, and the molten salt in a heat exchanger is melted and transfers the heat to the water. Thus, steam is generated, and the resulting steam is used to spin the engine along with a generator as shown in Fig. (2.12).

The maximum power output of 30W was produced at 700W/m^2 is reasonable compared to the size of the Fresnel lens and the amount of steam generated.
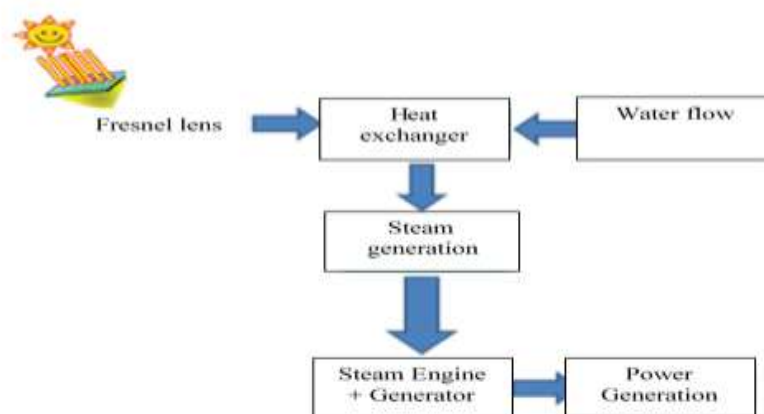
Fig. 2.12: Block diagram of Fresnel power house [26].

Krzysztof Sornek et. al. (2018) [27] improved the efficiency of the photovoltaic modules by using Fresnel lens. The experimental part of this study was performed using a linear Fresnel lens (75 x 50 cm dimensions) with a 20 W photovoltaic cell characterization was a 12-volt open circuit voltage and a short circuit current of 1.27 A (with dimensions of 45 x 34 cm), as shown in Fig. (2.13). The aim of the research is to improve the efficiency of the PV unit. The results show that the performance of the tested PV unit increased by approximately 7%.

Fig. 2.13: The configuration of the rig[27].

2.3 Solar Tracker Design

The output power produced by solar concentrator's or photovoltaic systems is related to the amount of solar energy obtained by the device, therefore it is necessary to track the sun's location with a high degree of precision.

The solar tracker is a device that tracks the sun wherever you go in the sky with the payload on it. This payload may be a solar cell or solar concentrate. There are two main types of solar tracking systems, which are single-axis solar tracking systems and dual-axis solar tracking systems based on their movement degrees of

freedom, [28]. The Solar tracking system can be categorized, dependent on their type of signal operation, as either closed-loop or open-loop type, [29]. A review of various types of solar tracking systems with solar concentrators is presented in Table 2.1.

Table 2.1 Review for various types of solar tracker with solar concentrators

Ref.	Researcher name	year	Application type
[30]	Palavras, Bakos	2006	Dish solar concentrator with flat aluminum plate absorber. Using sensors-electronic circuit and dual axis tracking system.
[31]	Kosuke, et. al.	2006	Heliostat with screen placed at 70 m from heliostat, With photo-sensor and dual axis tracking system.
[32]	Hassanain , Hayder	2011	Parabolic solar concentrator with stainless steel arc receiver, With Automatic east-west rotation tracking and manually north-south rotation.
[33]	Venegas, et. al.	2012	Parabolic trough concentrator with receiver tube unshielded and without a glass cover. With LABVIEW interface and single axis tracking system.
[34]	Fareed, et. al.	2012	Dish solar concentrator with cavity receiver. Using sun light tracking circuit system.
[35]	Xiaoshan, et. al.	2013	Large dish solar collector, with programmable logic controller and dual axis tracking system.
[36]	Jafari, et. al.	2015	Parabolic trough collector with pipe receiver. with microcontroller polar N–S axis, mechanism E–W tracking system

[37]	Pallavi, et. al.	2016	Parabolic dish concentrator. Using Arduino unit for automatic control and dual axis racking system.

2.4 Some Applications of Solar Concentrators

A review of various types of solar concentrator applications is presented in Table 2.1. Solar concentrators typically fall into two broad categories: type concentrated and type non-concentrated. The two most commonly used non-concentrating forms are the flat plate collectors and evacuated tube collectors.

The concentrated type generally employs parabolic, mirrors, and lens to focus on the collector surface of the total solar energy incident. So the surface of the collector is typically very large and the achieved temperature is very high. Some of the collectors are parabolic troughs, parabolic dish, Fresnel lens in this group [38].

Table 2.2. Review for various types of solar concentrators applications

Ref.	Researcher name	year	Application type
[39]	Ramalingam and Marimuthu	2011	Parabolic dish solar concentrator with flat surface absorption receiver. the efficiency is 63.3% for the straight flow path receiver with 80L/h, and the efficiency is 67.1 % for the curved flow path receiver during the 110 L/h
[40]	Atul A. Sagade	2013	Parabolic solar collector and a new helical coiled receiver in the form of a cone. the efficiency is 48.36% with a flow rate of 0.0076 kg/ s.

[41]	Arunkumar, et. al.	2013	Concentrator coupled with hemispherical basin solar still with and without PCM. the productivity is 4.46 L/m^2/day with PCM 3.52 L/m2/day with-out PCM
[42]	Imtiaz, Gwi Hyun	2014	Conical solar water heater (CSWH) , with or without a vacuum glass absorber. the maximum efficiency is 72% and 60% with and without vacuum glass absorber at 6L/min.
[36]	Jafari Mosleh, et. al.	2015	Parabolic through collector combined with a heat pipe and a twin-glass evacuated tube collector. The productivity is 0.27 kg/m^2.h
[43]	Arunkumar, et. al.	2016	Compound parabolic concentrator with tubular solar still (CPC-TSS), The productivity is (1.9 L/m2/day), and compound parabolic concentrator with concentric tubular solar still (CPC-CTSS) (2.5 L/m2/day), and pyramid solar still (2.6 L/m2/day) and single slope (2.9 L/m2/day) solar stills.
[44]	Srithar, et. al.	2016	Triple basin glass solar still (TBSS), and parabolic dish concentrator (PDC). The productivity is 16.94 kg/m^2.day
[45]	Rajamohan, et. al.	2016	Parabolic dish concentrator and conical absorber tube. the efficiency is 65.00 %
[46]	Bin Zou, et. al.	2016	Parabolic trough collector with direct water and a thermal storage tank with insulation. the efficiency is 69%

[47]	Reza, et. al.	2017	Parabolic dish collector (PDC) with cylindrical cavity receiver. Receiver thermal efficiency is 80 to 90%.
[48]	Ramalingam and Marimuthu.	2017	Scheffler parabolic dish and circular tank solar receiver with PCM. the efficiency is 45-58% without PCM, efficiency 60-65% with PCM
[49]	Ahmad Sedaghat et. al.	2018	Tank solar still combined with dish solar collector. Productivity is 2.6 L/day

2.5 Summary of Literature Review

Recently, many studies have been accomplished to investigate the effectiveness of solar concentrators to increase the concentration of the solar radiation using a solar tracking system, yet only a limited number mentioned in the literature examined the effect of Fresnel lens concentrator with solar tracking system.

The review of literatures presented in this chapter were classified in three sections for simplicity. Papers published to investigate the use of Fresnel lens were thirteen, of which five were linear type Fresnel lens and seven were circular type. The design of different solar tracker were inspected in ten papers, and twelve papers to investigate some applications of solar concentrators.

This work presents an experimental study of the use of Fresnel lens solar concentrator in the Iraq weather to produce very extreme temperature during wintertime. Two-axis tracking system are used to track the sun and maintain the focal stationary during the day. Various types of thermal applications models are proposed to check the efficacy of the system.

CHAPTER THREE

THEORETICAL STUDY

3. THEORETICAL STUDY

3.1. Introduction

This chapter explains the details of theoretical analysis of the device. The Fresnel lens solar concentrator with several different applications that installed in the focal point will be explain the theoretical analysis, as follows:

3.2 Fresnel lens Concentrator Geometry

The Fresnel lens geometry can be analyzed by calculates the angles of each surface of the prisms. The angles of the prisms increase as the groove becomes farther from the center. The refraction angle of the prisms (β') can be calculates by using the fallowing equation [25]:

$$\beta' = tan^{-1}\left(\frac{H}{f}\right) + \beta \qquad (3.1)$$

Where H is the height of the prism with respect to the reference system and f is the focal length, as shown in Fig. (3.1).

The prisms angle (β') can be calculates According to the Snell's law as follow [25]:

$$\frac{sin\beta}{sin\beta'} = \frac{n'}{n} \qquad (3.2)$$

The parameters n and n' represent the refractive indices for air and PMMA respectively, which equal to 1 for air and 1.49 for PMMA.
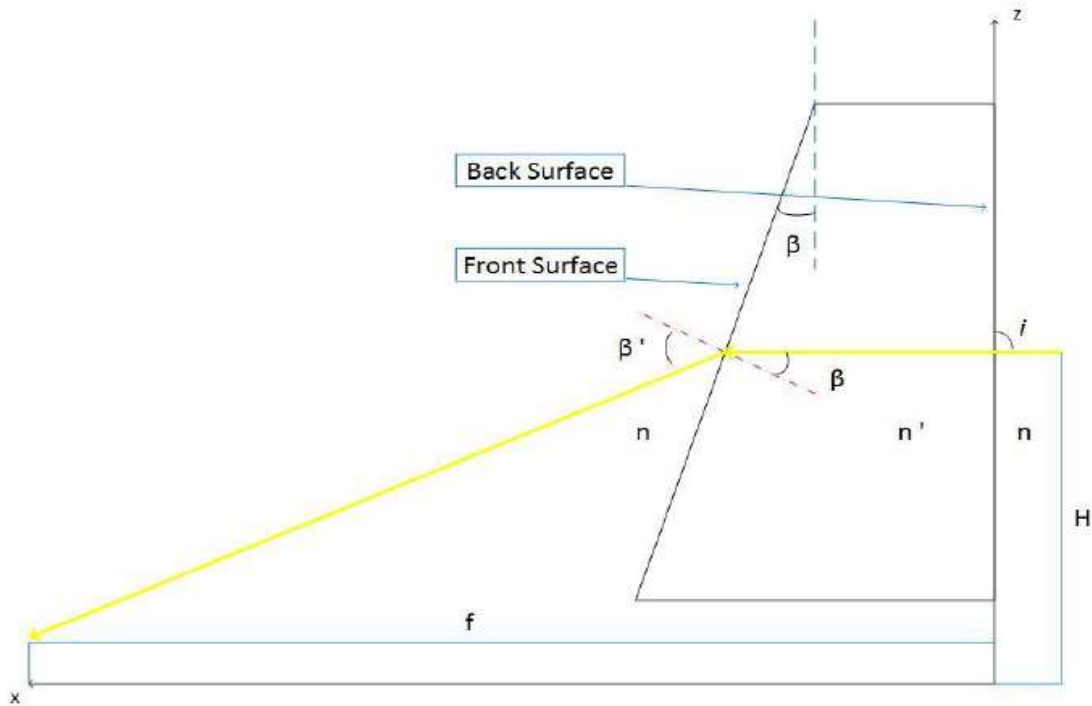
Fig. 3.1: Prims geometry and refraction principle [25].

3.3 The Sun Position

The sun position at a given time can be determined at a specific location of known longitude and latitude. The celestial coordinates needed to determine its position for a given location on Earth are the solar altitude angle (α) and the solar azimuth angle (Z). The time involved is the apparent solar time (AST) to express the time of day for a given location, which describes the exact time of the sun in relation to the local time, and is given by [50]:

$$AST = LST + ET \pm 4(SL - LL) \tag{3.3}$$

Where *LST* is local standard time, *SL* is standard longitude, *LL* is local longitude, and the *ET* is equation of time in minutes and is given by:

$$ET = 9.87 \, sin \, (2B) - 7.53 \, cos \, (B) - 1.5 \, sin \, (B) \tag{3.4}$$

Where

$$B = \frac{(N - 81)360}{364} \tag{3.5}$$

Where (N) is day of the year, and If the location is east of Greenwich, the sign of Eq. (3.1) is minus (-), and if it is west, the sign is plus (+).

The solar altitude angle (α) and solar azimuth angle (Z) are calculated mathematically for each month, day and hour of the year using Eq.3.6 and Eq.3.7 [50]:

$$\sin(\alpha) = \sin(L)\ \sin(\delta) + \cos(L)\cos(\delta)\cos(h) \tag{3.6}$$

$$\sin(Z) = \frac{\cos(\delta)\sin(h)}{\cos(\alpha)} \tag{3.7}$$

Where L is local latitude, δ is solar declination angle, h is hour angle and are given by [50]:

$$\delta = 23.45\sin\left[\frac{(284 + N)360}{365}\right] \tag{3.8}$$

$$h = \pm 0.25 \text{ (Number of minutes from local solar noon)} \tag{3.9}$$

Where the sign of Eq. (3.7) is plus (+) applies to afternoon hours and the sign is minus (-) to morning hours.

3.4 Thermal Analysis for the Solar Still Model

The distillation process consists of two stages, the evaporation of water by solar energy and condensation of moister air to produce pure water. The energy is

transfer from basin to cover occurs by evaporation-condensation in addition to convection and radiation, and from the back of the still to the ground [4].

The energy balance for the water in the basin of solar still per unit area of basin, can be written as [4]:

$$I \, \tau_C \, \alpha_C = q_e + q_{r,b-g} + q_{c,b-g} + q_k + (m \, c_p)_b \frac{dT_b}{dt} \tag{3.10}$$

where e is evaporation-condensation, r is radiation, c is convection, k is conduction, The b and g refer to basin and glazing (cover), τ_C is the transmittance of the cover, α_C absorptance (thermal diffusivity).

The energy balance on the cover can be written as [4]:

$$q_e + q_{r,b-g} + q_{c,b-g} = q_{r,g-a} + q_{c,g-a} \tag{3.11}$$

The radiation exchange between basin and cover is given by :

$$q_{r,b-g} = 0.9\sigma\left(T_b{}^4 - T_g{}^4\right) \tag{3.12}$$

The convection heat transfer between the basin and cover is calculated by:

$$q_{c,b-g} = h_c{}'\left(T_b - T_g\right) \tag{3.13}$$

The convection coefficient in the still $h_c{}'$ is calculated mathematically using Eq.(3.14)

$$h_c{}' = 0.884 \left[(T_b - T \,) + \left(\frac{p_{wb}-p_{wg}}{2016-p_{wg}}\right) T_b \,\right]^{1/3} \tag{3.14}$$

Where p_{wb} and p_{wg} are the vapor pressures of water.

The heat transfer by evaporation-condensation is calculated by:

$$q_e = 9.15 \times 10^{-10} \ h_c'\left(p_{wb} - p_{wg}\right) h_{fg} \tag{3.15}$$

The heat loss to the ground can be written as:

$$q_k = U_G\left(T_b - T_g\right) \tag{3.16}$$

Where U_G is an overall loss coefficient of the still basin.

3.5 Thermal Analysis for the Heat Exchanger Model

The useful heat gain Q_u by the heat transfer flued in the receiver is expressed [48]:

$$Q_u = m^. \ Cp(To - Ti) \tag{3.17}$$

The collector thermal efficiency (η) was computed by the following equation [17]:

$$\text{η} = \frac{m^. \ Cp(To - Ti)}{I \ A} \tag{3.18}$$

Where $m^.$ is mass flow rate of heat transfer fluid in kg/s, Cp is specific heat of fluid at the outlet temperature, T_i is fluid inlet receiver temperature in °C, T_o is fluid outlet receiver temperature in °C, I is direct solar radiation in W/m² and A is the area of the high concentration point focus imaging Fresnel lens in m².

CHAPTER FOUR

EXPEREMANTAL WORK

4. EXPERIMANTAL WORK

4.1 Introduction

This chapter explains the details of the device design. This work presents an experimental study to utilize Fresnel lens to increasing the concentrator of solar radiation using a solar tracking system. The experimental rig consists of a freely rotating two-axis frame that is controlled by an electronic circuit that implements Arduino and stepper motors as a control system to adjust the position of the Fresnel lens focal by moving the motors accordingly. The focal of the sunray is to be maintained stationary at a fixed position to ensure continuity of heat flow on the absorber. Several different applications are used as absorption systems such as solar still, heat exchanger, container tank receiver. The experimental tests are performed with local weather conditions at the Engineering Technical College of Al Najaf, AL- Furat AL-Awsat Technical University located in Najaf - Iraq, at latitude 31.59 degrees north, 44.19 degrees east as shown in Fig. (4.1), thorough details about weather in Najaf city- Iraq from research unit in the college [51].

Fig. 4.1: Location of experimental test

4.2 Apparatus Components

The experimental apparatus consists of two main parts, namely the Fresnel lens solar concentrator and the some applications model of solar concentrators, manufacturing, properties, and operating of each part will be explained as follows:

4.2.1 Fresnel lens Solar Concentrator

The solar concentrator, used in this experiment, is a mechanism that allows a two-axis free motion to track the sunray during daylight. As shown in Fig. (4.2), the Fresnel lens was mounted to an aluminum frame that was connected to a one-direction moving joint (vertical direction) by four arms, which was controlled using a screw rod. When the screw rod moves to the top and bottom, the lens moves in the vertical direction. In order for the lens to be able to move in the second direction (horizontal direction), the moving joint is connected to a moving base. For the apparatuses to be stable, the two bases were placed on a stationary frame.
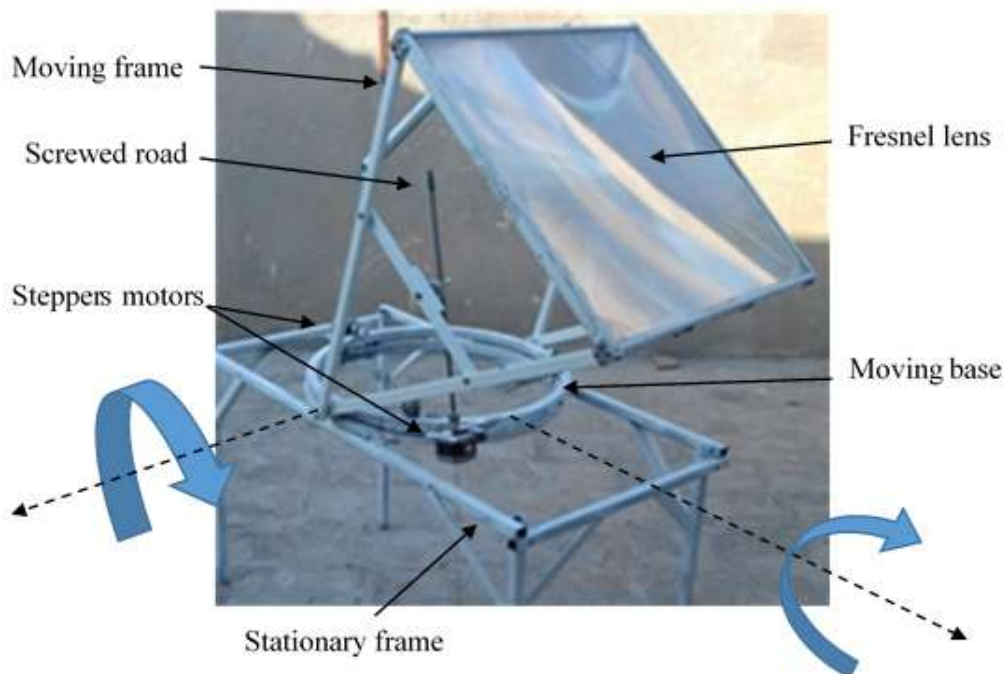
Fig. 4.2: Direct photograph the components of the Fresnel lens solar concentrator

The size of the Fresnel lens plays a crucial role in the amount of heat produced at the focal spot. In this work, the smaller available Fresnel lens is chosen, where a square Fresnel lens with the following specification is used (dimensions: 520 x 520 mm, Focal Length: 620 mm, thickness: 3 mm, Material: Optical PMMA), as shown in table. (4.1). The focal temperature is rather suitable for moderate solar applications in Iraq.

Figure (4.3) illustrates the details of the solar concentrator components, which are two discs and lens frame. The two arcs (fixed arc and rotating arc) are used to rotate the whole assembly towards the sun related to the vertical axes. The arcs were selected to provide an appropriate space in the focus allowing for various types of thermal applications. The outer diameter for each arc was 50 cm and the inner diameter for each arc is 46cm. The fixed arc was connected from the bottom side to a stationary frame and from the upper side was connected to the rotating arc by nine ball bearings to reduce friction between the two arcs. A stepper-motor was used to generate the motion around the vertical axis; the motor was placed on the rotating arc and, by a belt, connected to the fixed arc. The stationary frame was designed to be wide enough to balance the whole assembly while the lens is rotating.

The lens was mounted to a square aluminum frame with a side length of 540 mm; the frame has a rectangular cross-section with a special groove to hold the lens. The aluminum frame was connected to four arms to rotate the lens toward the sun related to the horizontal axes. The length of each arm is (640 mm). The lens frame is rotated toward the sun by using a second stepper-motor. The motor was connected with a rotating arc from one end by using a rotating base and connected to one of the arms by using a screwed rod from the second end. When the lens moves toward the sun, the focal of the sunray is to be maintained stationary at a fixed position.
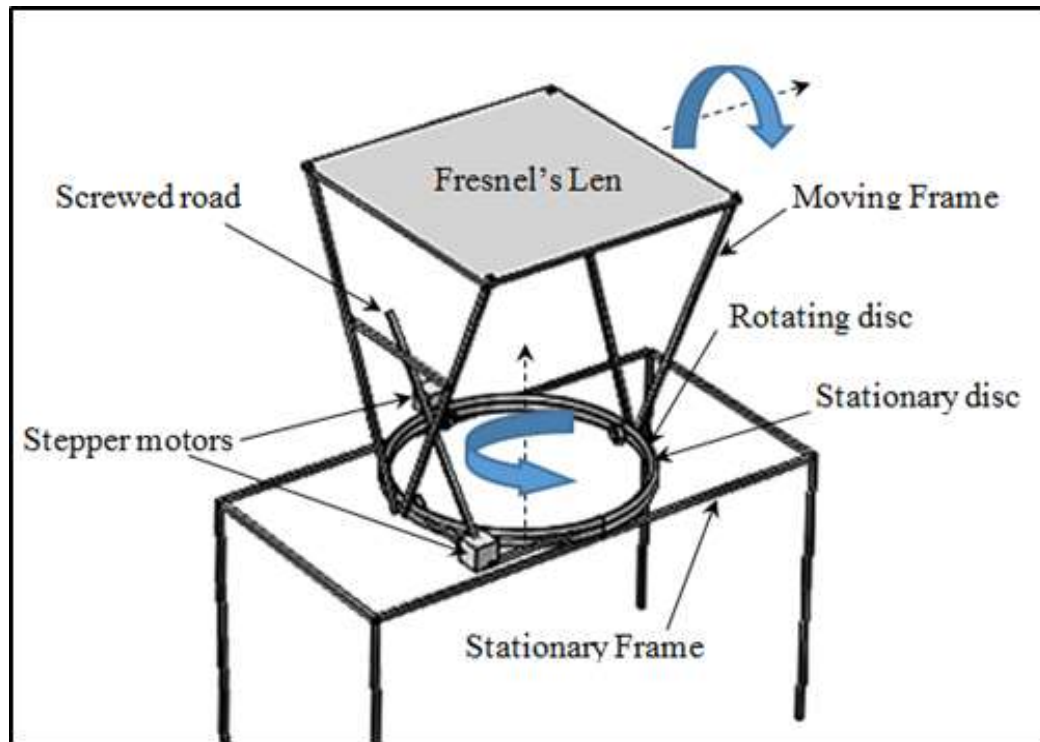
Fig. 4.3: Schematic diagram Fresnel lens solar concentrator

4.2.2 Sun Tracker Control System

The sun path can be tracked efficiently by sensing sunlight to specify the position and direction of the sun. Another way to track the sunlight efficiently is to calculate the position of the sun in the sky via calculation of altitude and azimuth angles for a given region, time and date. In this work, the second approach is used, where a control system is implemented to track the sunlight. The control system consists of a controlling circuit represented by an Arduino unit and two stepper motors to apply the motion to the tracking frame, one motor to move the frame vertically and the other one is to rotate the circular base horizontally. The Arduino unit is programmed such that the altitude and azimuth angles are calculated simultaneously based on the given date and time, as shown in Fig. (4.4). The control system is initiated by feeding the date and time beforehand.

35
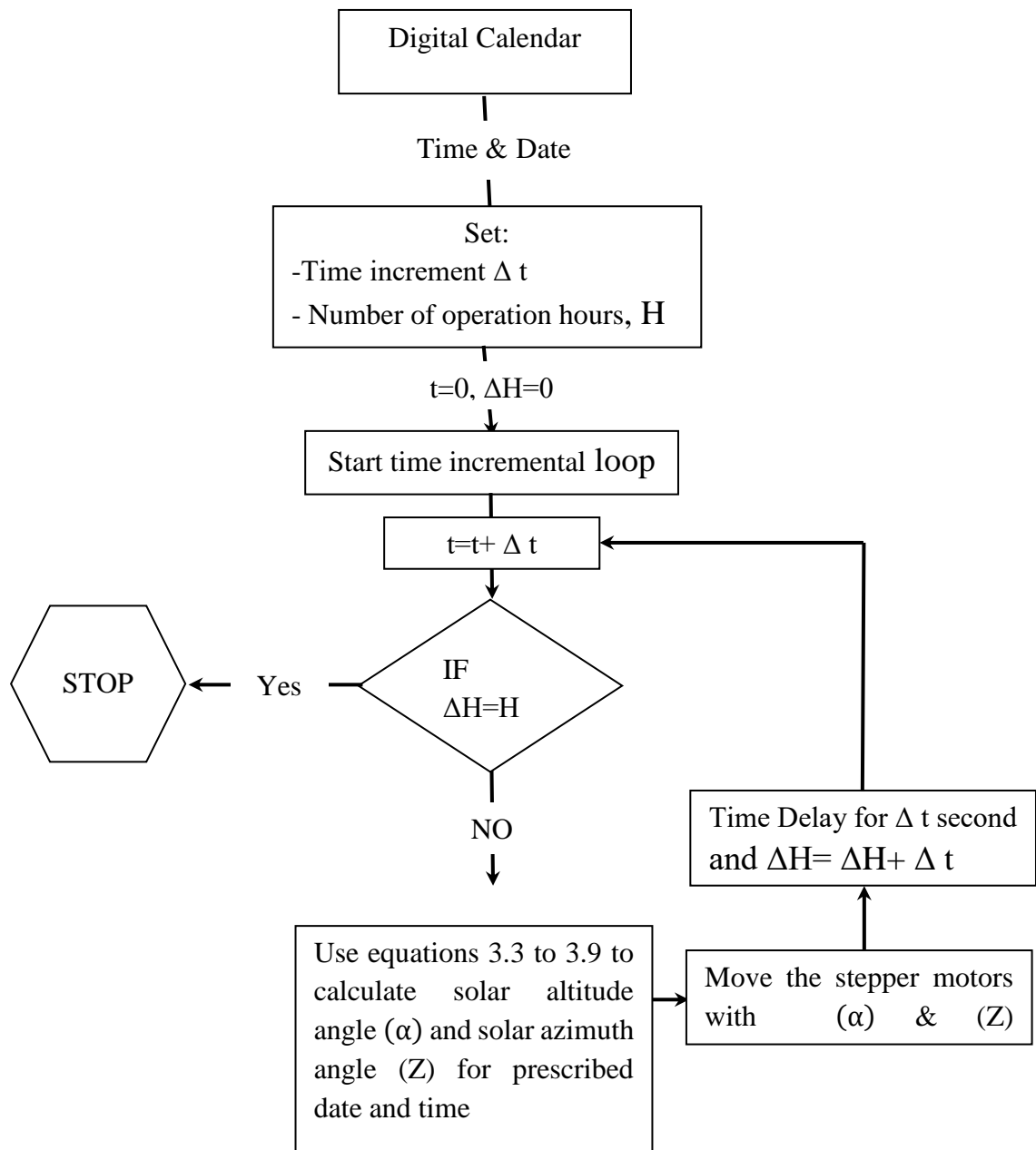
Fig. 4.4: Sun Tracker algorithm flowchart for Arduino control

It is worthy to mention that the tracking system cost can be divided into two costs, namely the initial cost which the price for each components individually where each motor has the pries of 10$, the tracking system frame has 50$ and Arduino has 10$, so the initial cost of the tracking system is 80$. Also there is a daily operating cost the system operate for six hours a day and because it moves every minute for a period of about one second of a motion then the entire

operation period for the two motors is going to be about 45 (3/4=0.75 hour) minutes a day. Moreover, the motor consumes a power of 25W (5V, 5A) hence, the operating cost for two motors is 50 Watt per day.

4.3 Applications Models

The applications consist of different types of solar thermal systems, solar still, heat exchanger, container tank receiver. That can be placed in the focus of the Fresnel lens concentrator to benefit from the continuity of solar heat energy by helping the solar tracking system. Following is a detailed illustration of the applications:

4.3.1 Model I

Two square plates (10 X 10 cm) made of different metals are used to study the thermal characteristics of the heat focal provided by the Fresnel lens. Two different plates are used, namely steel and aluminum, to study the temperature distribution on the plate, as shown in Fig. (4.5). This application can be useful for surface modifications of metallic materials [52].
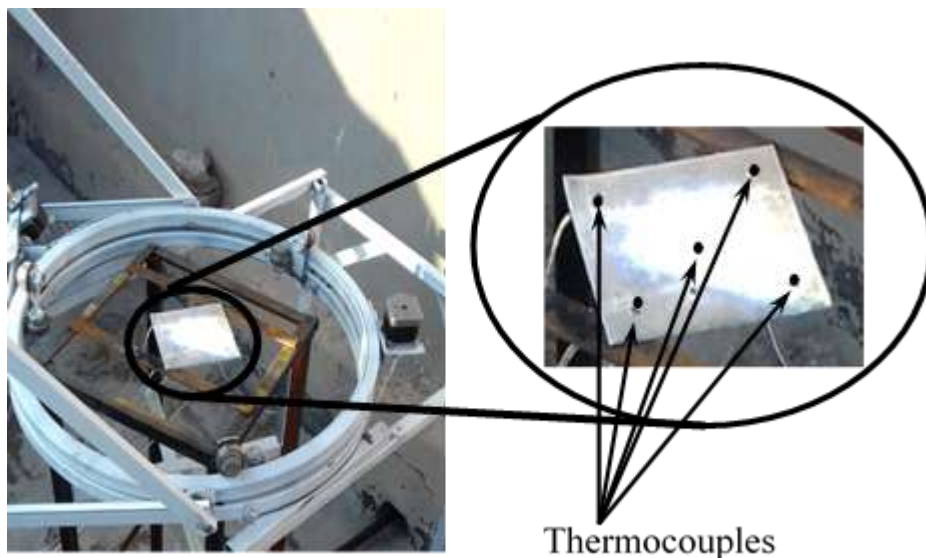
Fig. 4.5: Absorbing plate with the focal of the Fresnel lens and the thermocouples

4.3.2 Model II

The solar still, used in this experiment, is a model placed in the focus of the Fresnel lens concentrator. Two models of a cylindrical with con solar still (10 cm and 20 cm height) were manufactured from a cylinder glass with an angled italic 32 ° glass upper surface, the diameter of the cylinder is 13 cm as shown in Fig. 4.6 (a and b). It is placed in the focus of the lens to receive the refracted solar radiation from the lens. The still was connected with two plastic tubes, the first to inlet saline water and the second tube to outlet freshwater. An aluminum square water container (9x9cm) and height 1 cm, was placed at the still base to absorb the concentrated heat energy. The test was performed by putting the solar still at the lens' focus.

(a)

(b)
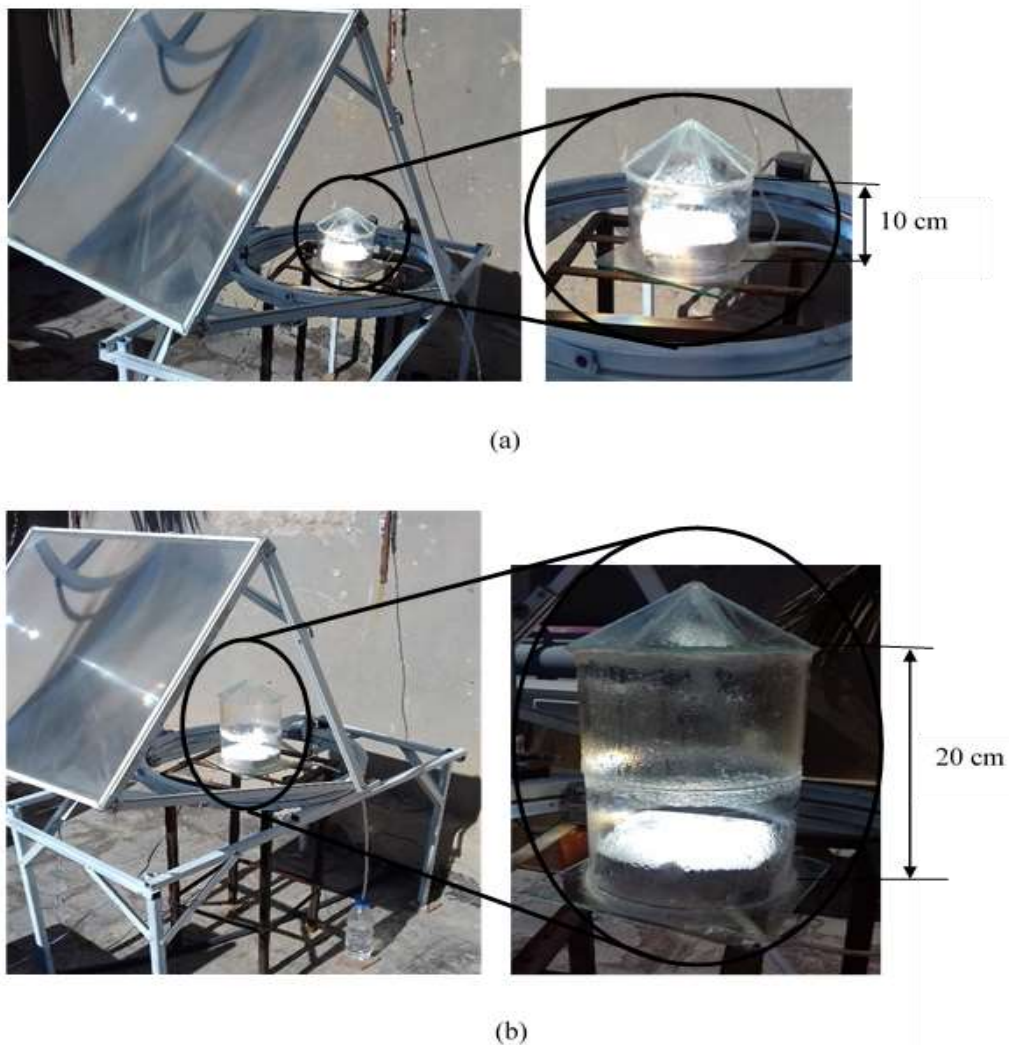
Fig. 4.6: Cylindrical with con solar still; (a) 10 cm height, (b) 20 cm height

4.3.3 Model III

Two models of the heat exchanger receivers are manufactured and tested. The models are conical pipe [17] and cubical tank heat exchangers [48]; both models are used to capture the concentrated thermal energy in the focus. The conical pipe heat exchanger consists of a copper tube with a diameter of 5 mm, twisted in a conical shape with an aperture of an upper diameter of 10 cm, a lower diameter of 4 cm, and a height of 10 cm, as shown in Fig (4.7). The outside of the conical pipe is covered by an aluminum plate with a thickness of 1 mm. Both the conical pipe and the aluminum plate are placed in an aluminum cylindrical container. The receiver is isolated from the surrounding by filling the space between the cylindrical container and the aluminum plate by polyurethane foam, to reduce the thermal loss by convection with the ambient.

The second model is the cubical tank heat exchanger which consists of an aluminum tank of a height of 1 cm, a length of 10 cm, and a width of 10 cm, as shown in Fig (4.8-a). The heat exchanger is provided with a number of internal grooves to circulate the water flow inside the tank, as shown in Fig (4.87-b). The model is painted with black to increase the absorption of solar radiation.
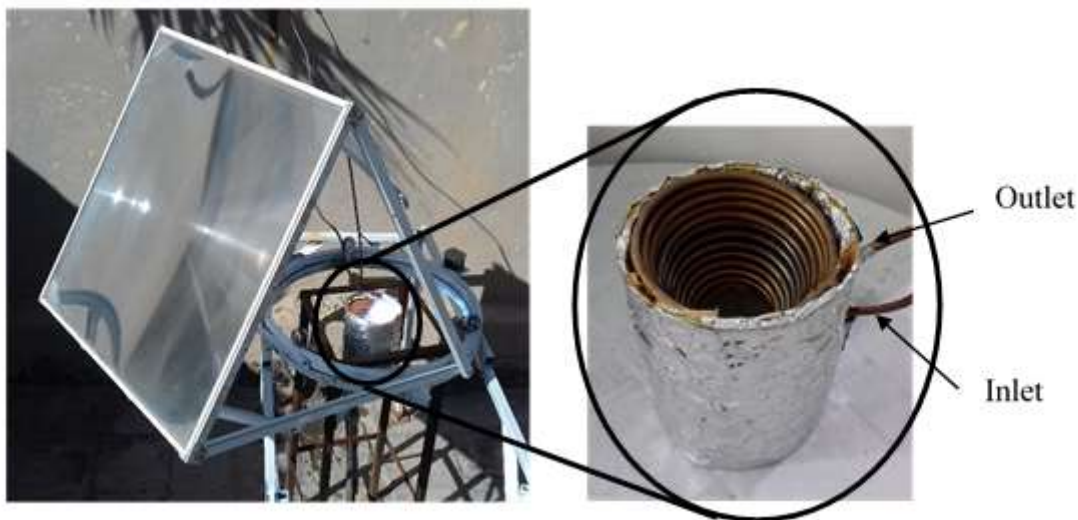
Fig. 4.7: conical pipe heat exchanger model
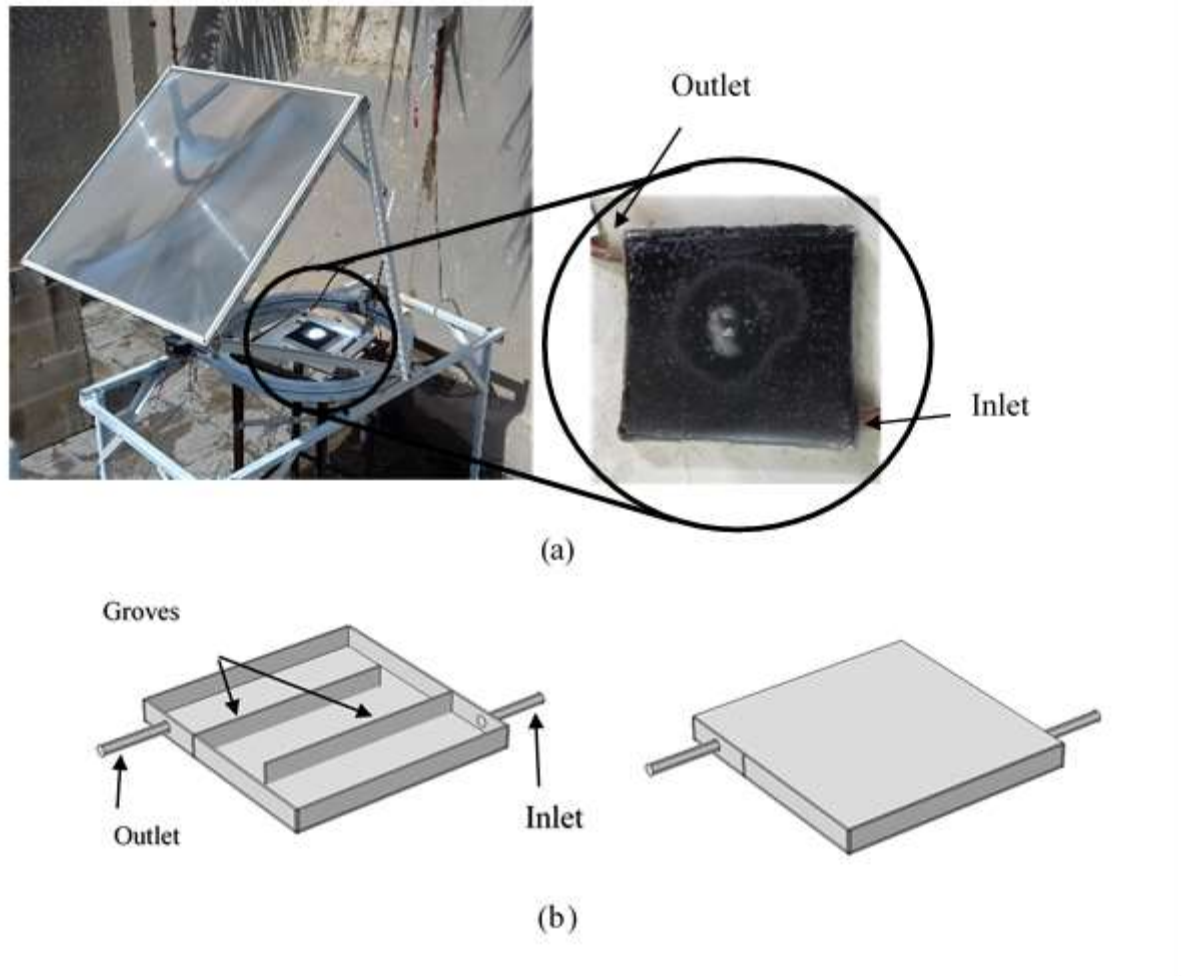
Fig. 4.8: cubical tank heat exchanger model

4.3.4 Model IIII

Cubical steel water tank (20 cm each side) which was manufactured with different metal finned cover is used to study the thermal characteristics of the heat focal provided by Fresnel lens as shown in Fig. (4.9-a). Two different metals finned covers are used, namely steel and aluminum. To study the temperature distribution in the tank, as shown in Fig. (4.9-b). The purpose of using fins is to evaluate the temperature distribution in the (depth) far away from the heat source (plate subjected to focal).

(a)
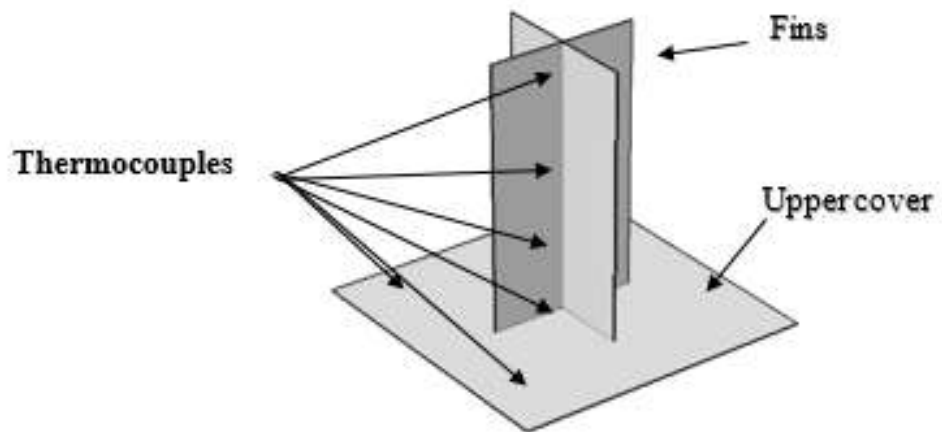
(b)

Fig. 4.9: Container tank receiver; (a) Cubical steel water tank, (b) fins cover.

4.4 Measuring Devices

Table 4.1. Geometrical specification of Fresnel lens concentrator and applications models system

Parameter	Value	Unit
Fresnel lens dimensions	52x52	cm
Fresnel lens Focal length	62	cm

41

Fresnel lens material	Optical PMMA	-
Fresnel lens thickness	0.3	cm
Fresnel lens frame material	Aluminum pipe	-
Fixed arc and rotating arc material	square steel pipe	-
Fixed arc and rotating arc outside diameter	50	cm
Fixed arc and rotating arc thickness	2	cm
Stationary frame thickness	2	cm
Stationary frame material	square steel pipe	-
Cylindrical type solar still diameter	13	cm
Cylindrical type solar still material	glass	-
Conical pipe aperture diameter	10	cm
Pipe coil diameter	0.5	cm
Cubical tank receiver dimensions	10x10x1	cm
Plate receiver dimensions (steel, aluminum)	10x10	Cm
Container tank receiver dimensions	20x20x20	cm
Thermal conductivity of steel	50.2	W/m .k
Thermal conductivity of aluminum	205.0	W/m .k
Thermal conductivity of copper	386.11	W/m .k

4.4.1 Measuring Temperature

To measure the temperature distribution of the receiver, the temperature of water inlet and outlet are obtained by using thermocouples type-K. It has a wide range of measuring the temperature from (-270 to 1260 °C). Thermocouples are joined with data logger temperature modal Applent 32 Channels Temperature Recorder for Heating Appliance (AT4532) with Measurement range (-200 – 1300 °C) and accuracy 0.2% + 1°C as shown in Fig. (4.10-a).

4.4.2 Intensity of Solar Irradiance Measurement

To calculate solar radiation reached on a Fresnel lens (Tenmars TM-207 Solar Power Meter) W/m^2 model is used. It has a range to measure solar intensity from (0 to 2000) W/m^2 as shown in Fig. (4.10-b); the accuracy of solar irradiation is ($\pm 0.5\%$)

(a)   (b)

Fig. 4.10: Measurement system; (a) Temperature meter(data logger) (b) Solar radiation measurement.

Chapter Five

RESULT

AND

DISCUSSIONS

5. RESULT AND DISCUSSIONS

5.1 Introduction

This chapter presents the results obtained from the experiments that were conducted using the Fresnel lens concentrator and the solar tracking system to simulate some applications of solar concentrator. In total, the study includes, three experiments to observe the temperature distribution on the surface of square plates (10×10 cm) made of different metals, six experiments to investigate the productivity of solar distillation for a cylindrical with con type solar still, six experiments to compute the useful heat gain for two types of heat exchangers, and two experiments to study the temperature distribution inside a container. The following is a detailed illustration of the experiments.

5.2 Model I

Practical experiments were conducted during the period 5 - 9 of Dec. 2019 from (9 AM - 3 PM), where the ambient temperature ranged from (12 - 22) °C and the solar radiation ranged from (824 - 1320) W/m^2, as shown in Fig. 5.1 (a and b).

The experiment was performed on 9-Dec.2019, where a square steel plate (10 X 10 cm) is used, and the sky was clear from the clouds and dust. The results are illustrated in Fig. (5.2-a), where the highest recorded temperature is 422 ° C at the center of the plate and 134 ° C at the edge when the intensity of the solar radiation is 1140 W/m^2 and the ambient temperature is 17 ° C. It is clear from Fig. (5.2-a) that the temperatures increase when the intensity of the solar radiation increases [39]. Whereas the temperature decreases significantly when the sky is unclear or cloudy weather, as it can be seen clearly in Fig. (5.2-b) where the test was performed on 5-Dec. 2019, at 11:00 the temperature decreased due to low solar radiation. Observing that, the increase in plate temperature is attributed to

the increase of the amount of solar incident radiation on the plate surface. Because of using the solar concentrator that focuses the sunlight from a large area on a small receiver, which was the result of using the solar tracking system that attributed to increase of solar energy collected, [49].
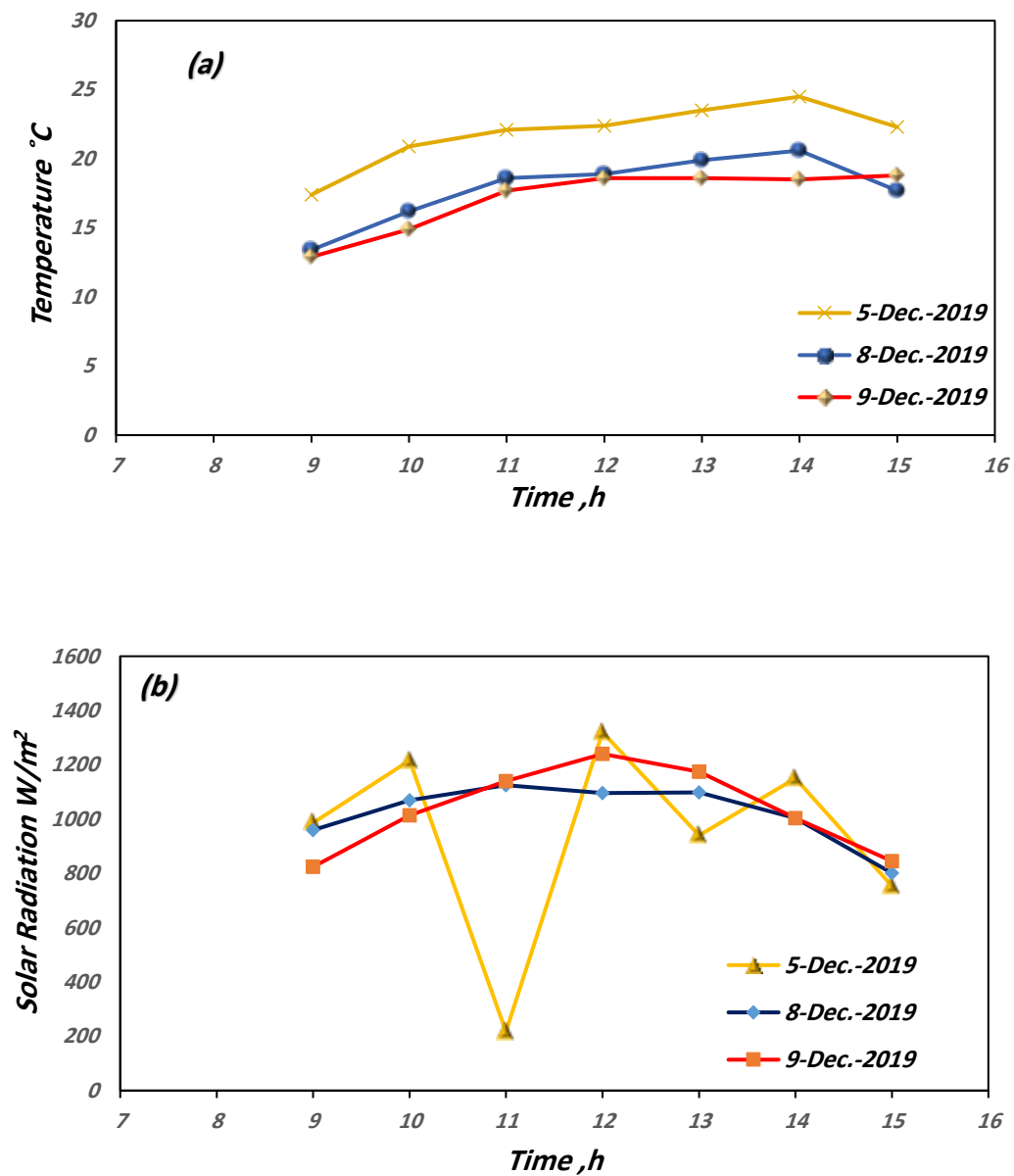
Fig. 5.1: Climatic conditions under which the experiments have been conducted of plate receiver: (a) ambient temperature, and (b) solar radiation, versus time.
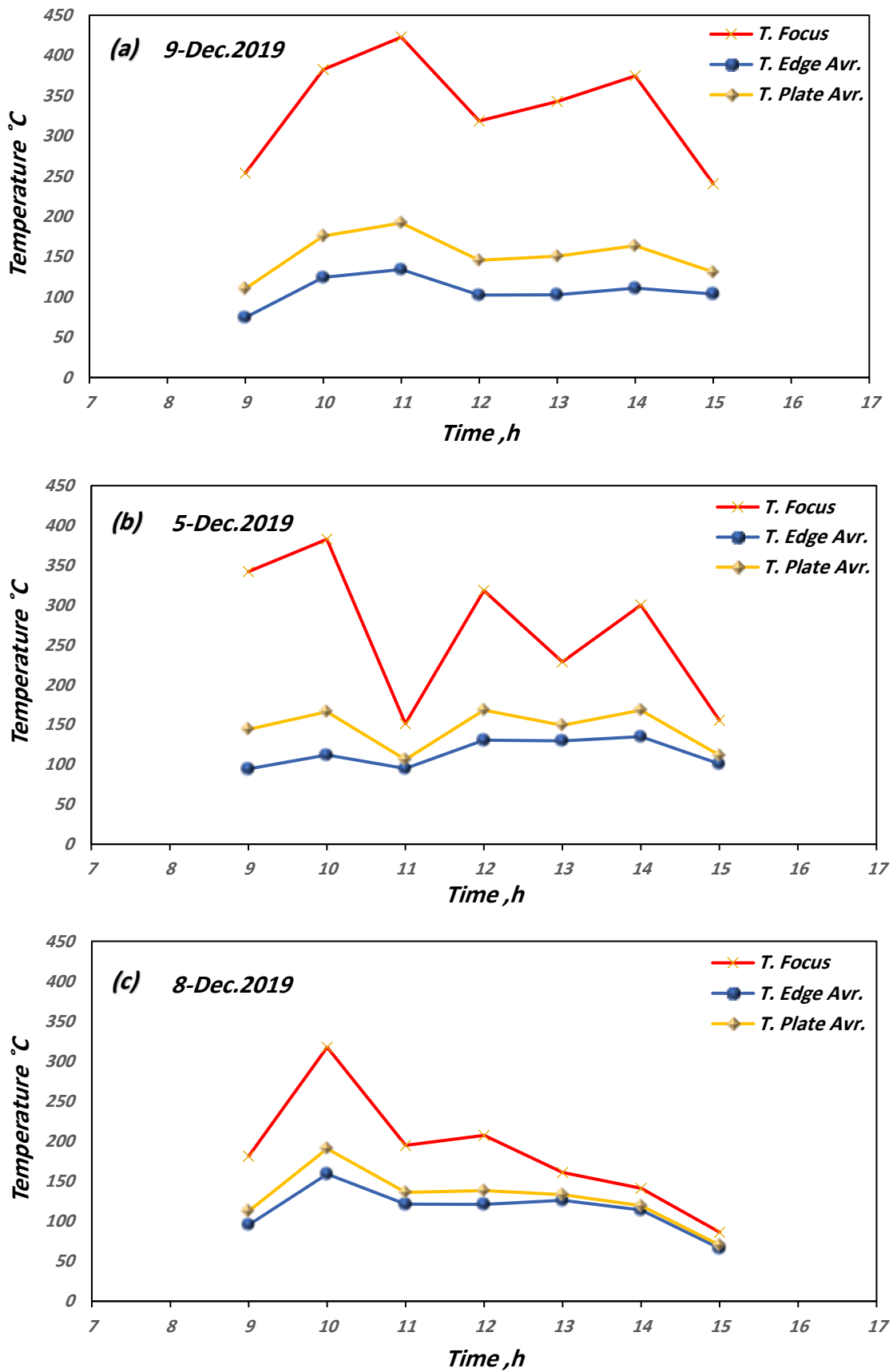
Fig. 5.2: Temperature of focus, edge average, plate average of plate receiver versus time (a) 9-Dec. 2019 (b) 5-Dec. 2019 (c) 8- Dec. 2019.

The same experiment was repeated on 8-Dec. 2019, where a square aluminum plate (10 X 10 cm) is used with the exact distribution and locations of thermocouples. Figure (5.2-c) illustrates the temperature distribution for the aluminum plate where the highest temperature obtained was at the focus which is 317 ° C and 130 °C at the edge when the intensity of the solar radiation is 1069 W/m^2 and the ambient temperature is 16.2 °C. However, it can be noticed that the steel plate recorded higher temperature than the aluminum and that is because of the difference in the coefficient of thermal conductivity which causes more heat dissipation to the surrounding, and also the solar radiation in the aluminum plate test was less, comparing by the other days.

Observing the results in experiments above, it gives an idea of promising abilities to using Fresnel lens in Iraqi weather, which can produce very extreme temperature up to 400 °C during winter time where the concentrator can be utilized efficiently in a wide range of renewable energy applications such as water desalination, water heating, and heat storage. On the other hand, the two-axis tracking system which is modeled and design to track the sun, can be maintain the focal stationary during the day without being affected by the weather condition, it continues to track the sun even when the weather is cloudy.

5.3 Model II

Practical experiments were conducted using cylindrical with con solar stills with different heights, 10 cm, and 20 cm. where in total, the study included six experiments. For the (10 cm height) solar still the experiments were performed three times in three days with similar weather conditions; and a similar procedure was followed for 20 cm height solar still, and the following is a detailed illustration of the experiments:

5.3.1 Solar Still of 10 cm in Height

The experiments were conducted during the period 25-27 of Jan. 2020 from (9AM – 3PM), where the ambient temperature ranged from (5 - 15) °C and the solar radiation ranged from (1150 - 1347) W/m^2 as shown in Fig. 5.3 (a and b). The three experiments were performed by using cylindrical with con solar still and can be summarized as follows:

Table (5.1) Summary of the experimental results for solar still of 10 cm in height

Run	Date (2020)	Weather Conditions	Ambient Temp. min-max °C	Solar Radiation min - max W/m^2	Cumulative Productivity for six hours ml
1	25-Jan	cloudy	7-13	170-1316	200
2	26-Jan	clear	5-15	1160-1347	500
3	27-Jan	clear	8-16	1150-1307	490

The results are summarized in table (5.1) are illustrated in figures 5.3 (a and b) and (5.4), where the Fresnel lens provides sufficient heat to generate steam for distillation from refracted solar radiation. The change in the amount of solar radiation affects the productivity of the freshwater. The greatest amount of freshwater production was on Jan-26 when the solar radiation was at its highest where the sky was clear (no clouds or dust). While the productivity of freshwater decreases when the intensity of the solar radiation decreases due to the unclear sky or cloudy weather [49], as it can be seen clearly where the test was performed on 25-Jan the cumulative productivity for six hours of fresh water was only 200ml, however this is not always true since most of the time the weather is sunny in Iraq.

Fig. 5.3: Climatic conditions under which the experiments have been conducted for solar still with 10 cm height : (a) ambient temperature, and (b) solar adiation, versus time.

Fig. 5.4: Cumulative productivity for six hours for solar still of 10 cm height.

49

5.3.2 Solar Still of 20 cm in Height

      The experiments were conducted during the period 30- Jan. through 1⁻ Feb. 2020 from (9AM - 3 PM), where the ambient temperature ranged from (8 - 21) °C and the solar radiation ranged from (980 – 1301) W/m², as shown in Fig. 5.5 (a and b). The three experiments were performed by using cylindrical with con solar still and can be summarized as follows:

Table (5.2) Summary of the experimental results for solar still of 20 cm in height

Run	Date (2020)	Weather Conditions	Ambient Temp. Min-Max °C	Solar Radiation Min - Max W/m²	Cumulative Productivity for six hours ml
1	30-Jan	cloudy	10-19	635-1010	350
2	31-Jan	clear	12-21	980-1278	500
3	1-Feb	Partial cloudy	8-16	420-1301	490

      The results are summarized in table (5.2) are illustrated in figures 5.5 (a and b) and (5.6). Where the greatest amount of fresh water cumulative productivity for six hours on Jan-31 is 500 ml, and the lowest amount on Jan-30 is 350 ml. This difference is caused by the variation in the intensity of solar radiation, which influences the evaporation process. Therefore, the amount of freshwater production is directly proportional to the intensity of solar radiation [53].
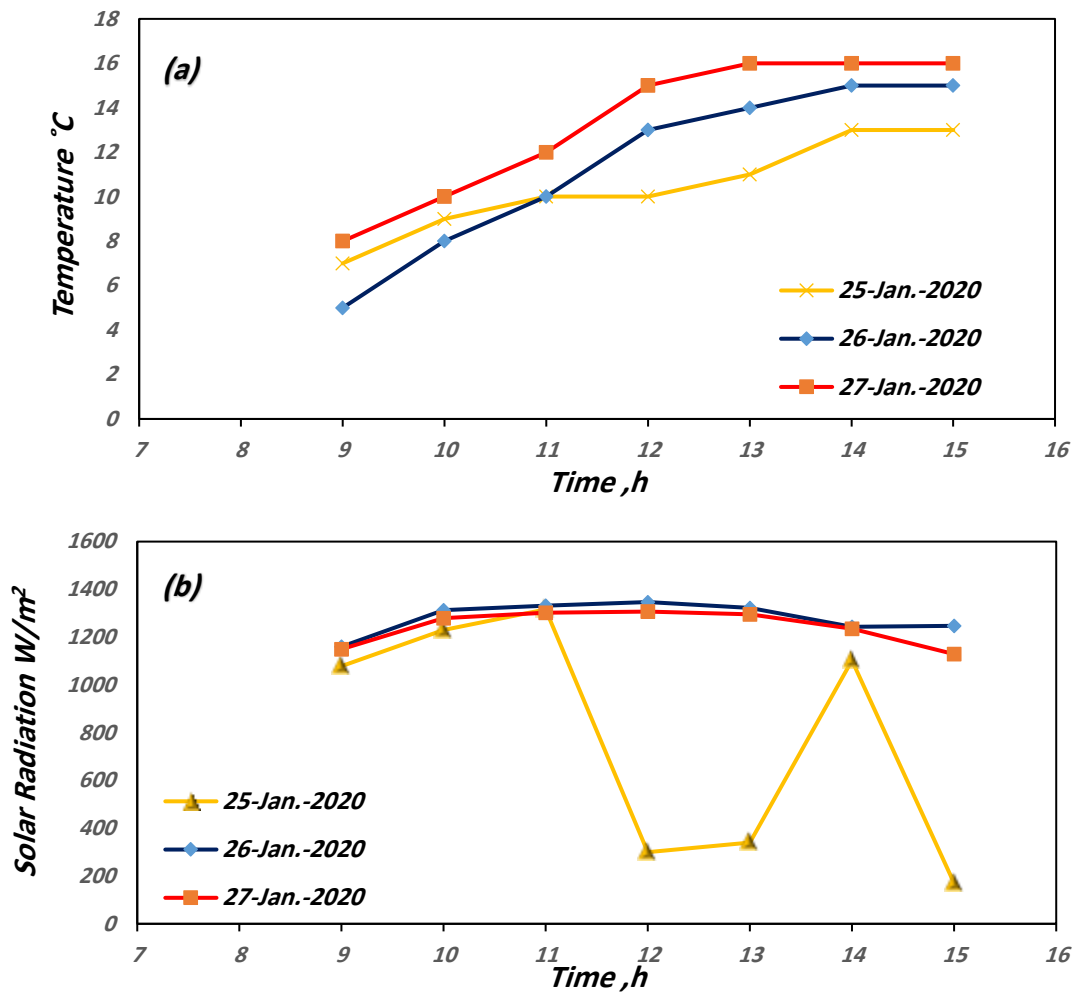
Fig. 5.5: Climatic conditions under which the experiments have been conducted of Solar still with 20 cm height: (a) ambient temperature, and (b) solar radiation, versus time.
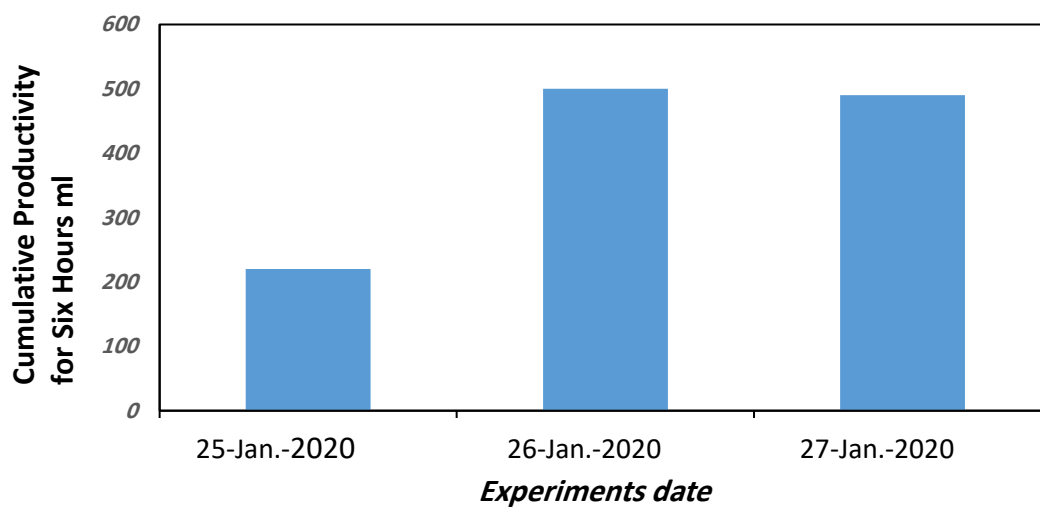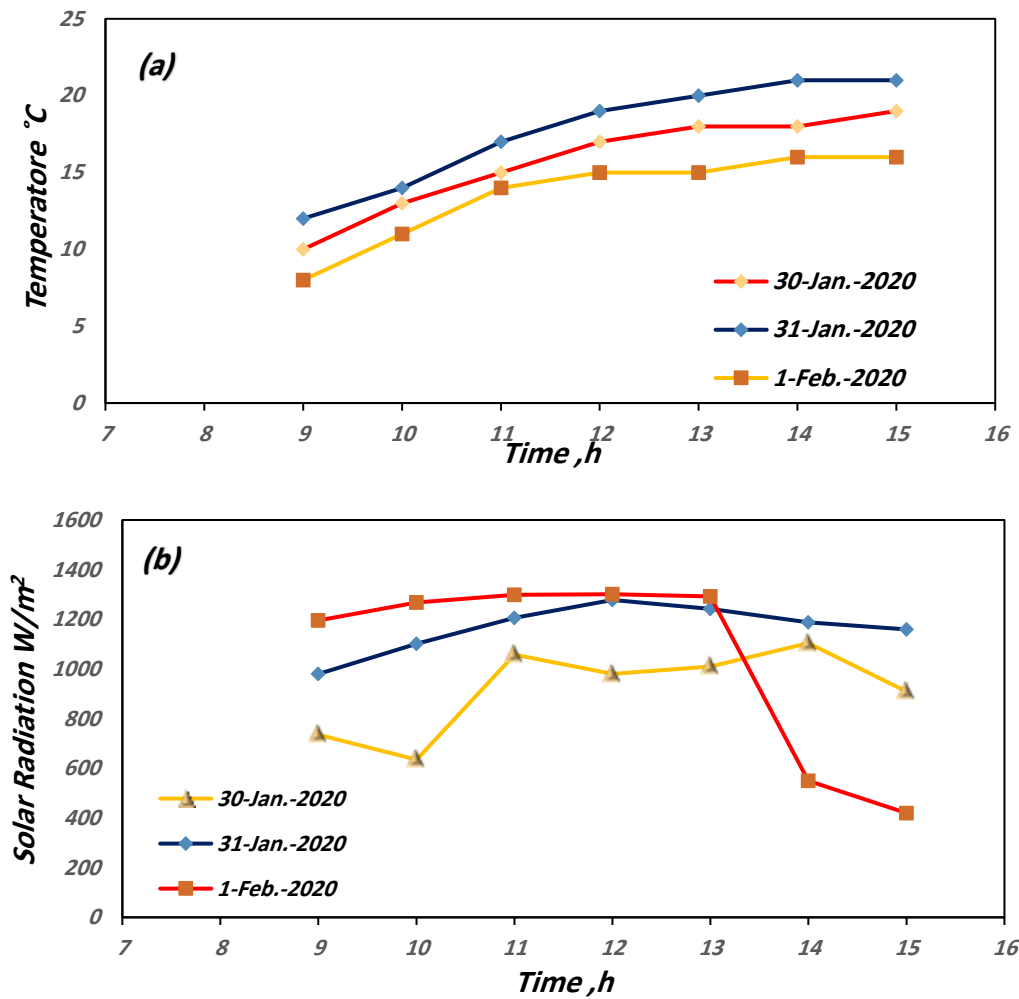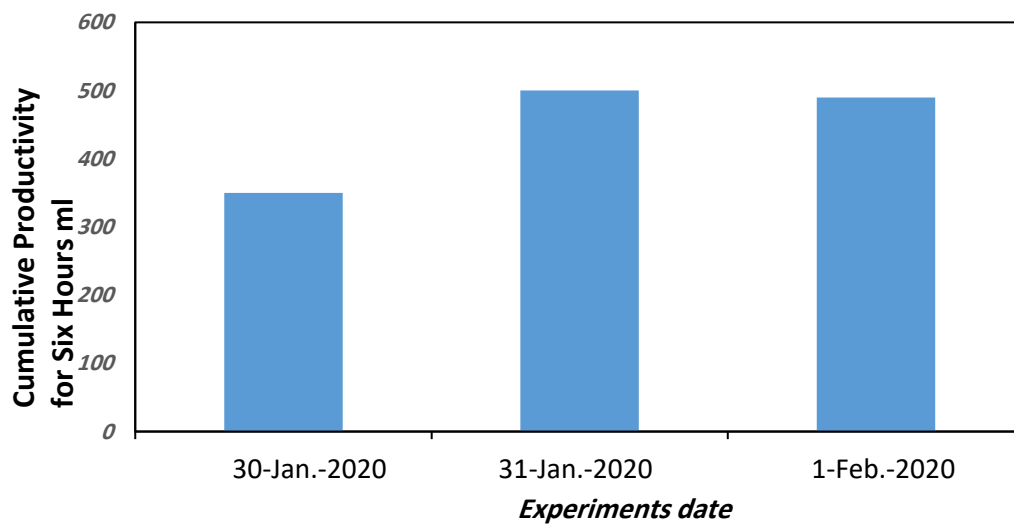

Fig. 5.6 : Cumulative productivity for six hours for solar still with 20 cm height.

In the experiments, focus in the main parameter investigated was the height of the solar still, we nominate the two values of the height 10 and 20 cm, respectively which implies the change of condensation area where the side area is doubled. As previously mentioned, the experiments were performed in six consecutive days so that the other contributing parameters, such as ambient temperature and solar radiation, will be in the same range. The results showed that the productivity of the solar still increased as the solar radiation increased. On the other hand, productivity is influenced by the height of the solar still and ambient temperature. However, the main parameter that affects productivity is the amount of solar radiation which has significant influence on the performance of solar still.

In solar stills, the area of condensation and temperature difference over the condensation glass cover surfaces play crucial roles in the productivity of the solar still. In this work the area was doubled in sake of showing that the increasing of the condensation area would cause a sensible difference in the results. The prototype can be modified to include a glass dome of a large area that is mounted on the top of the cylindrical with con solar still to ensure better condensation. Moreover, the amount of the water at the base of solar still can be decreased so as to improve the chance of evaporation with presence of extreme temperature produced by the focal of the Fresnel lens.

5.4 Model III

Practical experiments were conducted using two models of heat exchangers, namely conical pipe and cubical tank heat exchangers. In total, the study included six tests. For conical pipe heat exchanger, the experiment was performed three times in three consecutive days with different water flow rates (1, 2 and 4 L/h, respectively), and similar procedure was followed for cubical tank heat exchanger. The data was collected using two thermocouples type-K that are installed on the inlet and outlet pipes of the receivers. The temperature

measurement is recorded by means of a digital data logger and the experiments are performed as follows:

5.4.1 Conical Pipe Heat Exchanger

Practical experiments were conducted during the period 13-15 of Feb. 2020 from (9 AM - 3 PM), where the ambient temperature ranged from (8 – 19) °C and the solar radiation ranged from (950 – 1353) W/m^2, as shown in Fig. 5.7 (a and b).

Fig. 5.7: Climatic conditions under which the experiments have been conducted of conical pipe heat exchanger: (a) ambient temperature, and (b) solar radiation, versus time.

Figure (5.8-a) shows the relationship between the temperature of water inlet, outlet and useful heat gain versus time for the conical pipe heat exchanger at water flow rate was 2 *L/h* during the 13[-] Feb. 2020 , where the ambient temperature ranged from (8 – 16) °C and solar radiation in W/m^2 ranged from (950 – 1311). The average inlet water temperature is 14.2 °C and the average water outlet temperature is 41 °C. Useful heat gain ranged from (48 – 69) W. results were compared with the researchers Simoni Perini et. al. [25]

Figure (5.8-b) shows the relation between the temperature of water inlet, outlet and useful heat gain versus time for the conical pipe heat exchanger at water flow rate was 4 *L/h* during the 14[-]Feb. 2020 , where the ambient temperature ranged from (9 – 19) °C and the solar radiation in W/m^2 ranged from (972 – 1220). The average inlet water temperature is 15.7 °C and the average water outlet temperature is 32 °C. Useful heat gain ranged from (64 – 92) W.

Figure (5.8-c) shows the relationship between the temperature of water inlet, outlet and useful heat gain versus time for the conical pipe heat exchanger at water flow rate was 1 L/h during 15-Feb. 2020, where the ambient temperature ranged from (10 -19) °C and the solar radiation in W/m^2 ranged from (902 – 1353). The average inlet water temperature is 15 °C and the average water outlet temperature is 71°C. useful heat gain ranged from (43 – 80) W. Noting that at 14:00 the sky turned partially cloudy resulting in a reduction in amount of solar radiation to 982 W/m^2 causing a decrease in temperature of the water outlet to 69°C.

54
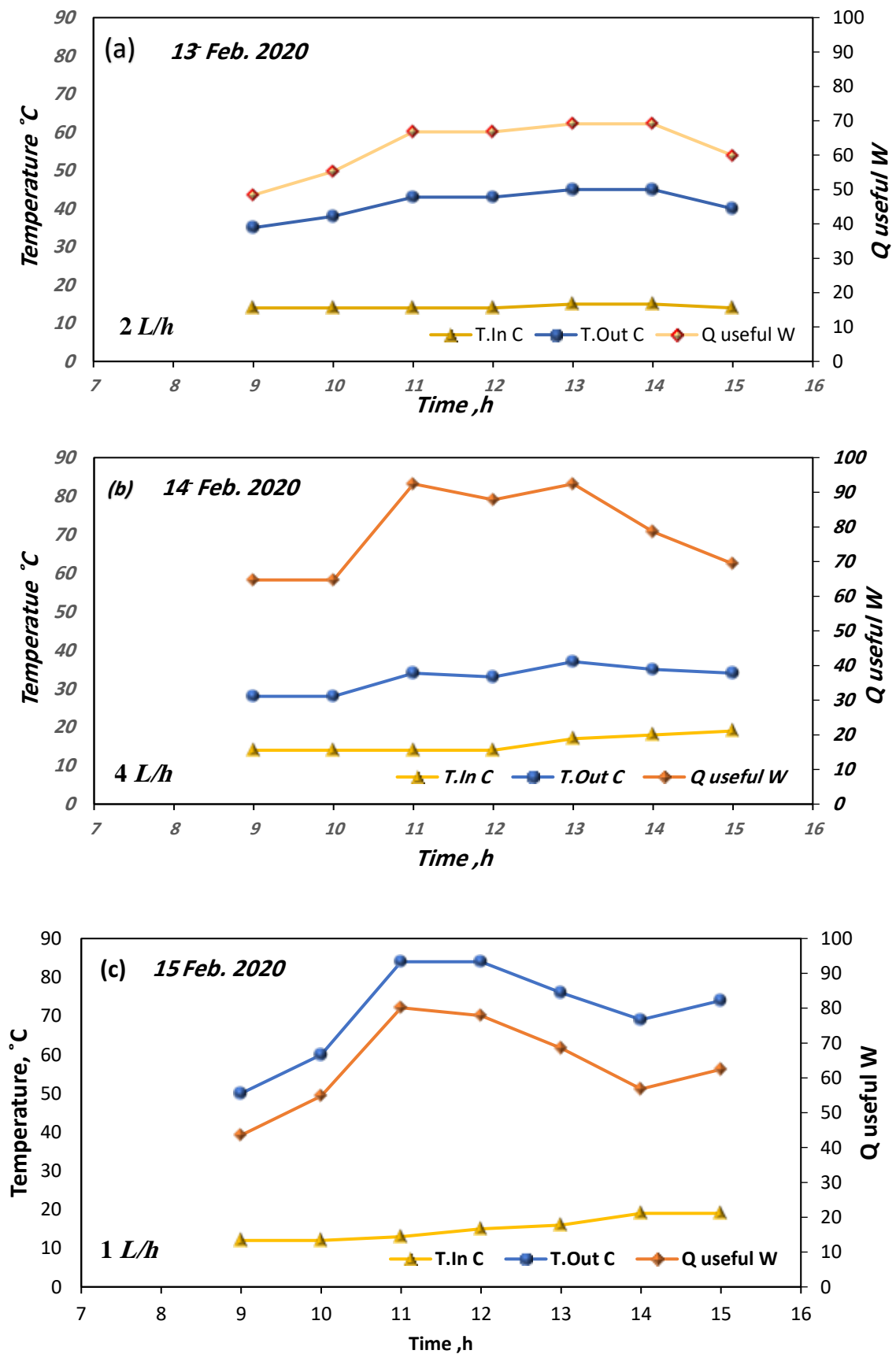
Fig. 5.8: Temperature of water inlet, outlet and useful heat gain versus time of conical pipe heat exchanger (a) *2 L/h* (b) *4 L/h* (c) *1 L/h*.

In experiments 1, 2, and 3, the main parameter investigated was the water flow rate, 2, 4, and 1 *L/h*, respectively. As previously mentioned, the experiments were performed in three consecutive days so that the other contributing parameters, such as ambient temperature and solar radiation, will be in the same range; for example, the minimum solar radiation was about 900 and the maximum solar radiation was about 1300. The difference in average temperature of water between outlet and inlet was 27, 17 and 56 °C respectively, which reflects a decreased temperature as the flow rate increased [47]. On the other hand, the useful heat gain increased with the increase of the flow rate, where the maximum useful heat gain was 92 W with a flowrate of 4 *L/h* [40].

5.4.2 Cubical Tank Heat Exchanger

Practical experiments were conducted during the period 22-28 of Feb. 2020 from (9AM – 3PM), where the ambient temperature ranged from (15 – 24) °C and the solar radiation ranged from (855 – 1387) W/m^2, as shown in Fig. 5.9 (a and b).
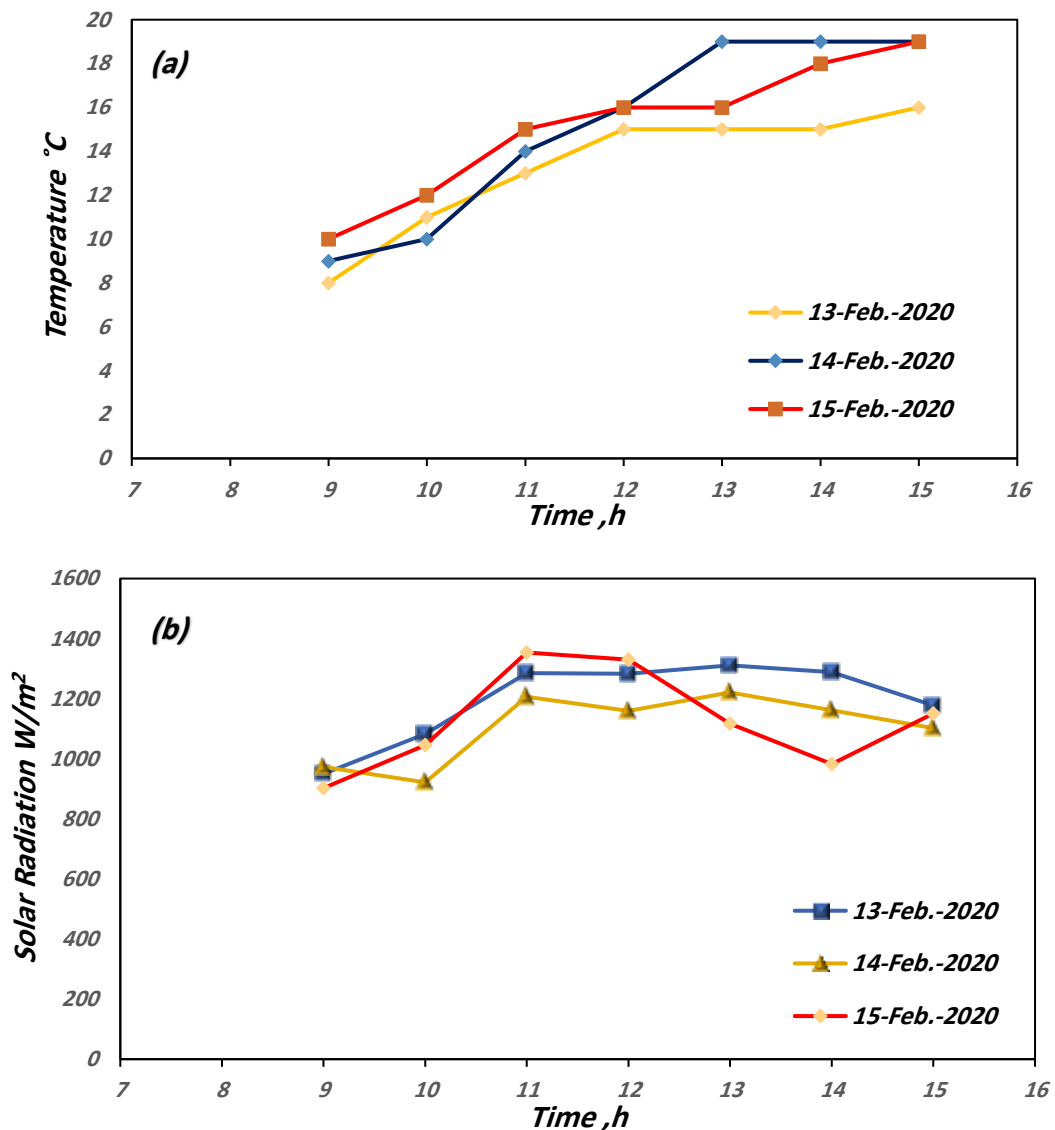
Figure (5.10-a) shows the relation between the temperature of water inlet, outlet and useful heat gain versus time for the cubical tank heat exchanger at water flow rate of 1 *L/h* during 22 Feb., where the ambient temperature ranged from (17 – 24) °C and the solar radiation in W/m^2 ranged from (950 – 1225) . The average inlet, outlet water temperatures and useful heat gain are 16 °C, and 58 °C and 48.9W respectively. Noting that at 13:00 the sky turned partially cloudy resulting in a reduction in amount of solar radiation to 412 W/m^2, causing a decrease in temperature of the water outlet to 34 °C.

Figure (5.10-b) shows the relationship between the temperature of water inlet, outlet and useful heat gain versus time for the cubical tank heat exchanger at water flow rate was 2 *L/h* during 26- Feb. 2020, where the ambient temperature ranged from (15- 21) °C and the solar radiation in W/m^2 ranged from (1159 –

1387). The average inlet, outlet water temperatures and useful heat gain are 17.5 °C, 50°C and 76 W respectively.

Figure (5.10-c) shows the relationship between the temperature of water inlet, outlet and useful heat gain versus time for the cubical tank heat exchanger at water flow rate was 4 *L/h* during 28⁻Feb. 2020, where the ambient temperature ranged from (17 – 22) °C and the solar radiation in W/m² ranged from (855 – 1387). The average inlet, outlet water temperatures, and useful heat gain are 18 °C, 33°C and 68 W respectively.
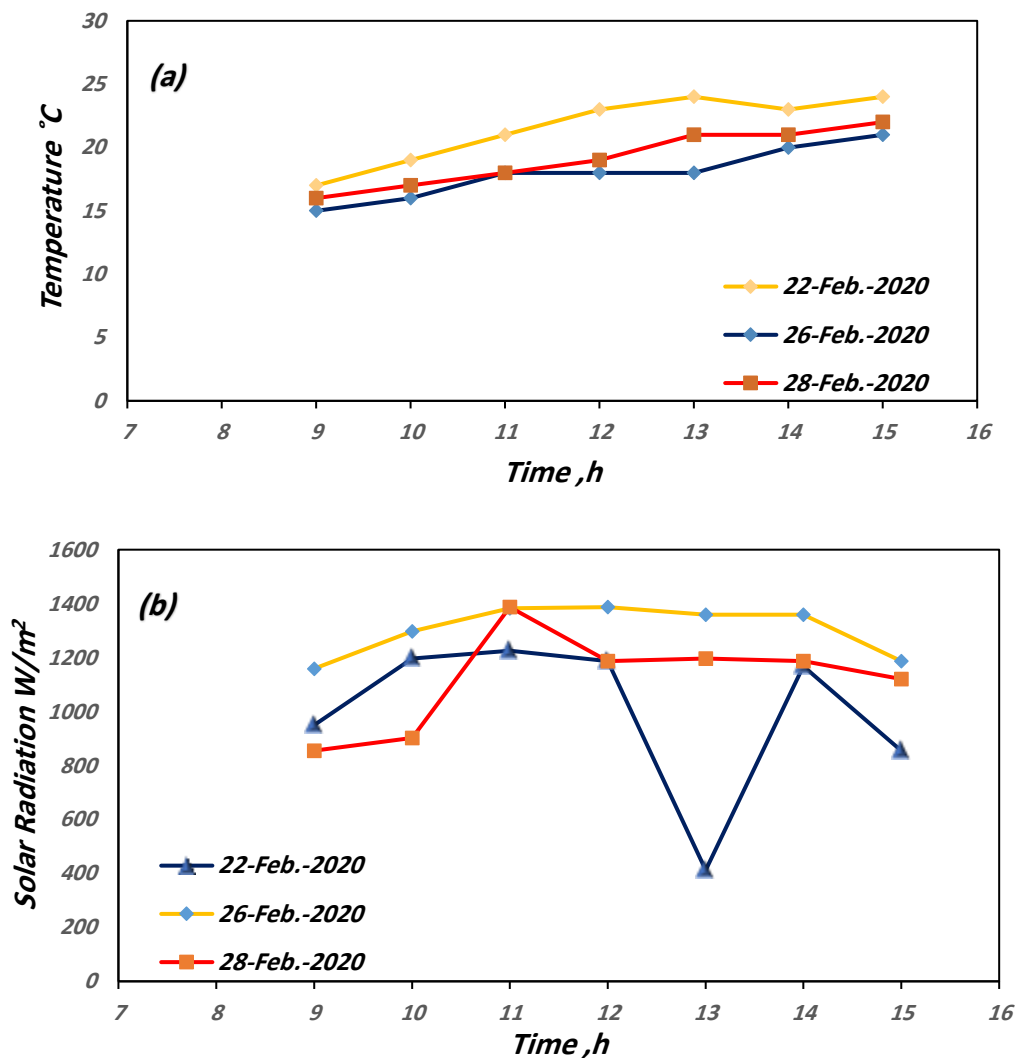

Fig. 5.9 : Climatic conditions under which the experiments have been conducted of cubical tank heat exchanger: (a) ambient temperature, and (b) solar radiation, versus time.
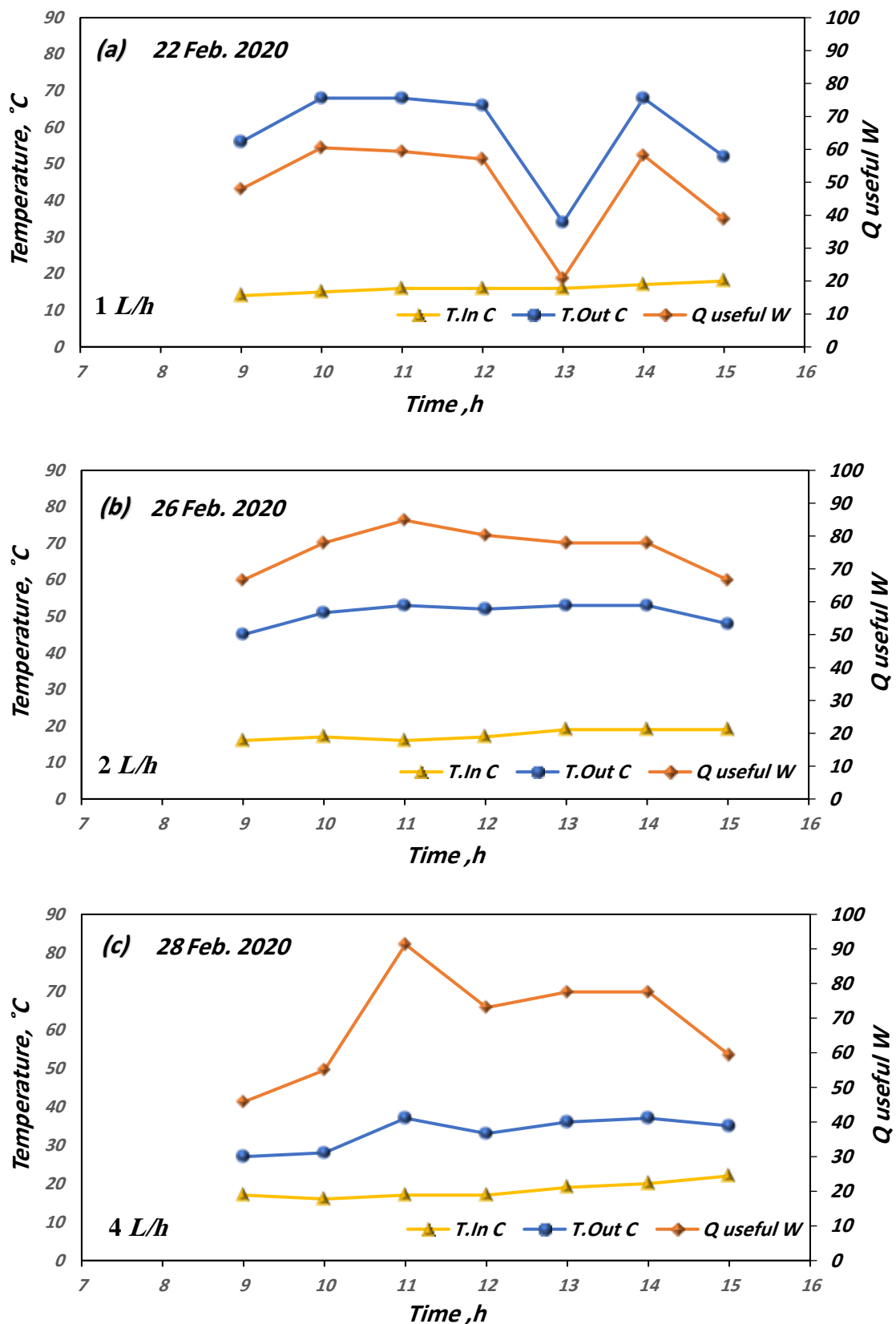
Fig. 5.10 : Temperature of water inlet, outlet and useful heat gain versus time of cubical tank heat exchanger (a) 1 *L/h* (b) 2 *L/h* (c) 4 *L/h*.

In experiments 4, 5, and 6, the main parameter investigated was the water flow rate, 1, 2, and 4 *L/h*, respectively. As previously mentioned, the experiments were performed in three consecutive days so that the other contributing parameters, such as ambient temperature and solar radiation, will be in the same range. The difference of average Temperature of water between outlet and inlet was 42, 33 and 15°C respectively, which reflects a decrease in the temperature as the flow rate increased [23]. On the other hand, the useful heat gain increased with the increase of the flow rate, where the maximum useful heat gain was 91 W with a flowrate of 4 *L/h* [48].

5.5 Model IIII

Practical experiments were conducted using cubical steel water container (20 cm each side), which manufactured with vertical metal fins connected to the upper cover of the container. Two different metals were used to manufacture the fins and the upper cover, namely steel and aluminum (one experiment for each type).

The data was collected using thermocouples type-K that are installed on the fins and the upper cover. Thermocouples were installed on the upper surface, to measure the heat distribution, and on the fins to measure the heat distribution inside the container depth. The temperature is recorded by means of a digital data logger. Following is a detailed illustration of the two experiments.

The first experiment was performed using steel fins and upper cover on 22-Nov.2019. The experiment started at 9AM and completed at 3PM. The ambient temperature ranged from (17 – 26) °C and the solar radiation in W/m² ranged from (1130 – 1251), as shown in Fig. (5.11).

Fig. 5.11: Ambient temperature and solar radiation versus time of container.

Figure (5.12) shows the relation between temperature distributions versus time for the steel upper cover. The average focus temperature is 183.8 °C, the average edge temperature is 79.6 °C and the average plate temperature is 100.5 °C.

Fig. 5.12: Temperature distribution of upper cover versus time of container of steel cover.

Figure (5.13) shows the relationship between temperature distributions along the steel fins versus time. The average temperature at 6 cm depth is 38.8 °C, the average temperature at 13 cm depth is 32.2 °C, and the average temperature at 19 cm depth is 29.9 °C. Noting that at 15:00 the sky turned partially cloudy resulting in reduction in amount of solar radiation to 260 W/m², causing a decrease in temperature of the focus to 48 °C. The results showed that the highest recorded temperature is 34 ° C at the depth 19 cm of the fins, which is suitable for melting some types of the (PCM).
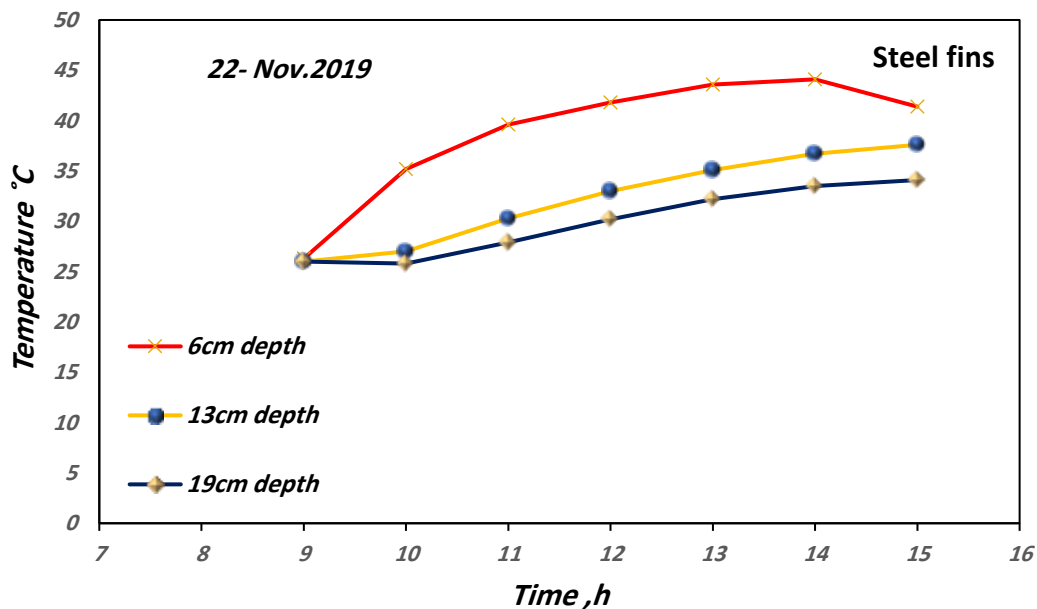
Fig. 5.13:Temperature distribution along the fins of the container of steel fins.

The other experiment was performed using an aluminum fins and upper cover of the container on 27-Nov. 2019. The experiment started at 9AM and completed at 3PM. The ambient temperature ranged from (19.6 - 25.3) °C and the solar radiation in W/m² ranged from (764 – 1008), as shown in Fig. (5.14).
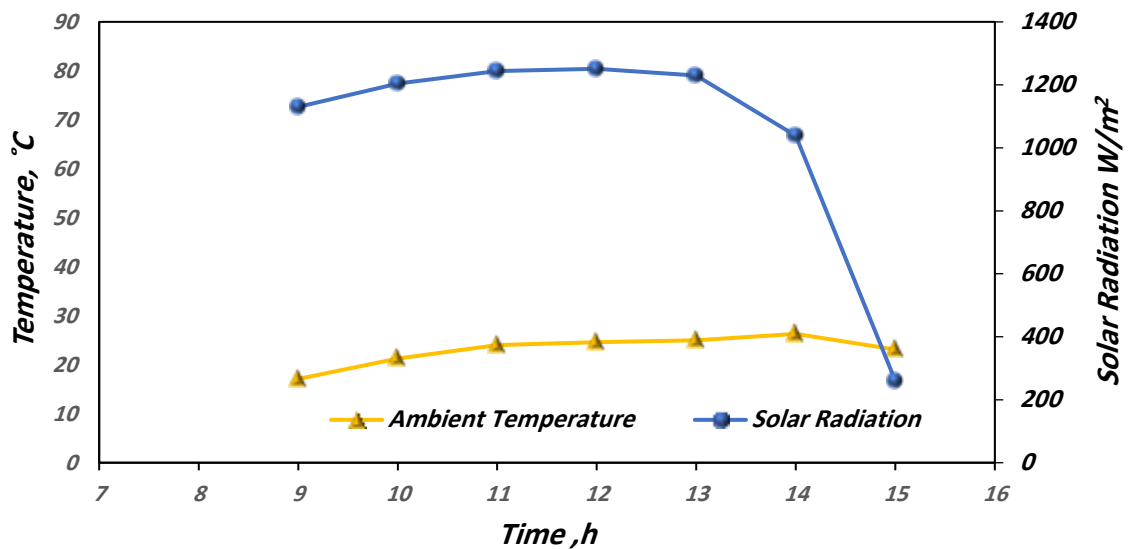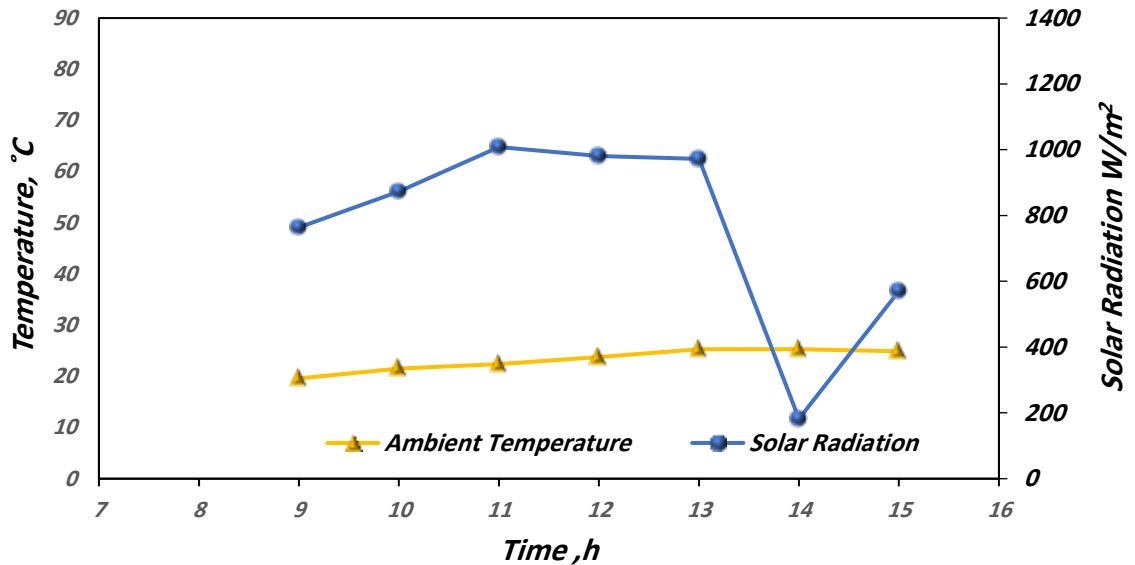
Fig. 5.14: Ambient temperature and solar radiation versus time of container.

Figure (5.15) shows the relationship between temperature distributions versus time for the aluminum upper cover. The average focus temperature is 60.9 °C, the average edge temperature is 51.6 °C and the average plate temperature is 53.5 °C.
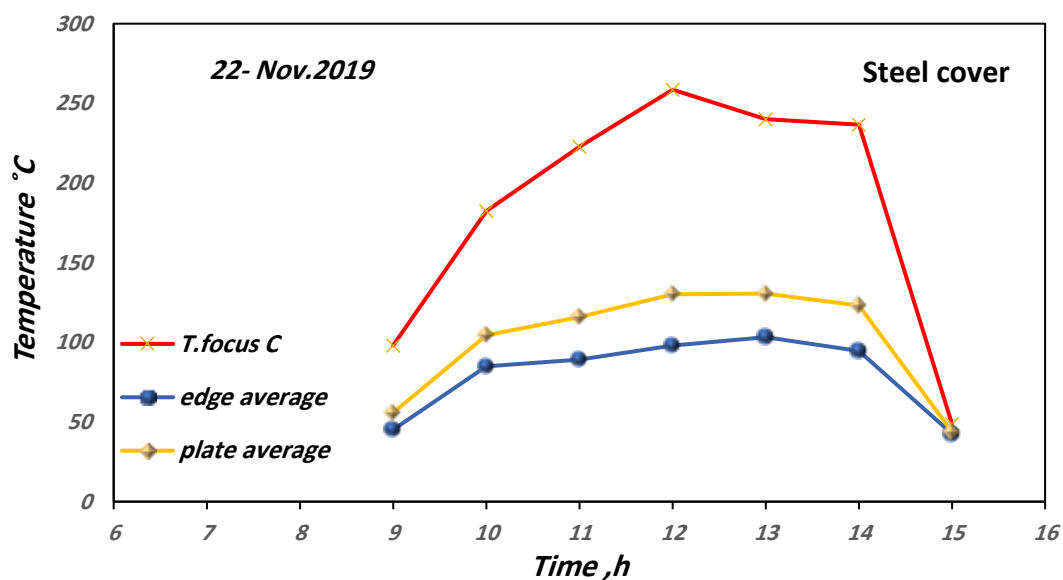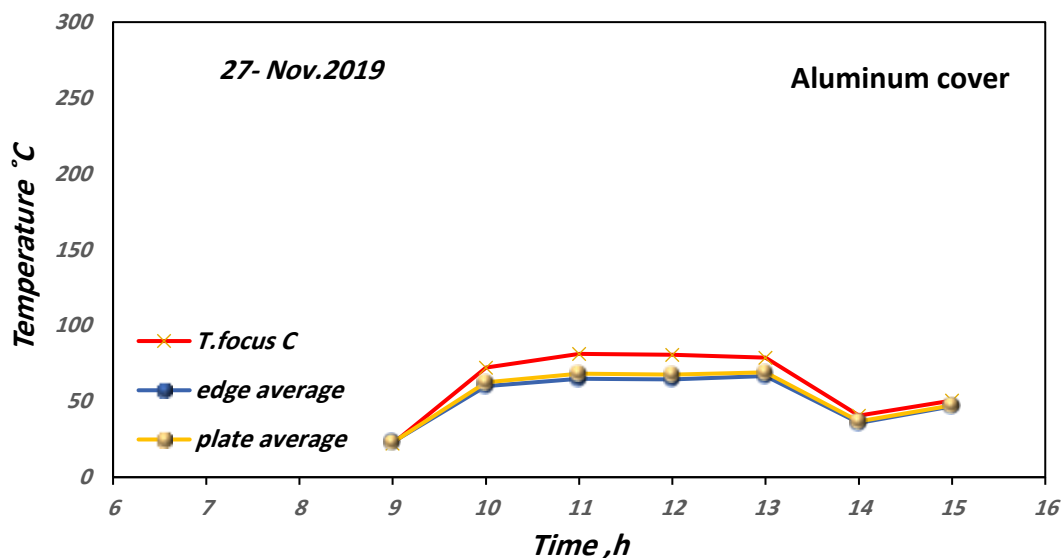

Fig. 5.15: Temperature distribution of upper cover versus time of container of aluminum cover.

Figure (5.16) shows the relationship between temperature distributions along the aluminum fins versus time. The average temperature at 5 cm in depth is

30.4 °C, the average temperature at 15 cm in depth is 24.5°C, and the average temperature at 19 cm in depth is 24.1 °C. It can be noticed that at 14:00 the sky turned partially cloudy resulting in a reduction in the amount of solar radiation to 182 W/m^2, causing a decrease in the temperature of the focus to 40.7 °C. From the results shown in figures above, one can see that the highest recorded temperature is 30 ° C at the depth 15 of the fins, which is suitable for melting some types of the (PCM). Note that the steel fins and upper cover recorded higher temperature than the aluminum fins and upper cover of the container and that is because of the difference in the coefficient of thermal conductivity which causes more heat dissipation to the surrounding, and also the solar radiation in the aluminum finned cover test was less, comparing by the other test [54].

Fig. 5.16:Temperature distribution along the fins of the container of aluminum fins.

Chapter six

CONCLUSIONS AND RECOMMENDATIONS

6. CONCLUSIONS AND RECOMMENDATIONS

6.1 Introduction

This work presents an experimental study to utilize extreme sunlight temperature via a Fresnel lens concentrator using a solar tracking system. The experimental tests are performed with the local weather condition in Najaf city/Iraq at latitude 31.59 degrees north, 44.19 degrees east. The experimental rig consists of a freely rotating two-axis frame that is controlled by an electronic circuit that implements Arduino and stepper motors as a control system to adjust the position of the Fresnel's lens focal by moving the motors accordingly. The focal of the sunlight is to be maintained stationary at a fixed position to ensure continuity of heat flow on the absorption system. Different types of solar thermal receivers, heat exchangers, solar still, and container tank were placed in the focus of the Fresnel lens concentrator. Therefore, the following conclusions can be stated based on the study results.

6.2 Conclusion

1. The results of the experiments show the focal temperature on the absorption steel plate reached as high as 400° C when the ambient temperature was 20° C. Whereas, The temperature distribution for the aluminum plate where the highest temperature obtained was at the focus which is 317 ° C when the ambient temperature is 16.2 ° C. However, the temperature of the focal for both aluminum and steel plates is high and can be implemented in many different solar applications.

2. The productivity of the freshwater in the solar still is strongly proportional to the amount of the solar radiation, where the intensity of the solar radiation influences the heat produced by the focal and hence it increases the productivity of the solar still. Although, the area of the solar still is increased to enhance the productivity, but the effect of the solar radiation is still the dominant parameter that rules the performance of the solar still at same weather conditions (ambient temperature and wind speed). The results show that the maximum freshwater cumulative productivity for six hours output for, 10 and 20 cm height, solar still during the experiment period was 500 ml when the average solar radiation was 1280 W/m^2 and 1165 W/m^2 respectively.

3. For solar water heater the experimental tests are performed using two models of heat exchangers, namely conical pipe and cubical tank heat exchangers. The experiments was performed three times in three consecutive days, for each models of heat exchangers, with different water flow rates (1, 2 and 4 liter per hour, respectively). The results showed that the highest useful heat gain recorded for the conical pipe heat exchanger is 92 W when the intensity of solar radiation is 1206 W/m^2 and the ambient temperature is 14 ° C. The highest obtained useful heat gain of the cubical tank heat exchanger was 91 W when the intensity of solar radiation is 1387 W/m^2 and the ambient temperature is 18 ° C.

4. The experimental tests was performed using cubical steel water container (20 cm each side) vertical metal fins connected to the upper cover of the container. The results show that the steel fins and upper cover recorded higher temperature than the aluminum fins and upper cover of the container and that

is because the difference in the coefficient of thermal conductivity which causes more heat dissipation to the surrounding, and also the solar radiation in the aluminum finned cover test was less, comparing by the other test
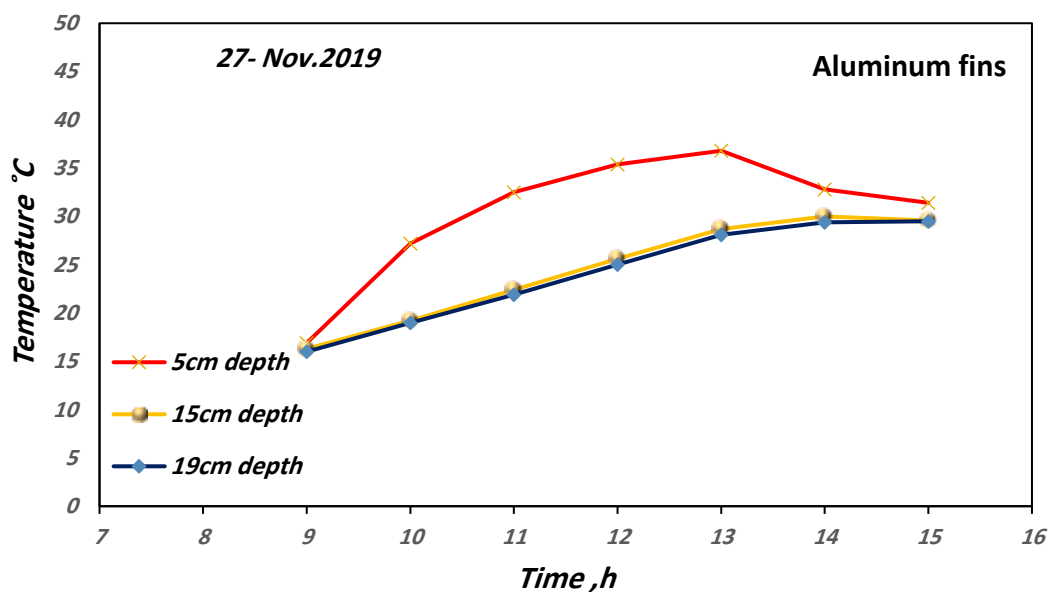
2.6 Recommendation

Observing the conclusion above, gives an idea of promising ability to use the Fresnel lens, during wintertime under Iraqi weather, in a wide range of renewable energy applications such as heating, heat storage, and water desalination applications. However, the following recommendations for future work

1. Using a larger Fresnel lens for greater amount of solar radiation to obtain a larger solar thermal energy, which can beneficial for domestic or industrial uses.

2. Using further modification in solar applications models such as using a glass cover for the conical pipe heat exchanger to reduce convection heat loss in the cavity aperture.

3. For the solar still can be modified to include a glass dome of a large area or a glass chimney that is mounted on the top of the cylindrical with con solar still to ensure better condensation.

References

7. REFRENCES

[1] F. M. Sukki, R. R. Iniguez, S.G. McMeekin, B.G. Stewart and B. Clive, "Solar concentrators," Int. J. Appl. Sci., vol. 1, no. 1, pp. 1–15, 2010.

[2] S. A. Kalogirou, "Solar thermal collectors and applications," Prog. Energy Combust. Sci., vol. 30, no. 3, pp. 231–295, 2004.

[3] H. H. Al-Kayiem and S. T. Mohammad, "Potential of renewable energy resources with an emphasis on solar power in Iraq: An outlook," Resources, vol. 8, no. 1, pp. 1–20, 2019.

[4] J. A. Duffie, W. A. Beckman, and J. McGowan, Solar Engineering of Thermal Processes, vol. 53, no. 4. 1985.

[5] "https://solargis.com/maps-and-gis-data/download/world" .

[6] "https://solargis.com/maps-and-gis-data/download/iraq" .

[7] C. Sierra and A. J. V Azquez, "High solar energy concentration with a Fresnel," J. Mater. Sci., vol. 40, no. 6, pp. 1339–1343, 2005.

[8] A. Ummadisingu and M. S. Soni, "Concentrating solar power - Technology, potential and policy in India," Renew. Sustain. Energy Rev., vol. 15, no. 9, pp. 5169–5175, 2011.

[9] L. E. Vieira de Souza and A. M. Gilmanova Cavalcante, "Concentrated Solar Power deployment in emerging economies: The cases of China and Brazil," Renew. Sustain. Energy Rev., vol. 72, no. May, pp. 1094–1103, 2017.

[10] Y. Tripanagnostopoulos, C. Siabekou, and J. K. Tonui, "The Fresnel lens concept for solar control of buildings," Sol. Energy, vol. 81, no. 5, pp. 661–675, 2007.

[11] M. Hasan Nia, A. Abbas Nejad, A. M. Goudarzi, M. Valizadeh, and P. Samadian, "Cogeneration solar system using thermoelectric module and fresnel lens," Energy Convers. Manag., vol. 84, pp. 305–310, 2014.

[12] M. Imtiaz Hussain, A. Ali, and G. H. Lee, "Performance and economic analyses of linear and spot Fresnel lens solar collectors used for greenhouse heating in South Korea," Energy, vol. 90, pp. 1522–1531, 2015.

[13] P. Durkaieswaran and K. K. Murugavel, "Various special designs of single basin passive solar still - A review," Renew. Sustain. Energy Rev., vol. 49, pp. 1048–1060, 2015.

[14] T. Rajaseenivasan, K. K. Murugavel, T. Elango, and R. S. Hansen, "A review of different methods to enhance the productivity of the multi-effect solar still," Renew. Sustain. Energy Rev., vol. 17, no. November, pp. 248–259, 2013.

[15] I. L. Mohammed, "Design and Development of a Parabolic Dish Solar Thermal Cooker," Int. J. Eng. Res. Appl. www.ijera.com, vol. 3, no. 4, pp. 1179–1186, 2013.

[16] P. D. Menghani, R. R. Udawant, A. M. Funde, and S. V Dingare, "Low Pressure Steam Generation by Solar Energy WithFresnel Lens : A Review," IOSR J. Mech. Civ. Eng., no. April, pp. 60–63, 2013.

[17] W. T. Xie, Y. J. Dai, and R. Z. Wang, "Numerical and experimental analysis of a point focus solar collector using high concentration imaging PMMA Fresnel lens," Energy Convers. Manag., vol. 52, no. 6, pp. 2417–2426, 2011.

[18] M. M. Valmiki et al., "A novel application of a Fresnel lens for a solar stove and solar heating," Renew. Energy, vol. 36, no. 5, pp. 1614–1620, 2011.

[19] P. J. Sonneveld, G. L. A. M. Swinkels, B. A. J. va. Tuijl, H. J. J. Janssen, J. Campen, and G. P. A. Bot, "Performance of a concentrated photovoltaic energy system with static linear Fresnel lenses," Sol. Energy, vol. 85, no. 3, pp. 432–442, 2011.

[20] I. Soriga and C. Neaga, "Thermal analysis of a linear Fresnel lens solar collector with black body cavity receiver," UPB Sci. Bull. Ser. D Mech. Eng., vol. 74, no. 4, pp. 105–116, 2012.

[21] M. Lin, K. Sumathy, Y. J. Dai, and X. K. Zhao, "Performance investigation on a linear Fresnel lens solar collector using cavity receiver," Sol. Energy, vol. 107, pp. 50–62, 2014.

[22] D. A. S. T. Prakash Kumar1, "Development of Fresnel Powerhouse Prototype With Thermal Energy Storage Concentrated Solar Power," Int. J. Technol. Res. Eng., vol. 1, no. 5, pp. 2347–4718, 2014.

[23] M. Imtiaz Hussain and G. H. Lee, "Experimental and numerical studies of a U-shaped solar energy collector to track the maximum CPV/T system output by varying the flow rate," Renew. Energy, vol. 76, pp. 735–742, 2015.

[24] T. C. Cheng, C. K. Yang, and I. Lin, "Biaxial-type concentrated solar tracking system with a Fresnel lens for solar-thermal applications," Appl. Sci., vol. 6, no. 5, 2016.

[25] S. Perini, X. Tonnellier, P. King, and C. Sansom, "Theoretical and experimental analysis of an innovative dual-axis tracking linear Fresnel lenses concentrated solar thermal collector," Sol. Energy, vol. 153, no.

September, pp. 679–690, 2017.

[26] N. S. Al-Dohani, S. N. Nagaraj, A. Anarghya, and V. N. Abhishek, "Development of Powerhouse Using Fresnel lens," MATEC Web Conf., vol. 144, pp. 1–9, 2018.

[27] K. Sornek, M. Filipowicz, and J. Jasek, "The use of fresnel lenses to improve the efficiency of photovoltaic modules for building-integrated concentrating photovoltaic systems," J. Sustain. Dev. Energy, Water Environ. Syst., vol. 6, no. 3, pp. 415–426, 2018.

[28] A. Z. Hafez, A. M. Yousef, and N. M. Harag, "Solar tracking systems: Technologies and trackers drive types – A review," Renew. Sustain. Energy Rev., vol. 91, no. March, pp. 754–782, 2018.

[29] C. Lee, P. Chou, C. Chiang, and C. Lin, "Sun Tracking Systems: A Review," Sensors, pp. 3875–3890, 2009.

[30] I. Palavras and G. C. Ã. Bakos, "Development of a low-cost dish solar concentrator and its application in zeolite desorption," Renew. Energy, vol. 31, pp. 2422–2431, 2006.

[31] K. Aiuchi, K. Yoshida, M. Onozaki, Y. Katayama, M. Nakamura, and K. Nakamura, "Sensor-controlled heliostat with an equatorial mount," Sol. Energy, vol. 80, no. 9, pp. 1089–1097, 2006.

[32] H. A. N. Hameed, Hassanain Ghani, "Experimental study for productivity enhancement of parabolic solar concentrator system," Al-Qadisiya J. Eng. Sci., vol. 4, no. 2, 2011.

[33] E. Venegas-Reyes, O. A. Jaramillo, R. Castrejón-García, J. O. Aguilar, and F. Sosa-Montemayor, "Design, construction, and testing of a parabolic

trough solar concentrator for hot water and low enthalpy steam generation," J. Renew. Sustain. Energy, vol. 4, no. 5, 2012.

[34] F. M. Mohamed, A. S. Jassim, Y. H. Mahmood, and M. A. K. Ahmed, "Design and Study of Portable Solar Dish Concentrator," Int. J. Recent Res. Rev., vol. III, no. September, pp. 52–59, 2012.

[35] X. Jin, G. Xu, R. Zhou, X. Luo, and Y. Quan, "A Sun Tracking System Design for a Large Dish Solar Concentrator," Int. J. Clean Coal Energy, vol. 02, no. 02, pp. 16–20, 2013.

[36] H. Jafari Mosleh, S. J. Mamouri, M. B. Shafii, and A. Hakim Sima, "A new desalination system using a combination of heat pipe, evacuated tube and parabolic through collector," Energy Convers. Manag., vol. 99, pp. 141–150, 2015.

[37] P. N. Patil, M. A. Khandekar, and S. N. Patil, "Automatic dual-axis solar tracking system for parabolic dish," Proceeding IEEE - 2nd Int. Conf. Adv. Electr. Electron. Information, Commun. Bio-Informatics, IEEE - AEEICB 2016, pp. 699–703, 2016.

[38] A. Jamar, Z. A. A. Majid, W. H. Azmi, M. Norhafana, and A. A. Razak, "A review of water heating system for solar energy applications," Int. Commun. Heat Mass Transf., vol. 76, pp. 178–187, 2016.

[39] R. Senthil and M. Cheralathan, "Effect of non-uniform temperature distribution on surface absorption receiver in parabolic dish solar concentrator," Therm. Sci., vol. 21, no. 5, pp. 2011–2019, 2017.

[40] A. A. Sagade, "Experimental investigation of effect of variation of mass flow rate on performance of parabolic dish water heater with non-coated receiver," Int. J. Sustain. Energy, vol. 34, no. 10, pp. 645–656, 2015.

[41] T. Arunkumar, D. Denkenberger, A. Ahsan, and R. Jayaprakash, "The augmentation of distillate yield by using concentrator coupled solar still with phase change material," Desalination, vol. 314, pp. 189–192, 2013.

[42] M. Imtiaz Hussain and G. H. Lee, "Thermal performance evaluation of a conical solar water heater integrated with a thermal storage system," Energy Convers. Manag., vol. 87, pp. 267–273, 2014.

[43] T. Arunkumar, R. Velraj, D. C. Denkenberger, R. Sathyamurthy, K. V. Kumar, and A. Ahsan, "Productivity enhancements of compound parabolic concentrator tubular solar stills," Renew. Energy, vol. 88, pp. 391–400, 2016.

[44] K. Srithar, T. Rajaseenivasan, N. Karthik, M. Periyannan, and M. Gowtham, "Stand alone triple basin solar desalination system with cover cooling and parabolic dish concentrator," Renew. Energy, vol. 90, pp. 157–165, 2016.

[45] G. Rajamohan, P. Kumar, M. Anwar, and T. Mohanraj, "Analysis of solar water heater with parabolic dish concentrator and conical absorber," IOP Conf. Ser. Mater. Sci. Eng., vol. 206, no. 1, 2017.

[46] B. Zou, J. Dong, Y. Yao, and Y. Jiang, "An experimental investigation on a small-sized parabolic trough solar collector for water heating in cold areas," Appl. Energy, vol. 163, pp. 396–407, 2016.

[47] R. Karimi, T. T. Gheinani, and V. Madadi Avargani, "A detailed mathematical model for thermal performance analysis of a cylindrical cavity receiver in a solar parabolic dish collector system," Renew. Energy, vol. 125, pp. 768–782, 2018.

[48] S. Rc. M, "Effect of the phase change material in a solar receiver on thermal performance of parabolic dish collector," Therm. Sci., vol. 21, no. 6, pp.

2803–2812, 2017.

[49] A. Sedaghat, E. H. B. Hani, S. Ali, F. Ali, A. Al-Mesbah, and M. Malallah, "Experimental and Theoretical Analysis Of a Solar Desalination System Improved by Thermoelectric Cooler And Applying Sun Tracking System," Energy Eng. J. Assoc. Energy Eng., vol. 115, no. 6, pp. 62–76, 2018.

[50] S. A. Kalogirou, Solar Energy Engineering Processes and Systems. Oxford OX5 1GB, UK, Academic Press. 2014.

[51] D. M. Hachim, A. Alsahlani, and A. A. Eidan, "Measurements of Wind and Solar Energies in Najaf , Iraq," Adv. Nat. Appl. Sci., vol. 11, no. 9, pp. 110–116, 2017.

[52] C. Sierra and A. J. Vázquez, "NiAl coatings on carbon steel by self-propagating high-temperature synthesis assisted with concentrated solar energy: Mass influence on adherence and porosity," Sol. Energy Mater. Sol. Cells, vol. 86, no. 1, pp. 33–42, 2005.

[53] A. E. Kabeel and M. Abdelgaied, "Observational study of modified solar still coupled with oil serpentine loop from cylindrical parabolic concentrator and phase changing material under basin," Sol. Energy, vol. 144, pp. 71–78, 2017.

[54] R. Abu-malouh, S. Abdallah, and I. M. Muslih, "Design , construction and operation of spherical solar cooker with automatic sun tracking system," Energy Convers. Manag., vol. 52, no. 1, pp. 615–620, 2011.

APPENDICES

APPENDICES

Appendices- A: Sun tracker programming for Arduino control system

```
#include <LiquidCrystal_I2C.h>

LiquidCrystal_I2C lcd(0x27,2,1,0,4,5,6,7,3, POSITIVE);

#include <LCD.h>

#include "RTClib.h"

RTC_DS1307 rtc;


int smDirectionPin1 = 11; //Direction pin

int smStepPin1 = 12; //Stepper pin

int smDirectionPin2 = 10; //Direction pin

int smStepPin2 = 9; //Stepper pin

void setup () {

  pinMode(smDirectionPin1, OUTPUT);

 pinMode(smStepPin1, OUTPUT);

  pinMode(smDirectionPin2, OUTPUT);

 pinMode(smStepPin2, OUTPUT);

  pinMode(A0, INPUT_PULLUP); // sets analog pin for input

 lcd.begin(16, 2);

 while (!Serial); // for Leonardo/Micro/Zero

 Serial.begin(57600);

 if (! rtc.begin()) {

  Serial.println("Couldn't find RTC");

  while (1);

 }

 if (! rtc.isrunning()) {

  Serial.println("RTC is NOT running!");

  // following line sets the RTC to the date & time this sketch was compiled

  rtc.adjust(DateTime(F(__DATE__), F(__TIME__)));

  // This line sets the RTC with an explicit date & time, for example to set

  // January 21, 2014 at 3am you would call:

   // rtc.adjust(DateTime(2020, 2, 11, 23, 39, 0));

 }
```

```
}

void loop () {
 DateTime now = rtc.now();

int S=now.second();
int M=now.minute();
int H=now.hour();

   lcd.setCursor(0,0);
   lcd.print("TIME: ");
   lcd.print(now.hour(), DEC);
   lcd.print(":");
   lcd.print(now.minute(), DEC);
   lcd.print(":");
   lcd.print(now.second(), DEC);
   lcd.print("   ");

   lcd.setCursor(0,1);
   lcd.print("DATE: ");
   lcd.print(now.year(), DEC);
   lcd.print("/");
   lcd.print(now.month(), DEC);
   lcd.print("/");
   lcd.print(now.day(), DEC);
 int x=0;
 //-------------------------------from hear vertical axis ----------------
if( now.second()== 1&& now.hour()==9 ){
 while(x<    ){
 digitalWrite(smDirectionPin1,LOW);
   digitalWrite(smStepPin1,HIGH);
 delayMicroseconds(   );
 digitalWrite(smStepPin1,LOW);
 delayMicroseconds(   );
```

```
  x++;


  }


 }


if( now.second()== 1&& now.hour()==10 ){
 while(x<    ){
digitalWrite(smDirectionPin1,LOW);
  digitalWrite(smStepPin1,HIGH);
 delayMicroseconds(  );
 digitalWrite(smStepPin1,LOW);
 delayMicroseconds(  );
 x++;


 }


}


if( now.second()== 1&& now.hour()==11 ){
 while(x<   ){
digitalWrite(smDirectionPin1,LOW);
  digitalWrite(smStepPin1,HIGH);
 delayMicroseconds(  );
 digitalWrite(smStepPin1,LOW);
 delayMicroseconds(  );
 x++;


 }


}


if( now.second()== 1&& now.hour()==12 ){
 while(x<   ){
digitalWrite(smDirectionPin1,HIGH);
```

```
    digitalWrite(smStepPin1,HIGH);
 delayMicroseconds(   );
 digitalWrite(smStepPin1,LOW);
 delayMicroseconds(   );
  x++;


  }


}

if( now.second()== 1&& now.hour()==13 ){
 while(x<    ){
 digitalWrite(smDirectionPin1,HIGH);
    digitalWrite(smStepPin1,HIGH);
 delayMicroseconds(   );
 digitalWrite(smStepPin1,LOW);
 delayMicroseconds(   );
  x++;


  }


}

if( now.second()== 1&& now.hour()==14 ){
 while(x<    ){
 digitalWrite(smDirectionPin1,HIGH);
    digitalWrite(smStepPin1,HIGH);
 delayMicroseconds(   );
 digitalWrite(smStepPin1,LOW);
 delayMicroseconds(   );
  x++;


  }


}
```

```
//----------------------------------------------for hear vertical axis   --------------
//----------------------------------------------from hear horizontal axis --------------
if( now.second()== 20&& now.hour()==9 ){
  while(x<     ){
  digitalWrite(smDirectionPin2,HIGH);
  digitalWrite(smStepPin2,HIGH);
  delayMicroseconds(    );
  digitalWrite(smStepPin2,LOW);
  delayMicroseconds(    );
    x++;
  }
 }
 if( now.second()== 20&& now.hour()==10 ){
  while(x<     ){
  digitalWrite(smDirectionPin2,HIGH);
  digitalWrite(smStepPin2,HIGH);
  delayMicroseconds(    );
  digitalWrite(smStepPin2,LOW);
  delayMicroseconds(    );
    x++;
  }
 }

if( now.second()== 20&& now.hour()==11 ){
  while(x<     ){
  digitalWrite(smDirectionPin2,HIGH);
  digitalWrite(smStepPin2,HIGH);
  delayMicroseconds(    );
  digitalWrite(smStepPin2,LOW);
  delayMicroseconds(    );
    x++;
  }
 }

if( now.second()== 20&& now.hour()==12 ){
```

```
 while(x<    ){
 digitalWrite(smDirectionPin2,HIGH);
 digitalWrite(smStepPin2,HIGH);
 delayMicroseconds(   );
 digitalWrite(smStepPin2,LOW);
 delayMicroseconds(   );
   x++;
 }
 }

if( now.second()== 20&& now.hour()==13 ){
 while(x<    ){
 digitalWrite(smDirectionPin2,HIGH);
 digitalWrite(smStepPin2,HIGH);
 delayMicroseconds(   );
 digitalWrite(smStepPin2,LOW);
 delayMicroseconds(   );
   x++;
 }
 }

if( now.second()== 20&& now.hour()==14 ){
 while(x<    ){
 digitalWrite(smDirectionPin2,HIGH);
 digitalWrite(smStepPin2,HIGH);
 delayMicroseconds(   );
 digitalWrite(smStepPin2,LOW);
 delayMicroseconds(   );
   x++;
 }


}
//------------------------------------------------for hear horizontal axis  ---------------
delay(1000);
 }
```

Appendices-B: Table of Experimental data calculations

date	Time, h	T.In ˚C	T.Out ˚C	I W/m2	V L/h	m kg/s	Qu W
13/02/2020	9;00	14	35	950	2	0.000551	48.37653
13/02/2020	10:00	14	38	1083	2	0.000551	55.28747
13/02/2020	11:00	14	43	1285.35	2	0.000551	66.80569
13/02/2020	12:00	14	43	1282.5	2	0.000551	66.80569
13/02/2020	13:00	15	45	1311	2	0.000551	69.10933
13/02/2020	14:00	15	45	1288.2	2	0.000551	69.10933
13/02/2020	15:00	14	40	1178	2	0.000551	59.89476
date	Time h	T.In ˚C	T.Out ˚C	I W/m2	V L/h	m kg/s	Qu W
14/02/2020	09:00	14	28	972.8	4	0.001106	64.69711
14/02/2020	10:00	14	28	921.5	4	0.001106	64.69711
14/02/2020	11:00	14	34	1206.5	4	0.001106	92.42444
14/02/2020	12:00	14	33	1159	4	0.001106	87.80322
14/02/2020	13:00	17	37	1220.75	4	0.001106	92.42444
14/02/2020	14:00	18	35	1161.85	4	0.001106	78.56078
14/02/2020	15:00	19	34	1102	4	0.001106	69.31833

date	Time h	T.In ˚C	T.Out ˚C	I W/m2	V L/h	m kg/s	Qu W
15/02/2020	09:00	12	50	902.5	1	0.000274	43.54863
15/02/2020	10:00	12	60	1045	1	0.000273	54.78587
15/02/2020	11:00	13	84	1353.75	1	0.00027	80.1306
15/02/2020	12:00	15	84	1330	1	0.00027	77.8734
15/02/2020	13:00	16	76	1116.25	1	0.000273	68.552
15/02/2020	14:00	19	69	982.3	1	0.000272	56.77833
15/02/2020	15:00	19	74	1151.4	1	0.000272	62.45617
date	Time h	T.In ˚C	T.Out ˚C	I W/m2	V L/h	m kg/s	Qu W
22/02/2020	09:00	14	56	950	1	0.000273	47.93763
22/02/2020	10:00	15	68	1197	1	0.000273	60.49273
22/02/2020	11:00	16	68	1225.5	1	0.000273	59.35136
22/02/2020	12:00	16	66	1187.5	1	0.000273	57.06861
22/02/2020	13:00	16	34	412.3	1	0.000276	20.7746
22/02/2020	14:00	17	68	1168.5	1	0.000273	58.20998
22/02/2020	15:00	18	52	855	1	0.000273	38.80666
date	Time h	T.In ˚C	T.Out ˚C	I W/m2	V L/h	m kg/s	Qu W

| date	Time h	T.In ˚C	T.Out ˚C	I W/m2	V L/h	m kg/s	Qu W
26/02/2020	09:00	16	45	1159	2	0.000549	66.60366
26/02/2020	10:00	17	51	1296.75	2	0.000548	77.92913
26/02/2020	11:00	16	53	1382.25	2	0.000548	84.80523
26/02/2020	12:00	17	52	1387	2	0.000548	80.22117
26/02/2020	13:00	19	53	1358.5	2	0.000548	77.92913
26/02/2020	14:00	19	53	1358.5	2	0.000548	77.92913
26/02/2020	15:00	19	48	1187.5	2	0.000549	66.60366
date	Time h	T.In ˚C	T.Out ˚C	I W/m2	V L/h	m kg/s	Qu W
28/02/2020	09:00	17	27	855	4	0.001096	45.79422
28/02/2020	10:00	16	28	902.5	4	0.001096	54.95307
28/02/2020	11:00	17	37	1387	4	0.001092	91.30978
28/02/2020	12:00	17	33	1187.5	4	0.001092	73.04782
28/02/2020	13:00	19	36	1197	4	0.001092	77.61331
28/02/2020	14:00	20	37	1187.5	4	0.001092	77.61331
28/02/2020	15:00	22	35	1121	4	0.001092	59.35136

Appendices C: Calibration of thermocouples.

The calibration of temperature sensor (thermocouples) was done by recording readings at three different grades, then comparing them with the reading of the mercury thermometer at freezing temperature (0 °C), boiling water temperature (100 °C) and human body temperature (32 °C). The result of calibration as shown in Table. C-1

Table.C-1: Temperature Sensors Calibration.

Device No.	Freezing temperature = 0 ° C	Human body temperature = 37 ° C	Boiling temperature = 100 ° C
Hg thermometer	0	36.5	99.6
Sensor 1	0.17	36.2	98.8
Sensor 2	0.14	36.4	98.5
Sensor 3	0.15	36.7	99.4
Sensor 4	0.19	36.2	98.7
Sensor 5	0.18	36.3	98.6
Sensor 6	0.19	36.7	99.3
Sensor 7	0.2	36.6	98.9
Sensor 8	0.16	36.5	98.5
Sensor 9	0.17	36.6	98.8
Sensor 10	0.14	36.7	98.7
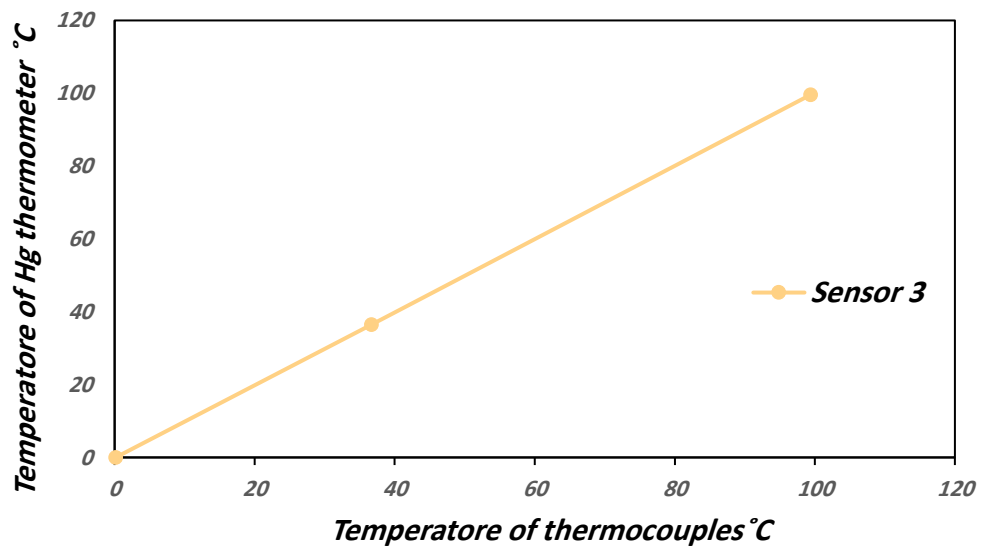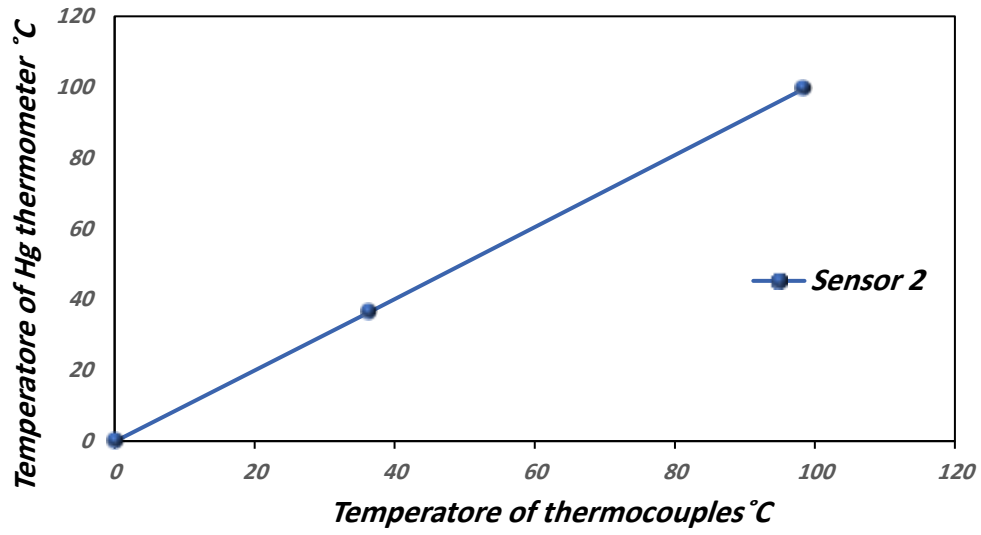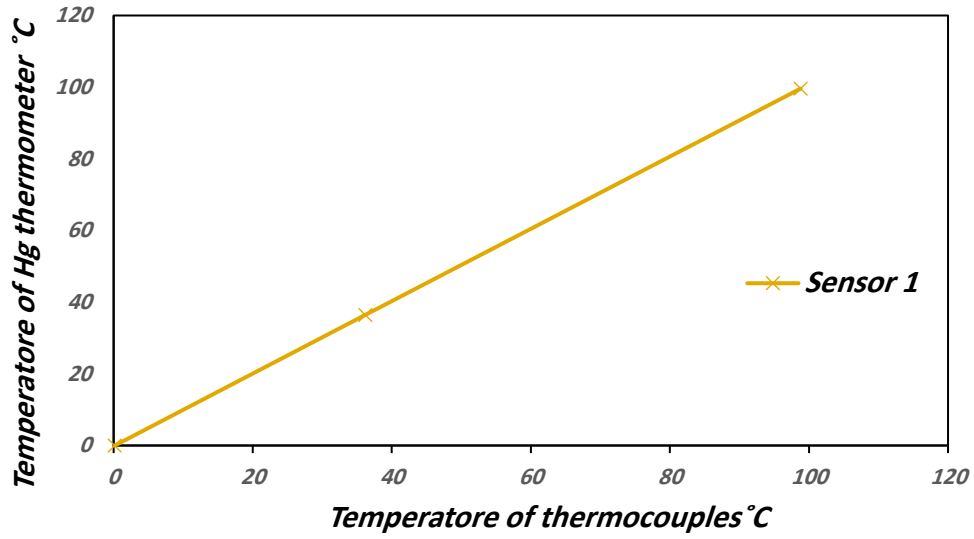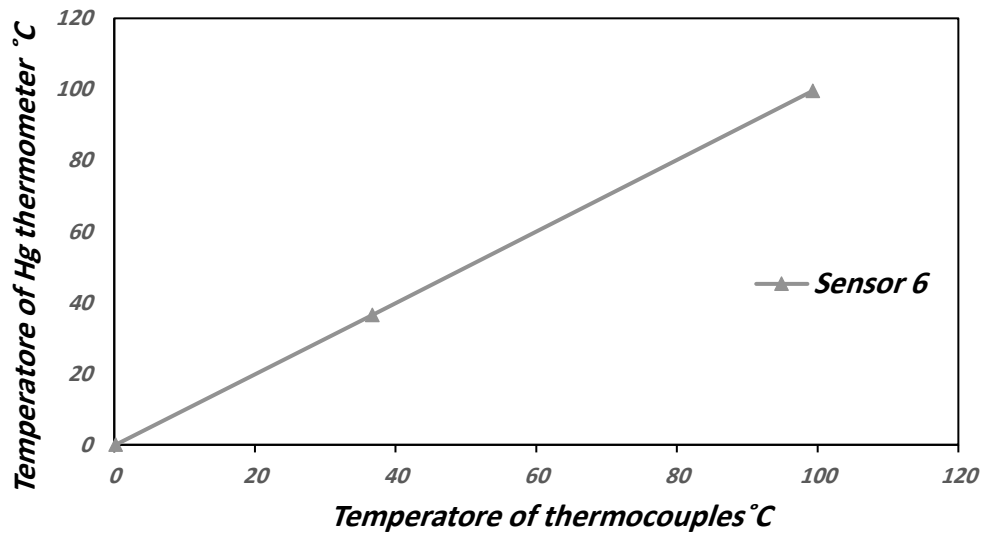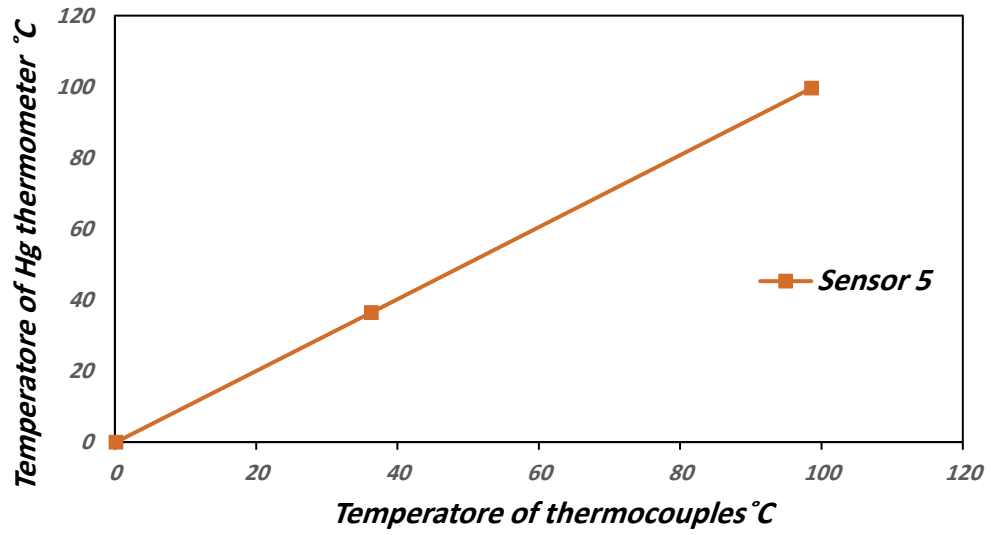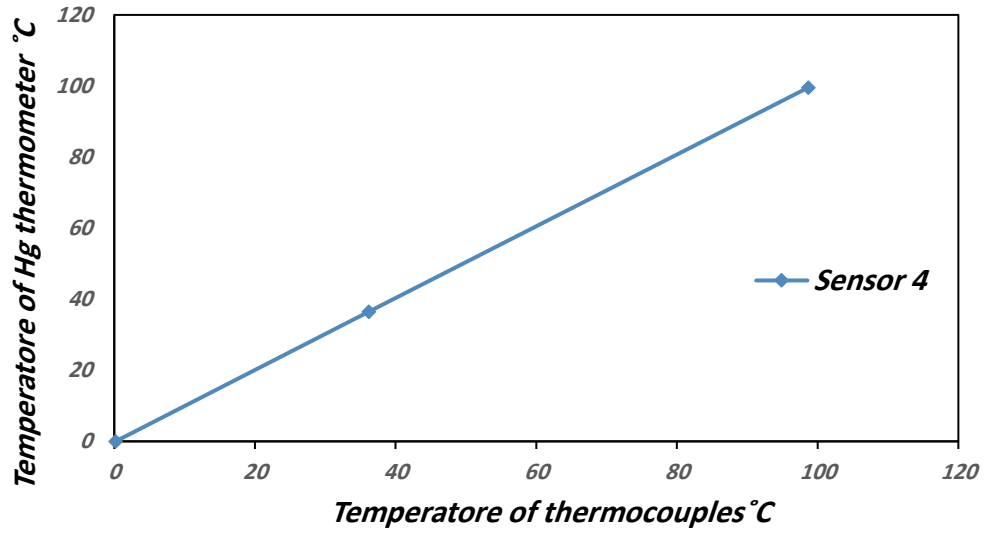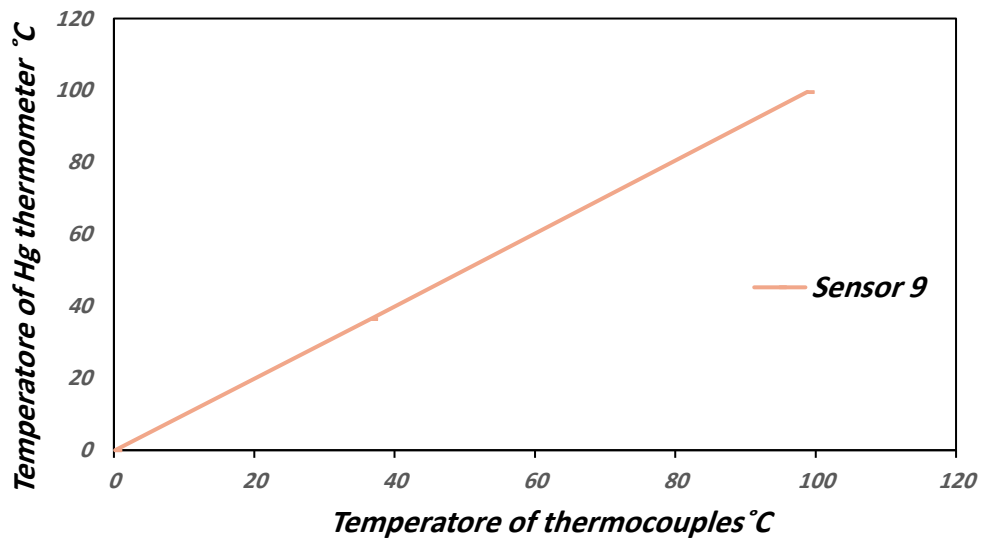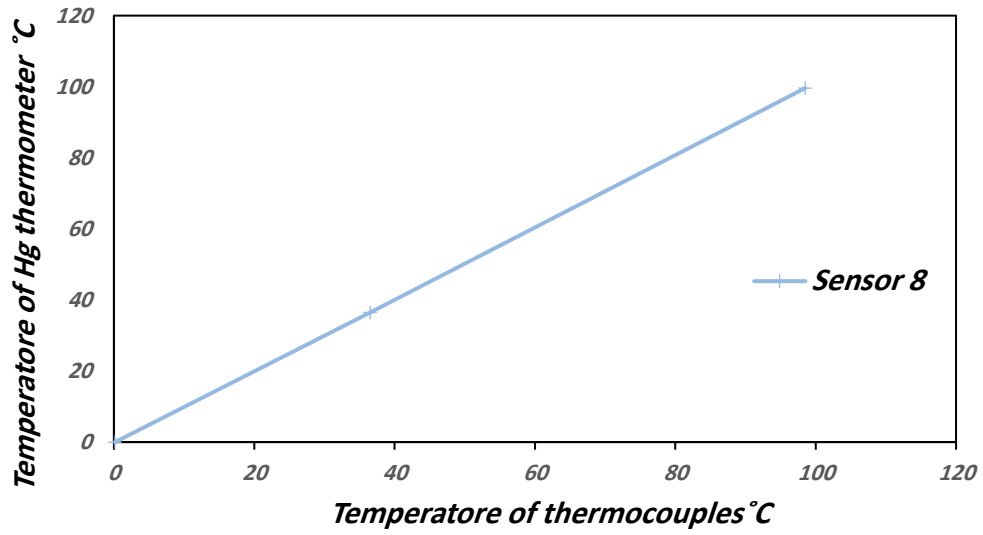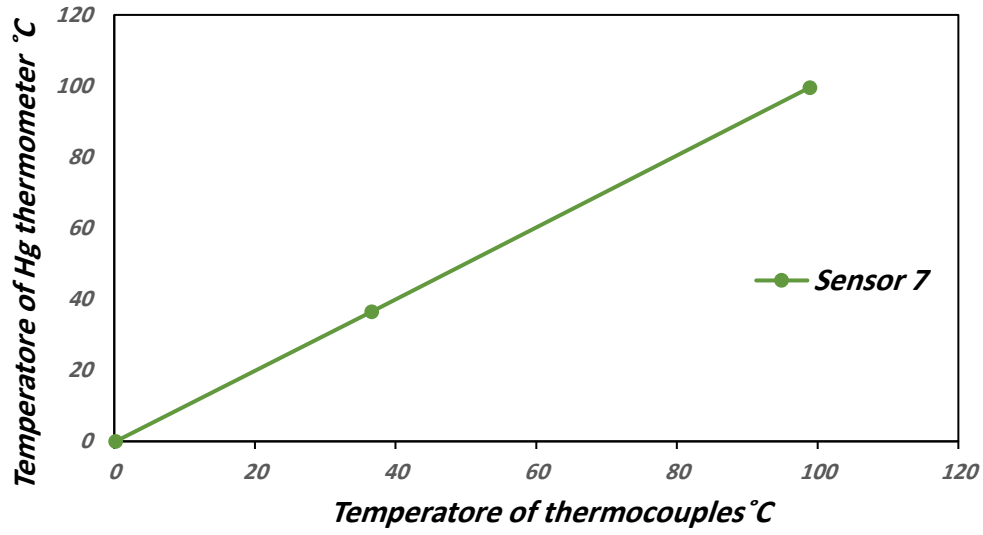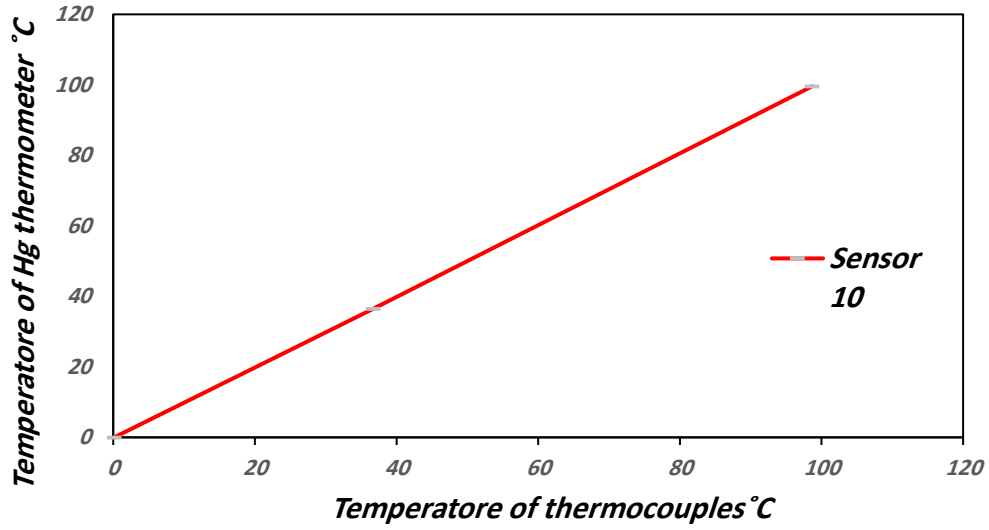
Fig. C.1: Calibration curves of thermocouples

Appendix-D: Calibration of solar power meter

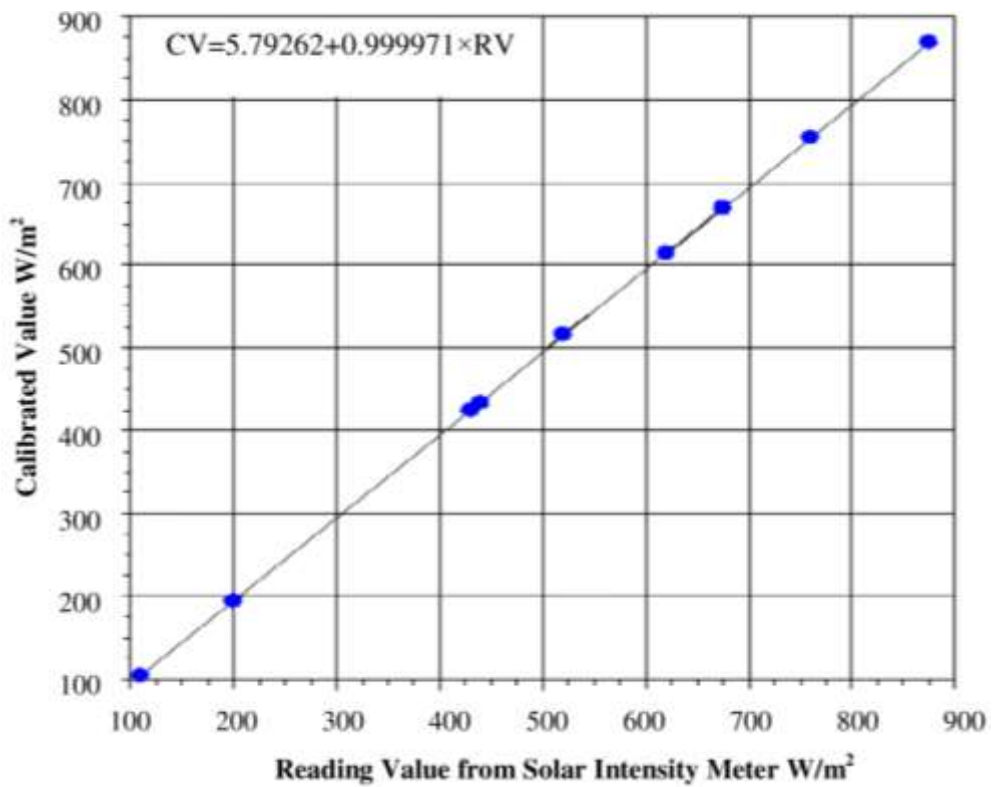$$CV = 5.79262 + 0.999971 \times RV$$

Fig. D.1: Calibration of solar power meter

Publications

Experimental Evaluation of Fresnel's lens solar concentrator in Iraq

Ahmed H. Obaid[a], Arsaad Al Sahlani[a], Adel A Eidan[b]

[a] Al-Furat Al-Awsat Technical University, Engineering Technical College of Al-Najaf, 31001, Iraq

[b] Al-Furat Al-Awsat Technical University, Najaf Technical Institute, 31001, Iraq

Abstract. This work presents an experimental study to utilize extreme sun rays temperature via Fresnel's lens concentrate using a solar tracking system. The experimental rig consists of a freely rotating two-axis frame that is controlled by an electronic circuit that implements Arduino and stepper motors as a control system to adjust the position of the Fresnel's lens focal by moving the motors accordingly. The focal of the sunray is to be maintained stationary at a fixed position to ensure continuity of heat flow on the absorption plate. The experimental results showed that the focal temperature reached as high as 422° C when the ambient temperature was 17° C. Observing the results, gives an idea of promising ability to use the Fresnel's lens in a wide range of renewable energy applications such as heating and heat storage.

1. Introduction

Solar energy is sustainable and so will never run out energy. Fossil fuels used in many energy sources are limited and decreased; in addition, it pollutes the environment as a result of the emissions of the combustion. Solar energy is one of the alternative solutions with its great potentials. Solar Energy can be utilities in many different forms. One of the forms is the solar concentrator where solar concentrators are devices that focus the sunlight from a large area, by reflection or refraction using parabolic or lens, respectively, on a small receiver. Such action increases the intensity of solar radiation on surface of the small receiver. As the sun change its relative location, the solar concentrators have to track the sun to be the solar radiation is directed on the absorption surface.

Many studies have been accomplished to investigate the effectiveness of solar tracking system with solar concentrator, yet only a limited number were mentioned in the literature that examined the effect of using solar tracking system with Fresnel lens concentrator. Zhai, H., et. al.(2010) [1] used linear Fresnel lens solar concentrator with evacuated tube absorber employing one-axis solar tracking system. The results showed that the thermal efficiency of this solar collector is higher than the commonly used flat-plate or evacuated tube solar collectors. Hussain,M.I., et. al.(2015) [2] examined two types of Fresnel lens collectors: linear Fresnel lens (LFL) and spot Fresnel lens (SFL), both types had the same surface area. the collectors were equipped with a dual-axis solar tracking system. They found that the (SFL) performance is 7-12% higher than the (LFL) collector. Sierra,C., et. al.(2005) [3] investigated the Fresnel lens concentrator of solar energy to achieve higher solar energy density and very high temperatures (1500–2000 K), such temperatures are useful for surface modifications of metallic materials. Hussain M.I.&Lee,G.H. (2015). [4] used Fresnel lenses and U-shaped solar energy receiver with concentrated photovoltaic thermal (CPV/T). the system was equipped with a two-axis solar tracking system. The results showed that the energy released depends on the ambient temperature and the intensity of the solar radiation. Xie,W.T., et. al.(2011) [5] used a Fresnel lens solar collector

Acceptance Letter

Dears : Ahmed H. Obaid, Assaad Al Sahlani, Adel A Eidan

Based on the recommendations of the reviewers and the local Scientific Committee, we are delighted to inform you that your manuscript entitled "Fresnel lens solar concentrator to utilize the Extreme solar Intensity in solar still receivers "has been accepted for publication in the 2nd International Scientific Conference of Al-Ayen University.

The accepted manuscripts will be published in the IOP publisher conference proceedings, which is Scopus indexed and has CiteScore 0.53 Q3 for 2019.

Shafik ... Shafik

Chairman of Organization

Committee

of ISCAU 2020

Al-Ayen University

جامعة العين

الخلاصة

يقدم هذا العمل دراسة تجريبية للاستفادة من درجة حرارة اشعة الشمس الشديدة باستخدام عدسة فريسنل كمركز شمسي و نظام التتبع الشمسي. يتكون العمل التجريبي من إطار يدور باتجاه ثنائي المحور يتم التحكم فيه عن طريق دائرة إلكترونية تتألف من دائرة Arduino و محركات stepper بحيث تعمل المجموعة كنظام تحكم لضبط موضع بؤرة عدسة فريسنل عن طريق تحريك المحركات وفقًا لذلك. يجب الحفاظ على بؤرة العدسة ثابتة في موضع ثابت لضمان استمرارية تدفق الحرارة على نظام الامتصاص.

تقدم الدراسة التجريبية الخصائص الحرارية لبؤرة العدسة. كاختبار أولي ، تم وضع لوحين من معدنين مختلفين وهما الفولاذ والألمنيوم في بؤرة العدسة لدراسة توزيع درجات الحرارة عليها. تم إجراء الاختبارات في مدينة النجف _ العراق (E° 44 ، N° 31) خلال فصل الشتاء وللفترة من تشرين الثاني 2019 إلى شباط 2020. وأظهرت النتائج أن درجة حرارة البؤرة وصلت إلى 400 درجة مئوية عندما كانت درجة الحرارة المحيطة 20 درجة مئوية. مراقبة النتائج اعطت فكرة عن القدرات الواعدة لاستخدام عدسة فريسنل في مجموعة واسعة من تطبيقات الطاقة المتجددة مثل تحلية المياه وتسخين المياه وتخزين الحرارة.

بالنسبة لتحلية المياه، تم استخدام نموذجين من المقطر الشمسي الزجاجي (بارتفاع 10 سم و 20 سم). لتسخين المياه، تم استخدام نموذجين من المبادلات الحرارية ، وهما الأنبوب المخروطي و الخزان المكعب. و تم استخدام حاوية مياه فولاذية مكعبة (20 سم لكل جانب)، تم تصنيعها مع زعانف معدنية عمودية متصلة بالغطاء العلوي للحاوية.

تم إجراء الاختبارات خلال الأيام المختلفة من شهر كانون الثاني وشباط 2020. وتم الحصول على أكبر إنتاجية للمقطر الشمسي هي (500مل) .

أجريت التجارب في شباط 2020. وأظهرت النتائج أن أعلى قيمة من الحرارة المستفادة تم الحصول عليها للمبادل الحراري الأنبوب المخروطي هي 92واط عندما كانت شدة الإشعاع الشمسي 1206 واط / م^2 ودرجة الحرارة المحيطة 14 درجة مئوية، وللمبادل الحراري الخزان المكعب هي 91واط عندما كانت شدة الإشعاع الشمسي 1387 واط / م^2 ودرجة الحرارة المحيطة 18 درجة مئوية. إنها فكرة واعدة لاستخدام عدسة فريسنل لتسخين المياه في درجات حرارة منخفضة نسبيًا.

تم إجراء الاختبارات خلال الأيام المختلفة من شهر تشرين الثاني 2019. وأظهرت نتائج التجارب، ان أعلى درجة حرارة مسجلة في بؤرة العدسة لحاوية المياه الفولاذية المكعبة هي 258.6 و 81.3 درجة مئوية على التوالي لكل من الغطاء المزعنف الستيل والالمنيوم عندما كانت درجة الحرارة المحيطة 24.6 و 22.4 م والشعاع الشمسي 1251و1008 واط /م^2 على التوالي.

جمهورية العراق

وزارة التعليم العالي والبحث العلمي

جامعة الفرات الاوسط التقنية

الكلية التقنية الهندسية نجف

التحقيق التجريبي لبعض التطبيقات الحرارية باستخدام مركز عدسة فريسنل في العراق

رسالة مقدمة الى

قسم هندسة تقنيات ميكانيك القوى كجزء من متطلبات نيل درجة الماجستير التقني
في هندسة الميكانيك_تخصص حراريات

تقدم بها

احمد حسين عبيد محمد

(بكالوريوس هندسة تقنيات التبريد والتكييف)

إشراف

الاستاذ المساعد الدكتور اسعد عواد عباس

الاستاذ المساعد الدكتورعادل عبد عزيز عيدان

شوال 1441